ELECTRON-LATTICE INTERACTION AND SUPERCONDUCTIVITY IN $BaPb_{1-x}Bi_xO_3$ AND $Ba_xK_{1-x}BiO_3$

Masafumi SHIRAI

OSAKA UNIVERSITY
GRADUATE SCHOOL OF ENGINEERING SCIENCE
DEPARTMENT OF MATERIAL PHYSICS
TOYONAKA OSAKA

ELECTRON-LATTICE INTERACTION AND SUPERCONDUCTIVITY IN $BaPb_{1-x}Bi_xO_3$ AND $Ba_xK_{1-x}BiO_3$

Masafumi SHIRAI

April 1989

Abstract

The oxide superconductor $BaPb_{1-x}Bi_xO_3$ (BPB) has attracted much attention because of its interesting properties of superconductivity. BPB becomes superconductor in the composition range $0<x<0.35$ and the maximum transition temperature T_c is about 13 K ($x=0.25$). Recently $Ba_xK_{1-x}BiO_3$ (BKB) has been found to have the highest T_c ($\sim$ 28 K at $x=0.7$) among oxide superconductors not containing Cu ions. Both BPB and BKB have perovskite-type structure and do not contain any transition-metal element. Hence, the magnetic mechanism may not be expected for the superconductivity in these compounds. Therefore, it is meaningful to investigate microscopically the superconductivity in BPB and BKB on the basis of the phonon mechanism.

The electron-lattice interaction is studied microscopically by using the realistic electronic bands of $BaPb_{0.7}Bi_{0.3}O_3$ and $BaBiO_3$ obtained by Mattheiss and Hamann. The conduction band which acrosses the Fermi level is well reproduced by the tight-binding (TB) model, and is a hybridized band consisting of O 2p and Bi (or Pb) 6s and 6p orbitals. We have calculated the electron-lattice coupling coefficient $g_\mu^\alpha(\mathbf{k},\mathbf{k}')$ which represents the strength of the coupling between two conduction band states k and k' caused by displacement of the μ-th atom along the α-direction ($\alpha=x,y,z$). It is found that $g_\mu^\alpha(\mathbf{k},\mathbf{k}')$ has strong wave-vector and mode dependences and is especially large for the vibration of O-atoms along the direction toward the nearest neighbouring Pb (or Bi) atoms.

The lattice dynamics of BPB and BKB is investigated by

diagonalizing the dynamical matrix in which the effective long range forces caused by the electron-lattice interaction are taken into account in addition to the short range forces. The electron-lattice interaction has turned out to lower the frequencies and to broaden the line-width of the longitudinal (L) O-stretching and/or breathing mode vibration. The phonon frequency renormalization shows remarkable wave-vector and x dependences.

We discuss the superconductivity of BPB and BKB in the framework of the strong coupling theory of the phonon mechanism. First, the spectral function $\alpha^2F(\omega)$ is calculated by making use of the calculated renormalized phonons. The frequency dependence of $\alpha^2F(\omega)$ is entirely different from that of the phonon density of states $F(\omega)$. It is noted that $\alpha^2F(\omega)$ has some prominent structures in the frequency range where the O-stretching/breathing mode phonons lie. Therefore, the O-stretching/breathing mode is expected to contribute dominantly to the superconductivity in BPB and BKB. As x increases, some main peaks in $\alpha^2F(\omega)$ shift to lower frequency side, reflecting the phonon frequency renormalization, and the magnitude of $\alpha^2F(\omega)$ increases remarkably in the wide frequency range. Such considerable change in $\alpha^2F(\omega)$ is expected to bring a remarkable x dependence of T_c.

The transition temperature T_c has been evaluated by solving the linearized Eliashberg equations. The calculated T_c increases rapidly with increasing x, and reaches 28 K at x=0.7 in case of $t'=4.05$ eV/A and $\mu^*=0.15$, where t' denotes the derivative of the transfer integral, and μ^* is the effective screened Coulomb replusion constant. In this case the dimensionless coupling

constant λ is evaluated to be 1.09, which suggests the strong electron-lattice coupling in BKB. Our results for T_c agree well with observed T_c in BKB, but disagree with those in BPB. One of reasons for this discrepancy may be that the rigid-band model is insufficient to describe BPB, because in BPB the Pb atom, which is one of constitutive elements of the conduction band, is substituted randomly by the Bi atom.

We have evaluated the isotope shift of T_c in BKB by calculating T_c when ^{16}O is replaced with ^{17}O and ^{18}O. A characteristic exponent α, defined as $T_c \propto M_0^{-\alpha}$, is found to be $\alpha=0.35\sim0.45$. Experimetally the value α is found to be 0.41 by Hinks et al and 0.35 by Kondoh et al. The principal reason why α differs from the value predicted by the BCS theory ($\alpha=0.5$) is that the vibration of atoms other than oxygens, such as Bi atoms, contribute appreciably to the superconductivity.

Further, the gap function $\Delta(\varepsilon)$ at T=0 K is calculated for BKB. The ratio $2\Delta_0/k_BT_c$ (Δ_0: superconducting energy gap) is found to have the value close to that predicted by the BCS weak coupling theory ($2\Delta_0/k_BT_c=3.5$). However, the tunneling differential conductance dI/dV shows a behavior which is characteristic to the strong coupling superconductor.

In conclusion, the observed superconducting properties in BKB can be understood by the phonon mechanism in the framework of the strong coupling theory. It is particularly emphasized that the significant renormalization of the L O-stretching/breathing mode phonons plays an important role for the high T_c in BKB.

Acknowledgements

The auther would like to express his sincere gratitude to Professor K. Motizuki, under whose guidance this work was done, for valuable suggestions and helpful discussions through the course of the work and also for her help in prepairing the manuscript. Without her continuous encouragement and help, this work would not have been completed. He also thanks Assistant Professor N. Suzuki for stimulative discussions and enlightening suggestions. Thanks are also due to all members of Motizuki Laboratory for discussions.

CONTENTS

§1. Introduction

Since the discovery of a superconductor with a high transition temperature ($T_c \sim$ 30 K) in La-Ba-Cu-O system,[1] much effort has been continuouslly made for investigating oxide superconductors. Oxide superconductor $BaPb_{1-x}Bi_xO_3$ (BPB) with a perovskite-type structure is a prototype of a series of the high T_c oxides. BPB exhibits a metallic behavior in the composition range $0 \leqq x < 0.35$ and becomes a superconductor with a relative high T_c.[2] On the other hand, BPB shows semiconducting properties over the wide range $0.35 < x \leqq 1$. The observed T_c shows a remarkable x dependence,[3] as shown in Fig.1-1, and takes its maximum T_c=12 K around x=0.25 which is extraordinarily high among superconductors not containing any transition elements. Such high T_c is a contrast to the experimental fact that BPB has a low carrier density, i.e. about 10^{21} cm^{-3} measured by the Hall effect,[3] which is smaller by an order of magnitude than that of typical superconductors. The specific heat measurement[4] has also confirmed that the density of states at the Fermi level $N(E_F)$ is quite small, about 10^{-1} states/(eV·unit cell·spin), in spite of its high T_c. Hence, it seems that the superconductivity in BPB may be attributed to strong electron-phonon interactions. The origin of such a strong electron-phonon coupling, however, has not been clarified yet theoretically.

As for the metal-semiconductor (M-S) transition in BPB with x=0.35, experimental studies have not been made so intensively

except for some electrical and optical measurements.[5),6)] Hence, the mechanism of the M-S transition has not been established so far. Various kinds of mechanism of the M-S transition, such as the local charge-density-waves (CDW),[7)] CDW with (Pb,Bi) ordering waves,[8)] have been proposed. It seems to be common that the substitution of Bi atoms with Pb atoms may be responsible for the M-S transition. Furthermore, the (Pb,Bi) substitution may stabilize the semiconducting phase and hence prevents the higher T_c in BPB.

In this connection the substitution of the Ba site of $BaBiO_3$, in place of the substitution of the Bi site, has been made to finding a possibility of high T_c. Such a possibility has been realized in $Ba_xK_{1-x}BiO_3$ (BKB).[9)] (It should be noted that the notation of composition x differs from the usual one, i.e. $Ba_{1-x}K_xBiO_3$, for convenience in dealing with both BPB and BKB simultaneously.) The perovskite-type oxide BKB with cubic symmetry exhibits superconductivity in the composition range $0.6<x<0.8$ relatively closer to $BaBiO_3$ as shown in Fig.1-1.[10)] Its maximum T_c of 28 K is a record so far except for the high T_c Cu oxide superconductors.

An unsolved question is whether the origin or mechanism of superconductivity in high T_c oxides is usual phonon mechanism or not. In order to clarify the mechanism of the superconductivity in the oxides various experimental studies, such as the isotope effect on T_c,[11)-16)] tunneling spectroscopy,[17)-19)] have been carried out. Both BPB and BKB are not exception of the

experimental objects. Therefore, it is important and meaningful to study theoretically the mechanism of superconductivity in BPB and BKB.

For this purpose the electron-lattice interaction in BPB and BKB is studied microscopically in Section 2, on the basis of realistic electronic band structure. In Sec.3 the lattice dynamics of these compounds is investigated taking account of the effect of the electron-lattice interaction. By utilizing the results obtained in Sec.2 and Sec.3, the superconductivity is discussed in Sec.4, on the basis of the strong coupling theory of the phonon mechanism.

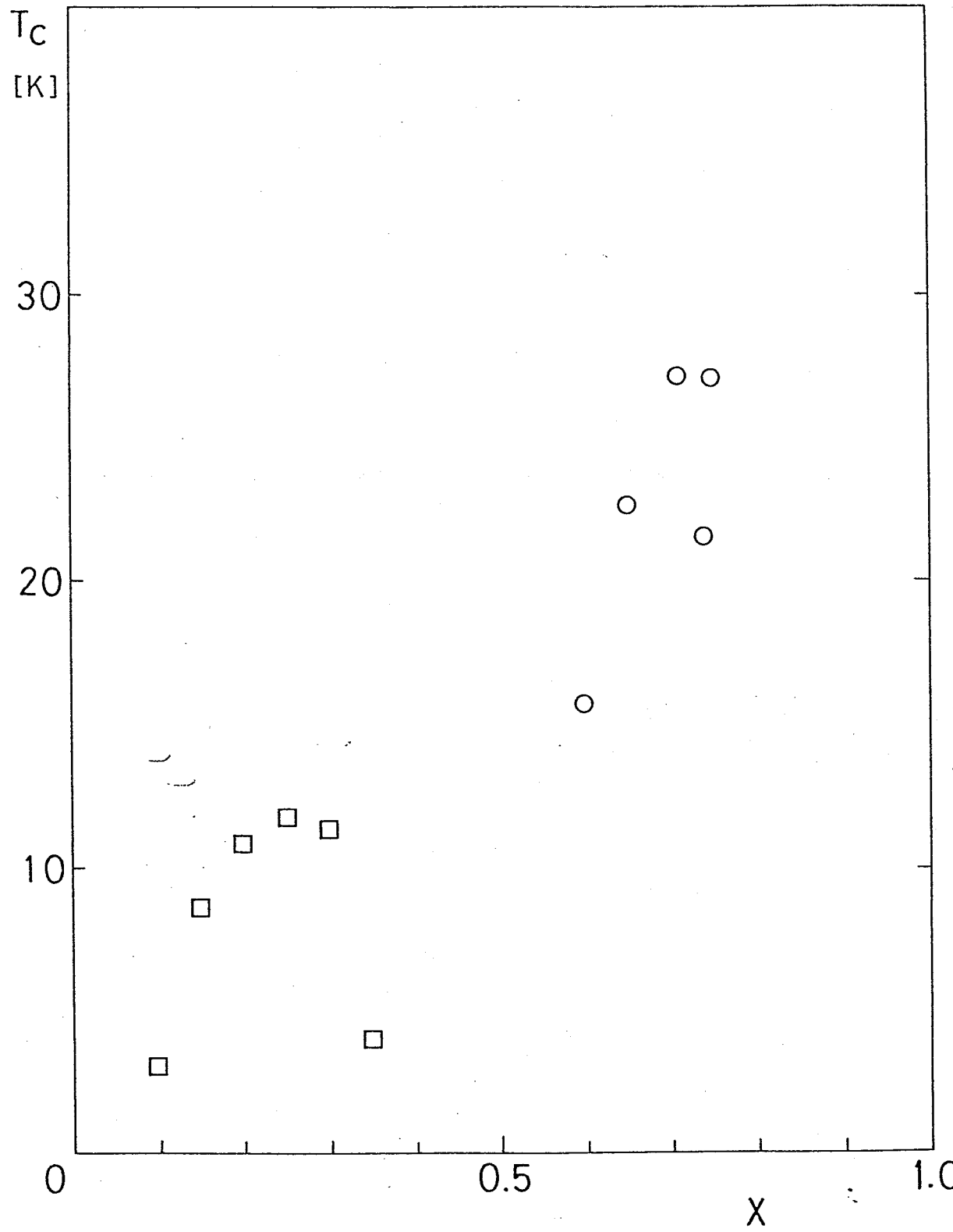

Fig.1-1. Superconducting transition temperatures T_c observed for BPB (open square) and for BKB (open circle).

§2. Electron-Lattice Interaction

2-1. Electronic Band Structure

The crystal structure of BPB at high temperatures (T>800 K) is cubic as shown in Fig.2-1. At lower temperatures, however, it takes a crystal structure of lower symmetry depending on the Bi concentration x. Cox and Sleight[20] has reported that the structure at room temperature changes as x increases from orthorhombic ($0<x<0.05$) to tetragonal ($0.05<x<0.35$), to orthorhombic ($0.35<x<0.9$) and finally to monoclinic ($0.9<x1$). Another group,[21] however, has shown that the structure at room temperature is orthorhombic in the whole range of $0<x<0.9$. Tanaka's group[22] have made systematic measurements on this compound using various kinds of experimental techniques, which include transport, Hall effect, specific heat, optical reflection or absorption, Raman scattering, and so on. According to their results physical properties of this compound with $0<x<0.2$ can be well understood within the rigid band model based on the band structure in the cubic phase calculated by Mattheiss and Hamann.[23]

The electronic band structure of BPB has been originally calculated by Mattheiss and Hamann[23] using the self-consistent scalar-relativistic linearized augumented plane wave (LAPW) method. They have carried out the LAPW band calculation for $BaPbO_3$, $BaPb_{0.7}Bi_{0.3}O_3$, and $BaBiO_3$ in the cubic structure.

Calculation for $BaPb_{0.7}Bi_{0.3}O_3$ has been performed by using the virtual crystal approximation. According to their results the conduction band consists mainly of a σ-bonding of O-2p and Pb (or Bi)-6s orbitals. There is a small overlap between the σ band and the O-2p non-bonding bands. Hence, $BaPbO_3$ is a semimetal with small number of conduction electrons. It has been shown that these band structures can be well understood in terms of a simple orthogonal tight-binding (OTB) model.

In the TB approximation the basis functions consist of the Bloch functions constructed from atomic orbitls $\phi_{\mu a}(\mathbf{r}-\mathbf{R}_{\ell\mu})$ as follows:

$$\Phi^{0}_{\mu a}(\mathbf{k};\mathbf{r}) = \frac{1}{\sqrt{N}} \sum_{\ell} e^{i\mathbf{k}\cdot\mathbf{R}_{\ell}} \phi_{\mu a}(\mathbf{r}-\mathbf{R}_{\ell\mu}) \quad , \tag{2-1}$$

where ℓ, μ and a specify unit cells, atomic sites in the unit cell and kinds of stomic orbitals, respectively. And the equilibrium position vector $\mathbf{R}_{\ell\mu}$ is expressed as

$$\mathbf{R}_{\ell\mu} = \mathbf{R}_{\ell} + \boldsymbol{\tau}_{\mu} \quad , \tag{2-2}$$

where $\mathbf{R}_{\ell}$ denotes the lattice vector of the ℓ-th unit cell, and $\boldsymbol{\tau}_{\mu}$ represents the position of the μ-th site in the unit cell. Energy eigen-values are determined by solving the following secular determinant equation:

$$\det\left|\mathbf{T}(\mathbf{k},\mathbf{k}') - E\,\mathbf{S}(\mathbf{k},\mathbf{k}')\right| = 0 \quad , \tag{2-3}$$

where $\mathbf{T}(\mathbf{k},\mathbf{k}')$ and $\mathbf{S}(\mathbf{k},\mathbf{k}')$ represent the transfer matrix and

orverlap matrix, respectively. Each matrix element of $\mathbf{T}(\mathbf{k},\mathbf{k}')$ and $\mathbf{S}(\mathbf{k},\mathbf{k}')$ is written as

$$T_{\mu a,\nu b}(\mathbf{k},\mathbf{k}') = \int d\mathbf{r}\ \Phi^{0}_{\mu a}(\mathbf{k})^{*}\ H_{el}\ \Phi_{\nu b}(\mathbf{k}') \quad , \tag{2-4a}$$

$$S_{\mu a,\nu b}(\mathbf{k},\mathbf{k}') = \int d\mathbf{r}\ \Phi^{0}_{\mu a}(\mathbf{k})^{*}\ \Phi_{\nu b}(\mathbf{k}') \quad . \tag{2-4b}$$

Here H_{el} is the one-electron Hamiltonian which can be given by

$$H_{el} = \frac{p^2}{2m} + \sum_{\ell\mu} V(\mathbf{r}-\mathbf{R}_{\ell\mu}) \quad , \tag{2-5}$$

where p denotes the momentum operator, m is the mass of an electron, and $V(\mathbf{r}-\mathbf{R}_{\ell\mu})$ represents the potential energy associated with the atom at the lattice site $\mathbf{R}_{\ell\mu}$ in the crystal.

If the potential energy retains the translational symmetry in the crystal, $\mathbf{T}(\mathbf{k},\mathbf{k}')$ and $\mathbf{S}(\mathbf{k},\mathbf{k}')$ are block-diagonalized with respect to the wave-vector $\mathbf{k}$:

$$\begin{aligned} T_{\mu a,\nu b}(\mathbf{k},\mathbf{k}') &= \delta_{\mathbf{k},\mathbf{k}'} T^{0}_{\mu a,\nu b}(\mathbf{k}) \\ &\equiv \delta_{\mathbf{k},\mathbf{k}'} \sum_{\ell-\ell'} e^{-i\mathbf{k}\cdot(\mathbf{R}_{\ell}-\mathbf{R}_{\ell'})}\ T^{0}_{\ell\mu a,\ell'\nu b} \quad , \end{aligned} \tag{2-6a}$$

$$\begin{aligned} S_{\mu a,\nu b}(\mathbf{k},\mathbf{k}') &= \delta_{\mathbf{k},\mathbf{k}'} S^{0}_{\mu a,\nu b}(\mathbf{k}) \\ &\equiv \delta_{\mathbf{k},\mathbf{k}'} \sum_{\ell-\ell'} e^{-i\mathbf{k}\cdot(\mathbf{R}_{\ell}-\mathbf{R}_{\ell'})}\ S^{0}_{\ell\mu a,\ell'\nu b} \quad , \end{aligned} \tag{2-6b}$$

with

$$T^0_{\ell\mu a,\ell'\nu b} = \int dr\ \phi^0_{\mu a}(r-R_{\ell\mu})^*\ H_{el}\ \phi_{\nu b}(r-R_{\ell'\nu}) \quad , \tag{2-7a}$$

$$S^0_{\ell\mu a,\ell'\nu b} = \int dr\ \phi^0_{\mu a}(r-R_{\ell\mu})^*\ \phi_{\nu b}(r-R_{\ell'\nu}) \quad . \tag{2-7b}$$

Then, the problem reduces to an eigen-value problem for each wave-vector k. The secular determinant equation (2-3) becomes

$$\det|T^0(k) - E^0_{nk}\ S^0(k)| = 0 \quad . \tag{2-8}$$

Here each matrix element of $T^0(k)$ and $S^0(k)$ is given by eqs.(2-6a) and (2-6b), respectively. And E^0_{nk} represents the eigen-energy of the Bloch state with band index n. Further, in the OTB approximation the basis functions are assumed to be orthogonal to each other. Hence, the overlap integral (2-7b) is given by

$$S^0_{\ell\mu a,\ell'\nu b} = \delta_{\ell,\ell'}\ \delta_{\mu,\nu}\ \delta_{a,b} \quad , \tag{2-9}$$

and the overlap matrix (2-6b) becomes a unit matrix 1. Then, the problem reduces to the usual eigen-value problem as follows:

$$\det|T^0(k) - E^0_{nk}\ 1| = 0 \quad . \tag{2-10}$$

The dispersion of the conduction band of BPB is well reproduced with the use of six parameters, three orbitals energies, E(2p), E(6s) and E(6p), and three transfer integrals,

$t(sp\sigma)$, $t(pp\sigma)$, and $t(pp\pi)$ in the Slater-Koster notation.[24] The values of these parameters determined for each compound are listed in Table 2-1. The dispersion curves calculated for x=0.3 are shown with the energy eigen-values utilized in determining the TB parameters (closed circles) in Fig.2-2. The Brillouin zone for cubic perovskite-type structure is given in Fig.2-3.

The dispersion curves of the conduction bands of $BaPbO_3$ and $BaPb_{0.7}Bi_{0.3}O_3$ are almost the same, and various physical propperties[25] of BPB with small Bi concentration can be well understood within the rigid-band model based on the conduction band structure of $BaPbO_3$ or $BaPb_{0.7}Bi_{0.3}O_3$. Recently Mattheiss and Hamann[26] have calculated the band structure for ordered alloy $Ba_{0.5}K_{0.5}BiO_3$, and it is confirmed that the conduction band of $BaBiO_3$ is little affected by substitution of K atoms for Ba atoms. In the following we discuss the electron-lattice interaction in BPB on the basis of the rigid-band model with the use of the conduction band of $BaPb_{0.7}Bi_{0.3}O_3$ whose dispersion is shown in Fig.2-4(a). To see the nature of wave functions we show in Fig.2-4(b) orbital components for the conduction band. It is clearly seen that both O-2pσ and Pb(Bi)-6s components are large except near the Γ point.

Density of states (DOS) of the conduction band is calculated by using the usual tetrahedron linear interpolation method.[27] In actual calculations the irreducible Brillouin zone, which has 1/48 volume of the first Brillouin zone, was devided into 64 small tetrahedra. The results are shown in Fig.2-5 with some

partial DOS defined by

$$N_{\mu a}(E) = \sum_{nk} |A_{n,\mu a}(k)|^2 \, \delta(E-E^0_{nk}) \quad , \tag{2-11}$$

where $A_{n,\mu a}(k)$ is the eigen-vector of the n-th conduction band and μ and a specify the atomic site and orbital in the unit cell, respectively. Then, the total DOS is given by the summation of the partial DOS as

$$\begin{aligned} N(E) &\equiv \frac{1}{N} \sum_{nk} \delta(E-E^0_{nk}) \\ &= \sum_{\mu a} N_{\mu a}(E) \quad . \end{aligned} \tag{2-12}$$

In Fig.2-5, O(2pσ) denotes the 2p-orbital of O atom which elongates along the direction connecting the relevant O atom and its nearest neighbouring (Pb,Bi) atoms. And 2p-orbitals of O atoms other than O(2pσ)'s are denoted by O(2pπ). It is found that the O(2pσ) and (Pb,Bi)(6s) components at E_F increases simultaneously when the E_F departs from the bottom of the conduction band with increasing the composition x. A share in percentage of each orbital component at the Fermi level for various composition x is listed in Table 2-2. It is found that (Pb,Bi) and O share their components by half with each other except for the vicinity of x=0. Further, tendency of saturation is seen in (Pb,Bi) 6s and 6p orbitals for x>0.4.

The Fermi surfaces have been drawn with changing x. Some of them are shown in Fig.2-6, i.e. for (a) x=0.1, (b) x=0.3, (c)

x=0.7 and (d) x=1.0 ($BaBiO_3$). It is clearly seen from the Figure that the Fermi surface expands gradually with increasing x or carriers in the conduction band. For small x, the Fermi surface is almost completely spherical. However, it becomes somewhat round cubic shape for rather large x such as $0.3<x<0.7$. The variation in the shape of the Fermi surface with changing x gives various nesting vectors Q for each x, e.g. for x=0.3 $Q=(\pi/a,0,0)$ which corresponds to the X point in the B.Z. However, the nesting feature of the Fermi surface is not so good because of the three dimensional character of the conduction band.

	$BaPbO_3$	$BaPb_{0.7}Bi_{0.3}O_3$ †	$BaBiO_3$
E(2p)	-0.5	-1.9	-2.5
E(6s)	-1.8	-4.1	-6.5
E(6p)	5.0	3.5	2.3
t(spσ)	2.2	2.2	2.0
t(ppσ)	2.6	2.7	2.6
t(ppπ)	-1.0	-0.9	-0.7

Table 2-1. Tight-binding band parameters. The unit of E and t is eV. †: Taken from Ref.23.

x	(Pb,Bi) 6s	(Pb,Bi) 6p	O 2pσ	O 2pπ
0.1	26.1 %	6.4 %	29.7 %	37.8 %
0.2	32.0	10.1	32.8	25.1
0.3	33.9	12.4	34.7	19.0
0.4	34.5	14.1	36.1	15.3
0.5	34.8	15.5	37.1	12.6
0.6	35.0	16.2	38.8	10.0
0.7	35.1	16.1	40.5	8.3
0.8	35.1	16.1	41.7	7.1
0.9	35.1	16.2	42.6	6.1
1.0	35.1	16.2	43.4	5.3

Table 2-2. Orbital components of the conduction band states at the Fermi level for each composition x.

Fig.2-1. Cubic perovskite-type crystal structure of BPB.

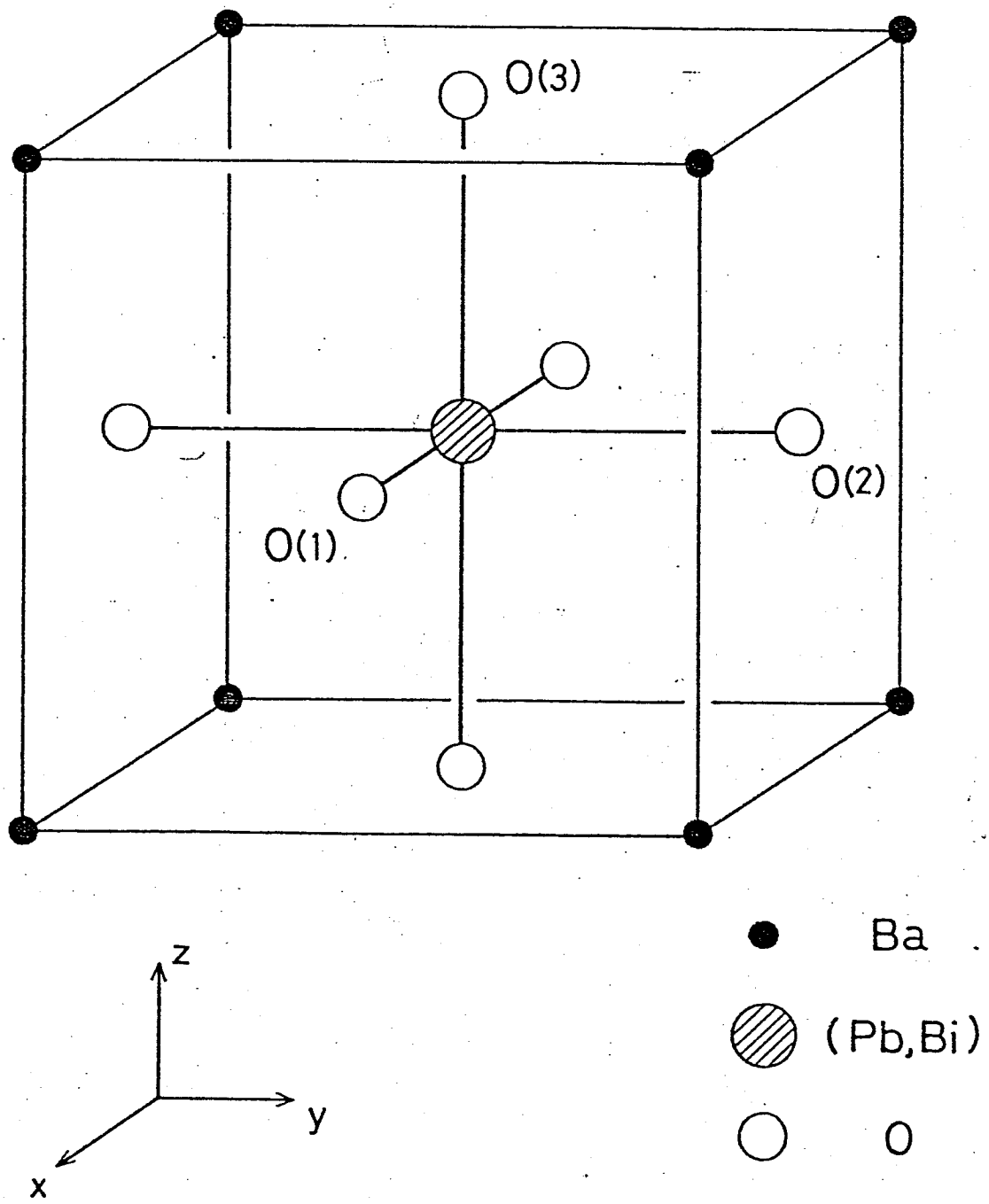

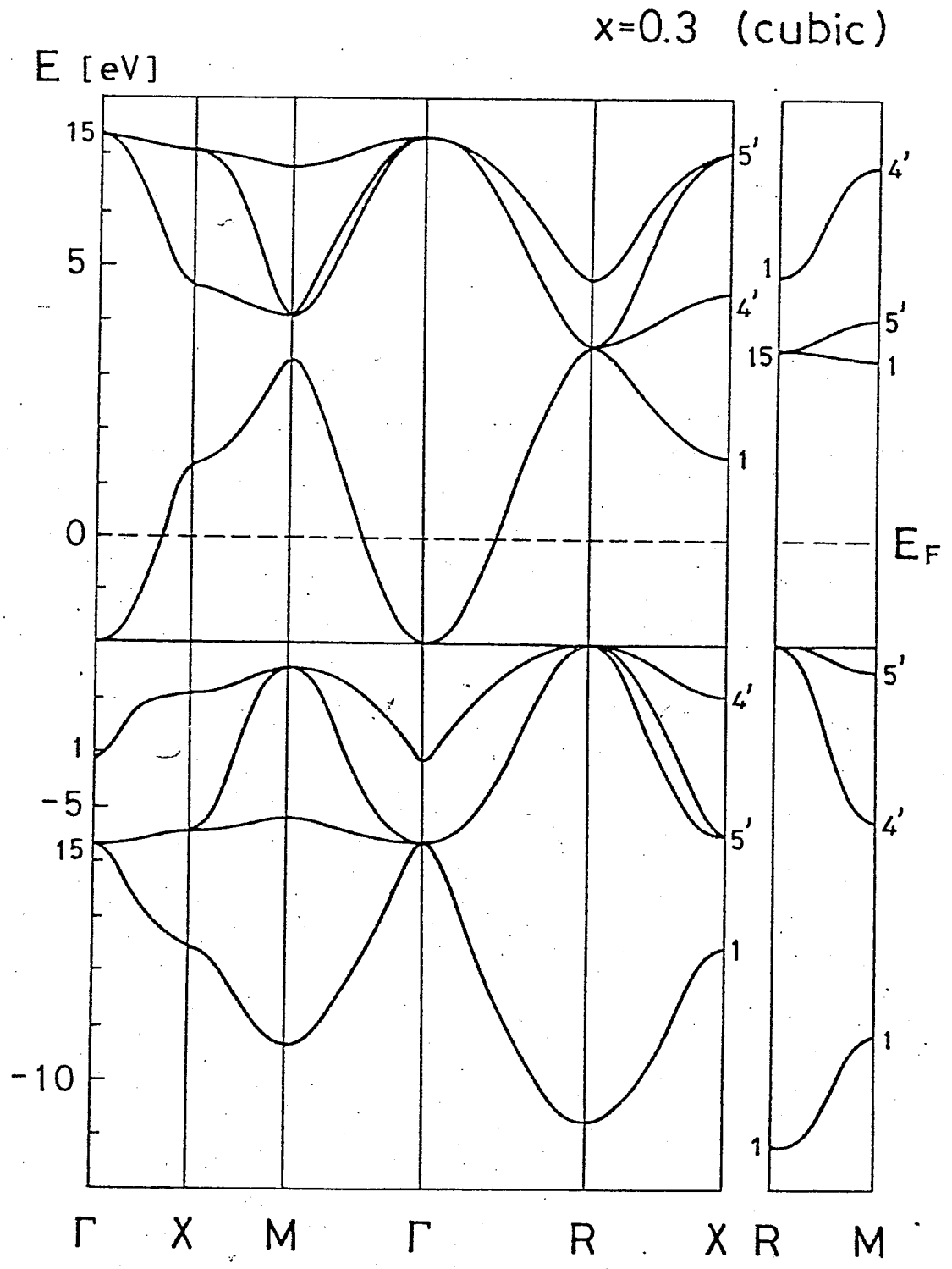

Fig.2-2. Dispersion curves of the electronic band calculated by the OTB method for cubic $BaPb_{0.7}Bi_{0.3}O_3$.

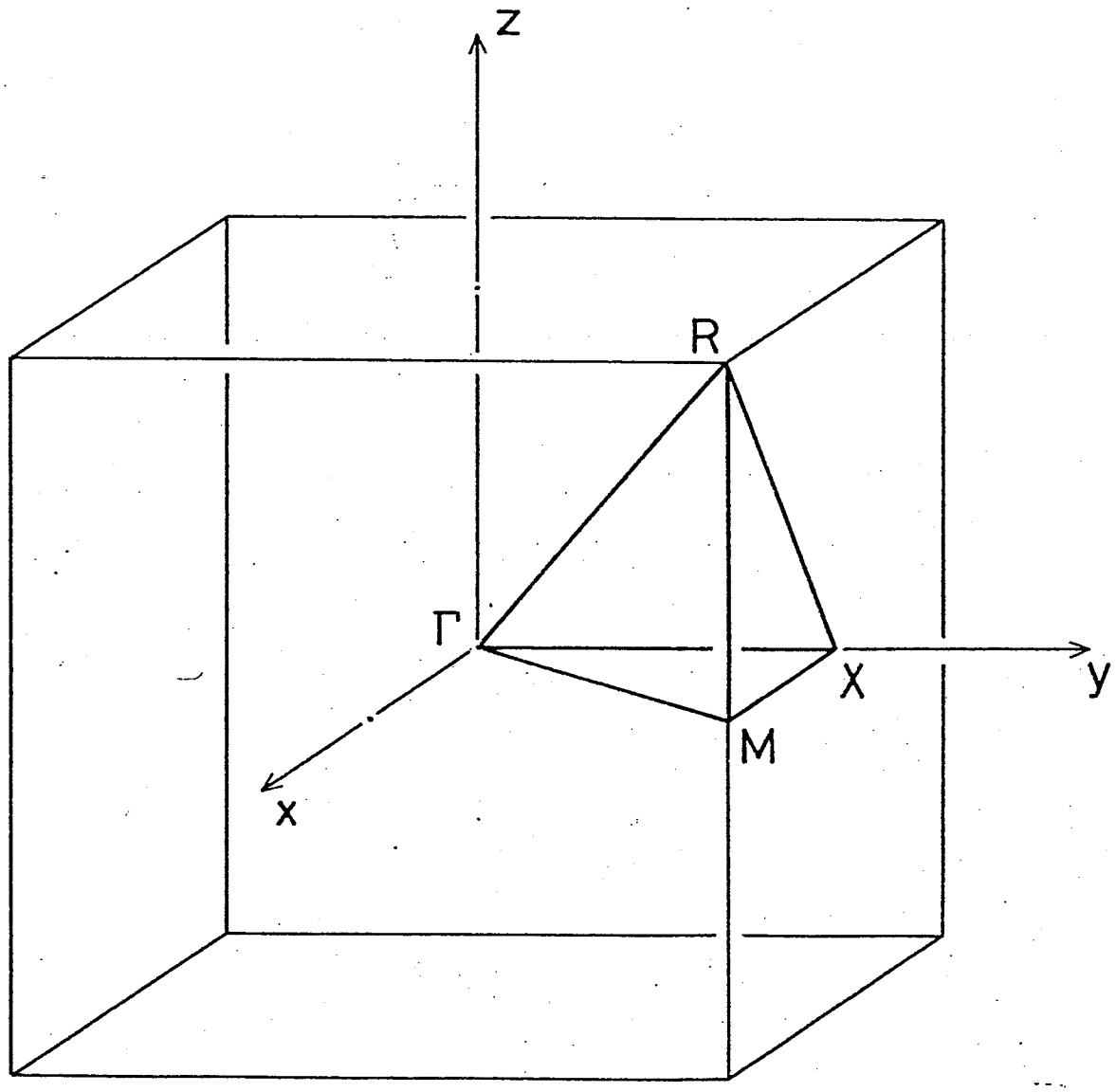

Fig.2-3. Brillouin zone for the cubic perovskite-type structure.

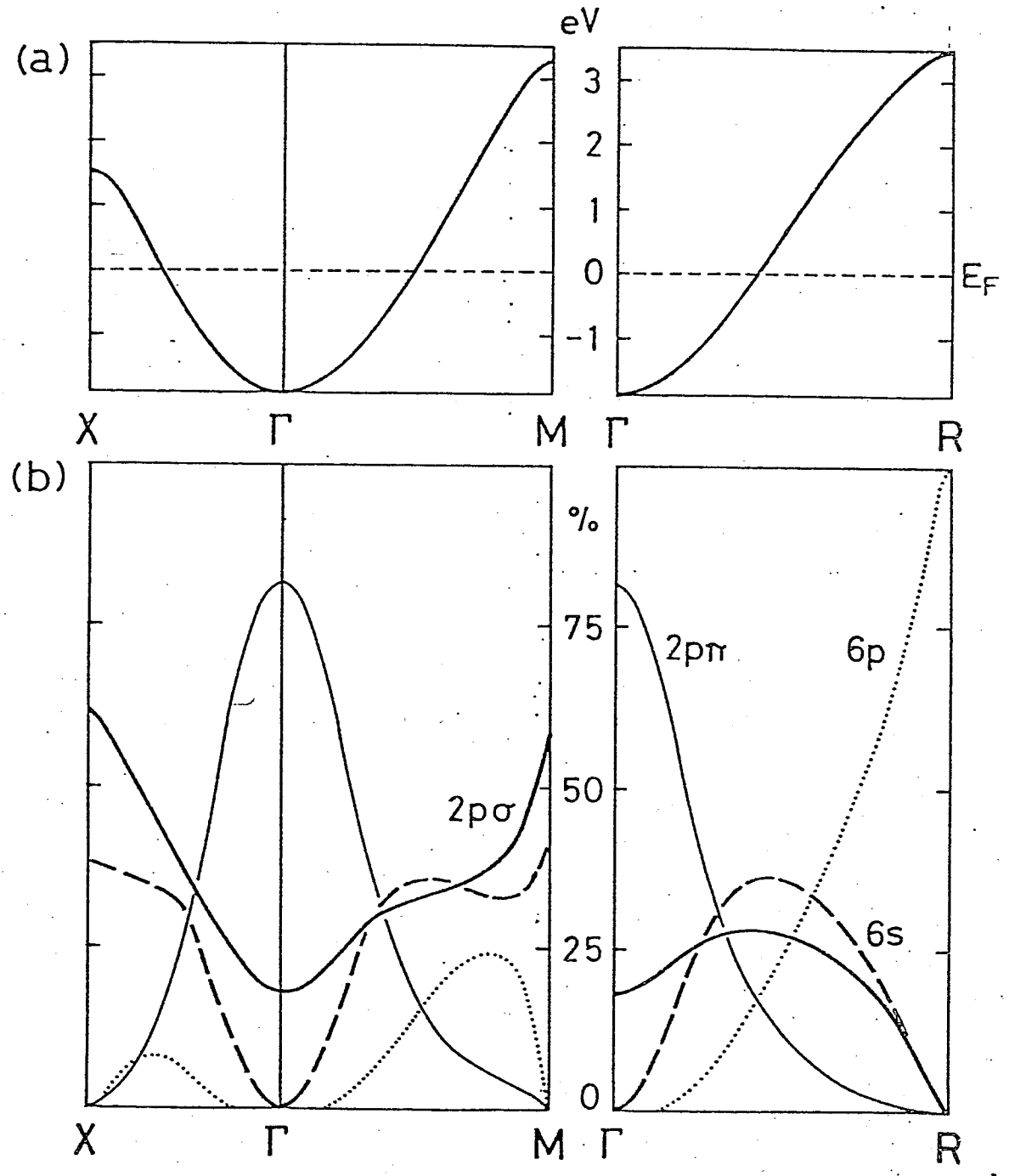

Fig.2-4.(a) Conduction band for the cubic $BaPb_{0.7}Bi_{0.3}O_3$ obtained by the OTB calculation.

(b) Orbital components of the conduction band states. 2pσ and 2pπ denote the orbitals of the O atoms, and 6s and 6p those of the Pb (or Bi) atoms.

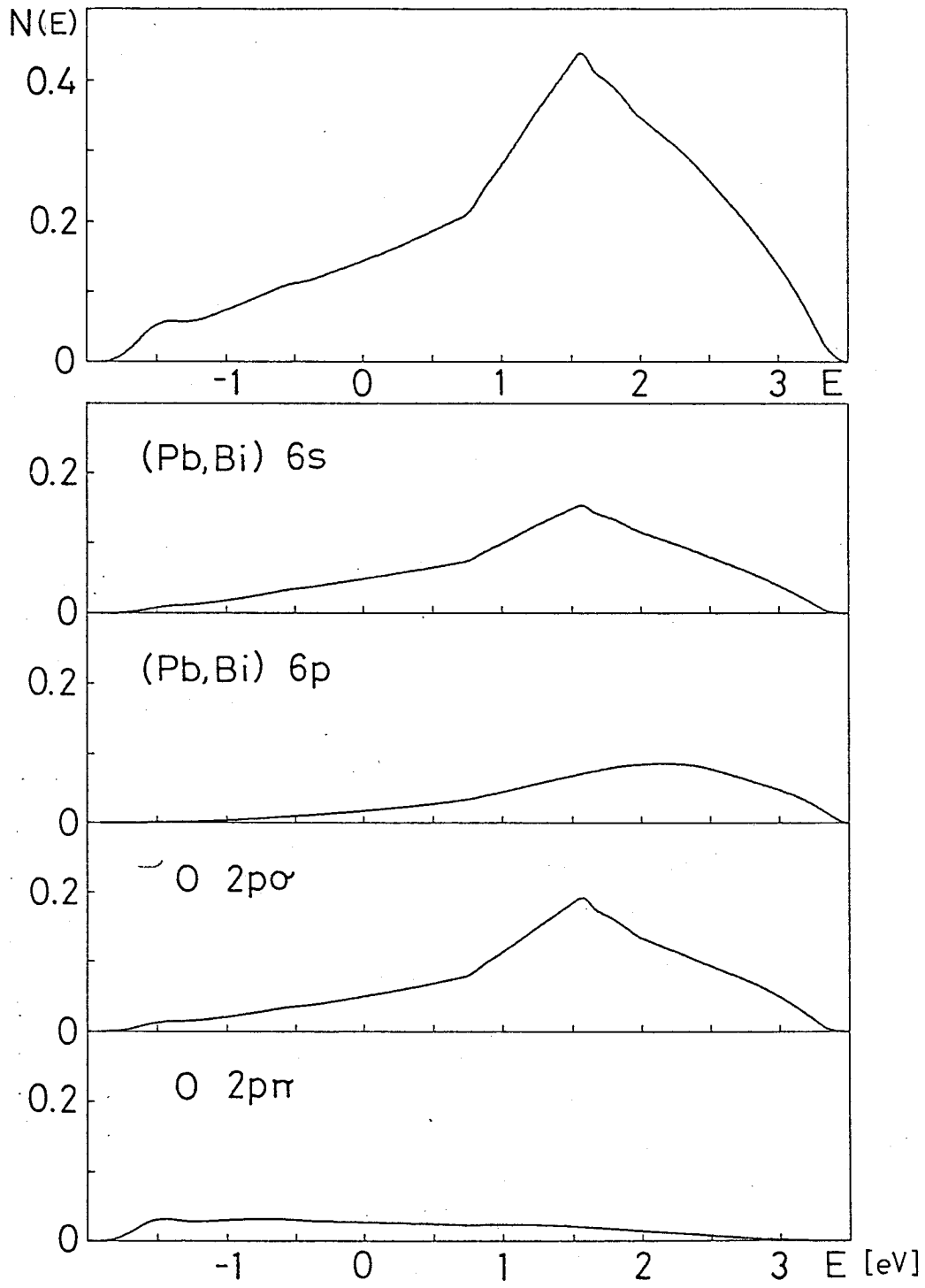

Fig.2-5. Density of states (DOS) for the conduction band. Partial DOS's devided into four kinds of orbital components are also shown.

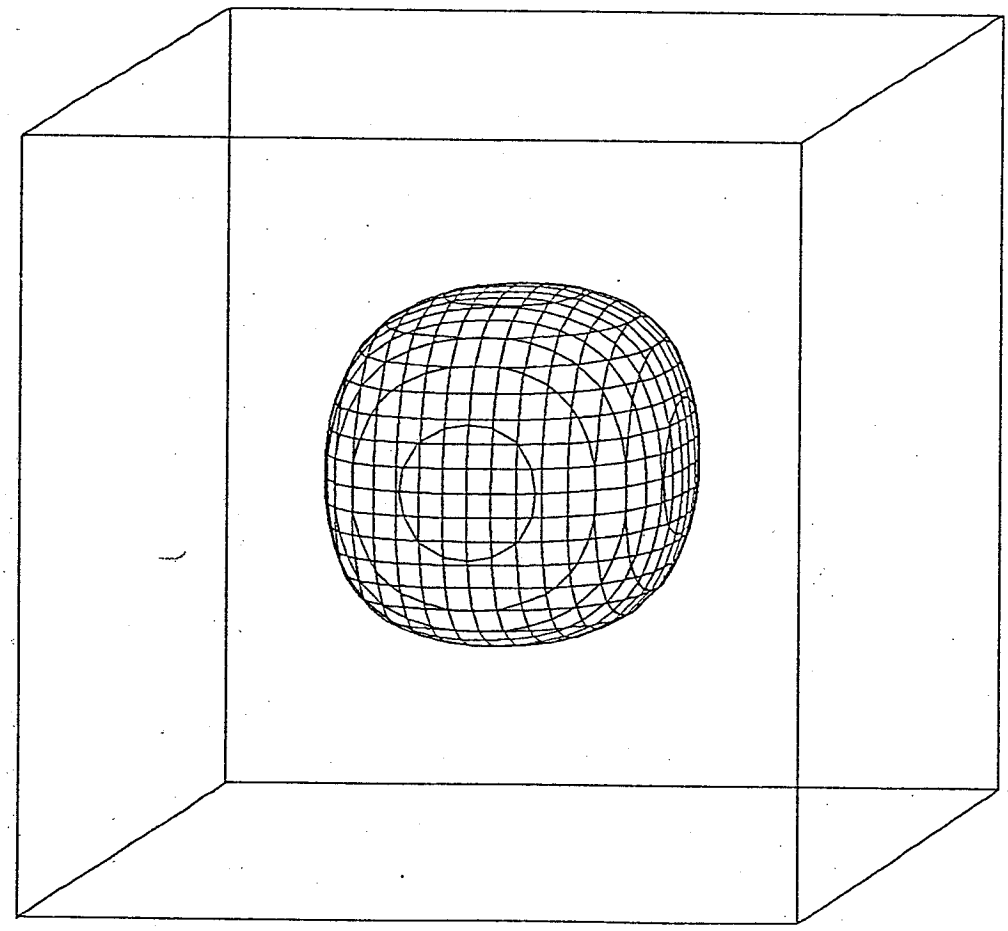

Fig.2-6.(a) Fermi surface for x=0.1. Occupied states are enclosed by the hatched surface centering around the Γ point.

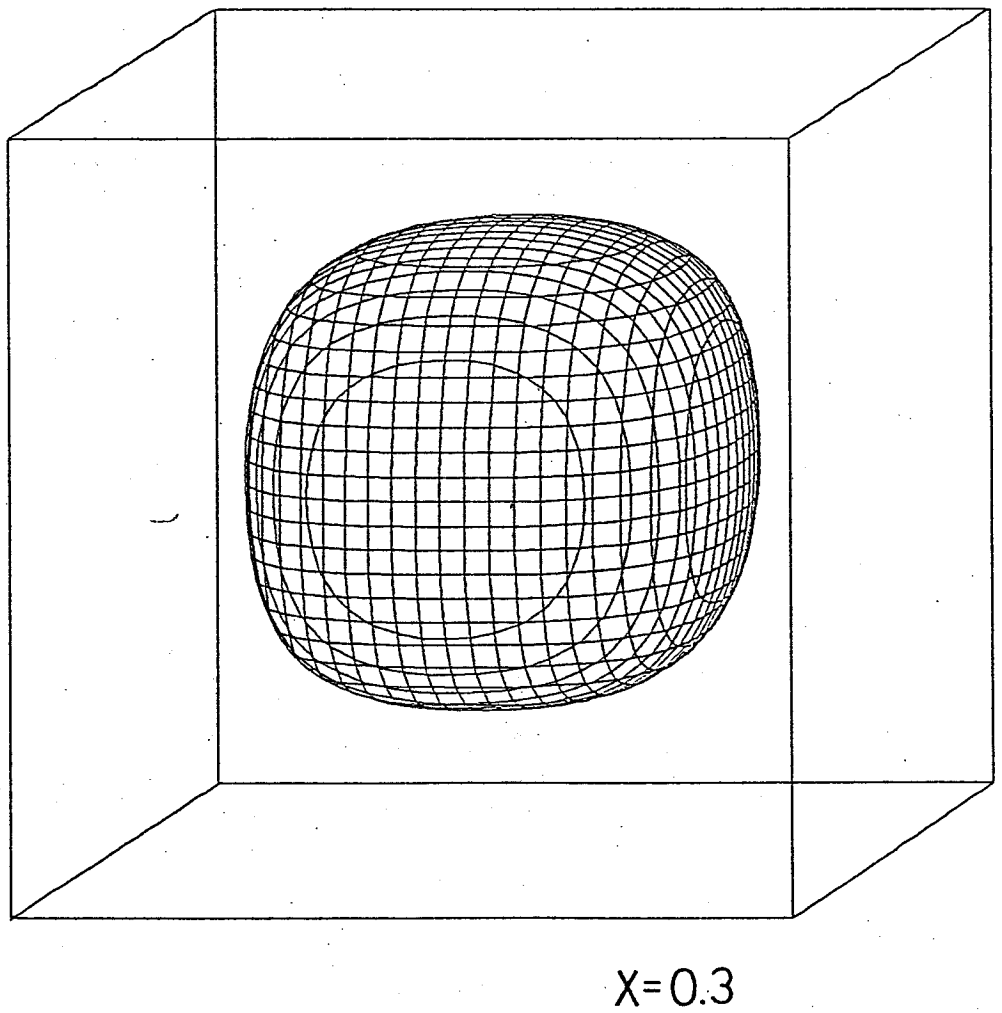

Fig.2-6.(b) Fermi surface for x=0.3.

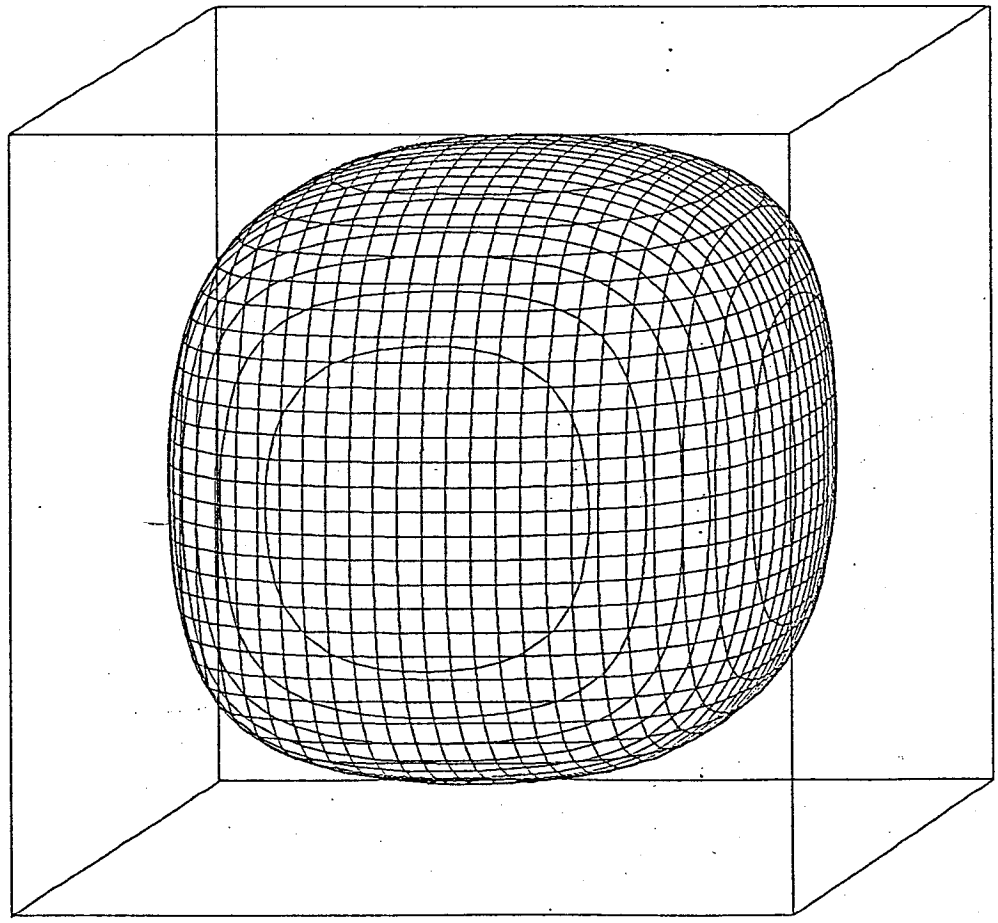

Fig.2-6.(c) Fermi surface for x=0.7.

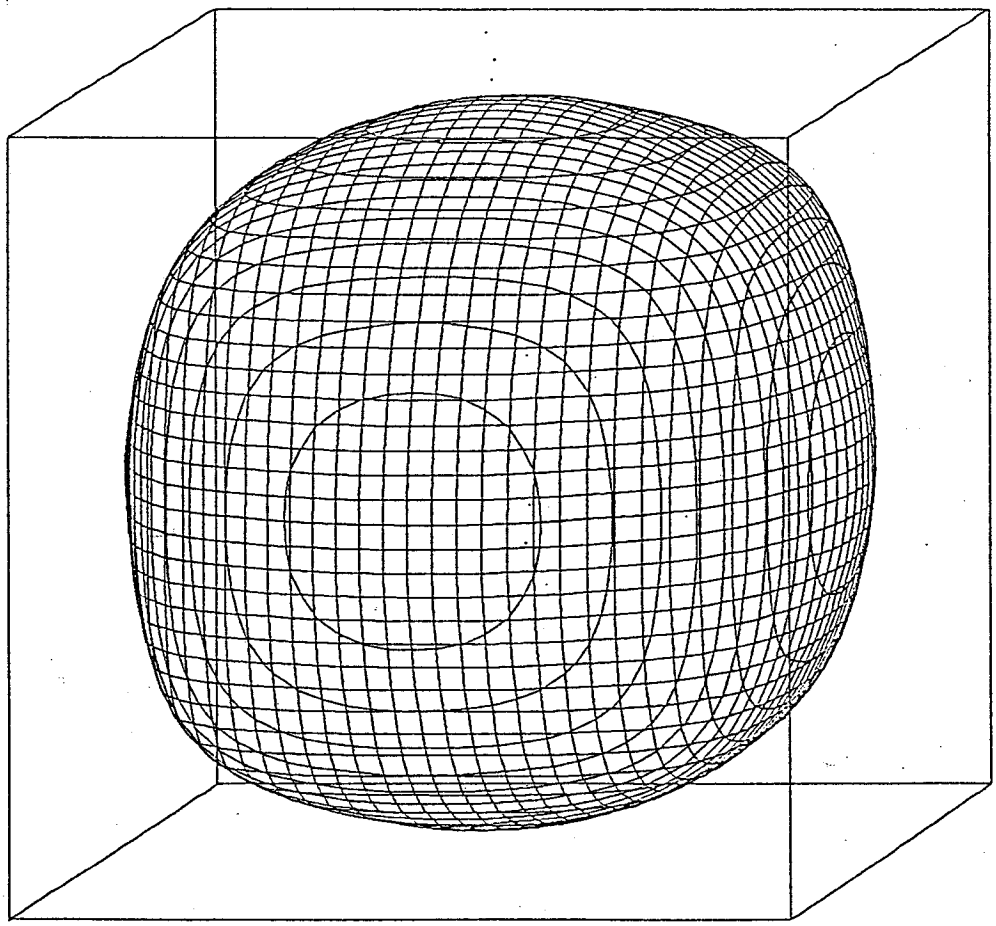

Fig.2-6.(d) Fermi surface for x=1.0 ($BaBiO_3$).

2-2. Electron-lattice coupling coefficient

In the orthogonal tight-binding (OTB) approximation the electron-lattice coupling is described in terms of derivatives of transfer integrals with respect to the atomic distance.[28] When the μ-th atom in the ℓ-th unit cell is displaced by small amount $\delta\mathbf{R}_{\ell\mu}$ from their equilibrium positions $\mathbf{R}_{\ell\mu}$, transfer integrals between orbitals of relevant atoms also change in propportion to the magnitude of atomic displacements:

$$T_{\ell\mu a,\ell'\nu b} = \int d\mathbf{r}\ \phi_a^*(\mathbf{r}-\mathbf{R}_{\ell\mu}-\delta\mathbf{R}_{\ell\mu})\ H_{e\ell}\ \phi_b(\mathbf{r}-\mathbf{R}_{\ell'\nu}-\delta\mathbf{R}_{\ell'\nu})$$

$$= T^0_{\ell\mu a,\ell'\nu b} + \sum_\alpha \nabla^\alpha T_{\ell\mu a,\ell'\nu b}\cdot(\delta R^\alpha_{\ell\mu}-\delta R^\alpha_{\ell'\nu}) \quad , \quad (2\text{-}13)$$

where $\nabla^\alpha T_{\ell\mu a,\ell'\nu b}$ is the gradient of the transfer integral in the equilibrium atomic position:

$$\nabla^\alpha T_{\ell\mu a,\ell'\nu b} = \frac{\partial}{\partial R^\alpha}\left(T_{\ell\mu a,\ell'\nu b}\right)\Big|_{R=\mathbf{R}_{\ell\mu}-\mathbf{R}_{\ell'\nu}} \quad , \quad (2\text{-}14)$$

Here the transfer integral is assumed to be a function of the difference R between the position vectors of the two atoms. In other words, the crystal field terms and the three-center integrals are neglected in the transfer integral.

Then, the transfer (Hamiltonian) matrix $\mathbf{T}(\mathbf{k},\mathbf{k}')$ may be expressed as follows within the linear approximation in atomic displacements:

$$[T(\mathbf{k},\mathbf{k}')]_{nn'} = E^{0}_{n\mathbf{k}}\,\delta_{\mathbf{k},\mathbf{k}'}\,\delta_{n,n'} + \sum_{q\mu\alpha}\sum g^{\alpha}_{\mu}(n\mathbf{k},n'\mathbf{k}')\,u^{\alpha}_{q\mu}\,\delta_{\mathbf{k}',\mathbf{k}-\mathbf{q}} \quad , \tag{2-15}$$

with

$$g^{\alpha}_{\mu}(n\mathbf{k},n'\mathbf{k}') = \sum_{\mu'a\nu'b}\sum [A^{\dagger}(\mathbf{k})]_{n,\mu'\alpha} \times [\dot{T}^{\alpha}_{\mu}(\mathbf{k},\mathbf{k}')]_{\mu'a,\nu'b}[A(\mathbf{k}')]_{\nu'b,n'} \quad , \tag{2-16}$$

where $E^{0}_{n\mathbf{k}}$ represents the unperturbed band energy of wave vector $\mathbf{k}$ and band index n, $u^{\alpha}_{\mu}(\mathbf{q})$ (α=x,y,z) denotes the Fourier transform of $\delta R^{\alpha}_{\ell\mu}$ defined by

$$u^{\alpha}_{\mu}(\mathbf{q}) = \frac{1}{\sqrt{N}}\sum_{\ell} e^{-i\mathbf{q}\cdot\mathbf{R}_{\ell}}\,\delta R^{\alpha}_{\ell\mu} \quad , \tag{2-17}$$

$[A(\mathbf{k})]_{\mu a,n}$ represent the transformation coefficients which diagonalize the unperturbed transfer matrix $T^{0}(\mathbf{k})$, and $[\dot{T}^{\alpha}_{\mu}(\mathbf{k},\mathbf{k}')]_{\mu'a,\nu'b}$ is expressed in termes of derivatives of transfer integrals as

$$[\dot{T}^{\alpha}_{\mu}(\mathbf{k},\mathbf{k}')]_{\mu'a,\nu'b} = \frac{1}{\sqrt{N}}\,[\delta_{\mu\mu'}T^{\alpha}_{\mu'a,\nu'b}(\mathbf{k}') - \delta_{\mu\nu'}T^{\alpha}_{\mu'a,\nu'b}(\mathbf{k})] \quad , \tag{2-18}$$

where $T^{\alpha}_{\mu'a,\nu'b}(\mathbf{k})$ is the Fourier transform of the gradient of the transfer integral defined by

$$T^{\alpha}_{\mu'a,\nu'b}(\mathbf{k}) = \sum_{\ell-\ell'} e^{-i\mathbf{k}\cdot(\mathbf{R}_{\ell}-\mathbf{R}_{\ell'})}\,\nabla^{\alpha}T_{\ell\mu'a,\ell'\nu'b} \quad . \tag{2-19}$$

If we express the atomic displacement $u_\mu^\alpha(\mathbf{q})$ in termes of phonon normal coordinates $Q_{\mathbf{q}\gamma}$ (γ specifying the mode of phonon), the second term of eq.(2-4) is expressed as follows:

$$\sum_{\mathbf{q}\gamma}\sum V^\gamma(nk,n'\mathbf{k}')\ Q_{\mathbf{q}\gamma}\ \delta_{\mathbf{k}',\mathbf{k}-\mathbf{q}}\ , \qquad (2\text{-}20)$$

where electron-phonon coupling coefficient $V^\gamma(nk,n'\mathbf{k}')$ is defined by

$$V^\gamma(nk,n'\mathbf{k}') = \sum_{\mu\alpha}\frac{1}{\sqrt{M_\mu}}\ \varepsilon_{\gamma,\mu\alpha}(\mathbf{k}-\mathbf{k}')\ g_\mu^\alpha(nk,n'\mathbf{k}')\ . \qquad (2\text{-}21)$$

Here $\varepsilon_{\gamma,\mu\alpha}(\mathbf{q})$ denotes the phonon polarization vector and M_μ is the mass of the μ-th atom.

The typical wave-vector dependences of $V^\gamma(\mathbf{k},\mathbf{k}-\mathbf{q})$ have been calculated and the reslts are shown in Fig.2-7 for $\mathbf{q}=(\pi/a)\times(1,1,1)$, the R-point in the Brillouin zone (BZ). Here only intra-band coupling of the conduction band has been indicated and the derivatives of transfer integrals have been taken as follows:

$$t'(sp\sigma) = -3.05\ \text{eV/A}\ (\equiv -t'),$$

$$t'(pp\sigma) = -3.15\ \text{eV/A},$$

$$t'(pp\pi) = 2.85\ \text{eV/A}.$$

An estimation of the derivatives will be given in detail in the next section. Normal modes of phonons at the R-point are listed in Table 2-3 and some of the normal modes are illustrated in Fig.2-8(a)~(f). Since the conduction band states consist of the O 2p and (Pb,Bi) 6s and 6p orbitals, the vibrations of the (Ba,K) atoms, which correspond to $R_{25}'(T_{2g})$ modes, cannot affect the

conduction band. And the displacements of O atoms along the directions which are tangential to nearest neighbouring (Pb,Bi)-O bonds have also no contribution to the electron-lattice interaction as long as we take into account only the first order coupling coefficients with respect to the displacements. Hence the coupling coefficients for the $R_{15}'(T_{1g})$ mode, which is the rotational mode of (Pb,Bi)-O_6 octahedron, and $R_{25}'(T_{2g})$ mode become zero definitely in the present case.

It is found from Fig.2-7 that R_1 (A_{1g}) mode, i.e. the so-called breathing mode, takes larger value than the other modes for wide region in the BZ. The strethcing-type deformation of (Pb,Bi)-O_6 octahedra corresponds to R_{12} (E_g) mode which turns out to have secondly strong electron-lattice coupling. The coupling coefficients for the vibration of (Pb,Bi) atoms, i.e. R_{15} (T_{1u}) mode, are almost an order of magnitude smaller than those for the R_1 and/or R_{12} modes, because the mass of (Pb,Bi) is greater about 13 times than that of O atoms (see eq.(2-21)). It is noted that the remarkable wave-vector and mode dependences of the coupling coefficient $V^{\gamma}(\mathbf{k},\mathbf{k}-\mathbf{q})$ may play an important role on the lattice dynamics and the superconductivity in BPB and BKB.

$R = R_1 + R_{12} + R_{15} + R_{15}' + R_{25}'$	
R_1 (A_{1g}) :	$[u^x_{O(1)} + u^y_{O(2)} + u^z_{O(3)}]/\sqrt{3}$
R_{12} (E_g) :	$[u^x_{O(1)} + u^y_{O(2)} - 2\cdot u^z_{O(3)}]/\sqrt{6}$
	$[u^x_{O(1)} - u^y_{O(2)}]/\sqrt{2}$
R_{15} (T_{1u}) :	$u^x_{(Pb,Bi)}$
	$u^y_{(Pb,Bi)}$
	$u^z_{(Pb,Bi)}$
$R_{15}'(T_{1g})$:	$[u^y_{O(1)} - u^x_{O(2)}]/\sqrt{2}$
	$[u^z_{O(2)} - u^y_{O(3)}]/\sqrt{2}$
	$[u^x_{O(3)} - u^x_{O(1)}]/\sqrt{2}$
$R_{25}'(T_{2g})$:	$c_1[u^y_{O(1)} + u^x_{O(2)}] + c_2\cdot u^z_{Ba}$
	$c_1[u^z_{O(2)} + u^y_{O(3)}] + c_2\cdot u^x_{Ba}$
	$c_1[u^x_{O(3)} + u^z_{O(1)}] + c_2\cdot u^y_{Ba}$

Table 2-3. Phonon normal modes of the cubic perovskite type structure at the R-point.

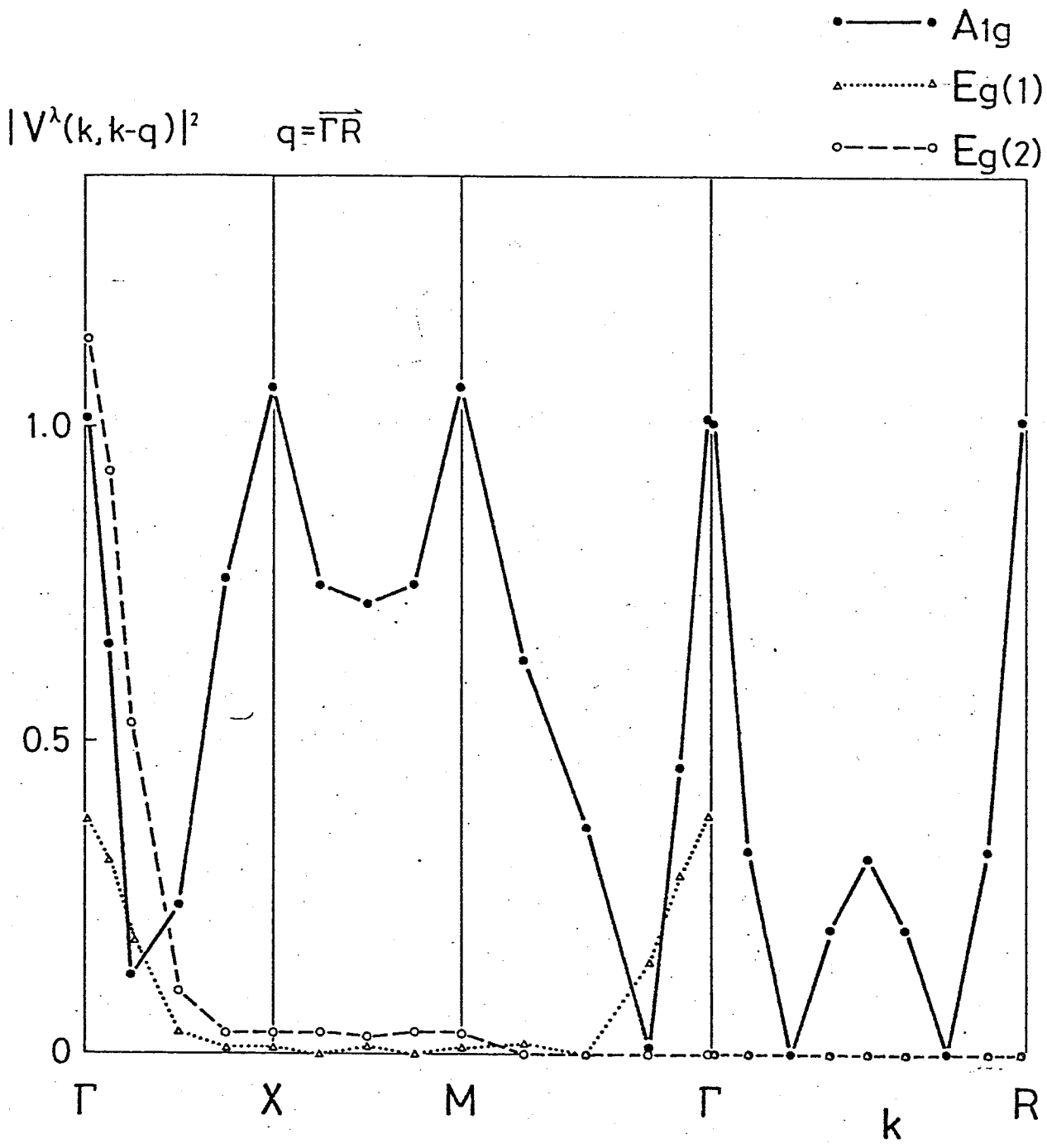

Fig.2-7. Typical wave-vector **k** and mode γ dependences of the electron-lattice coupling coefficient $V^{\gamma}(\mathbf{k},\mathbf{k}-\mathbf{q})$ calculated for **q** of the R point.

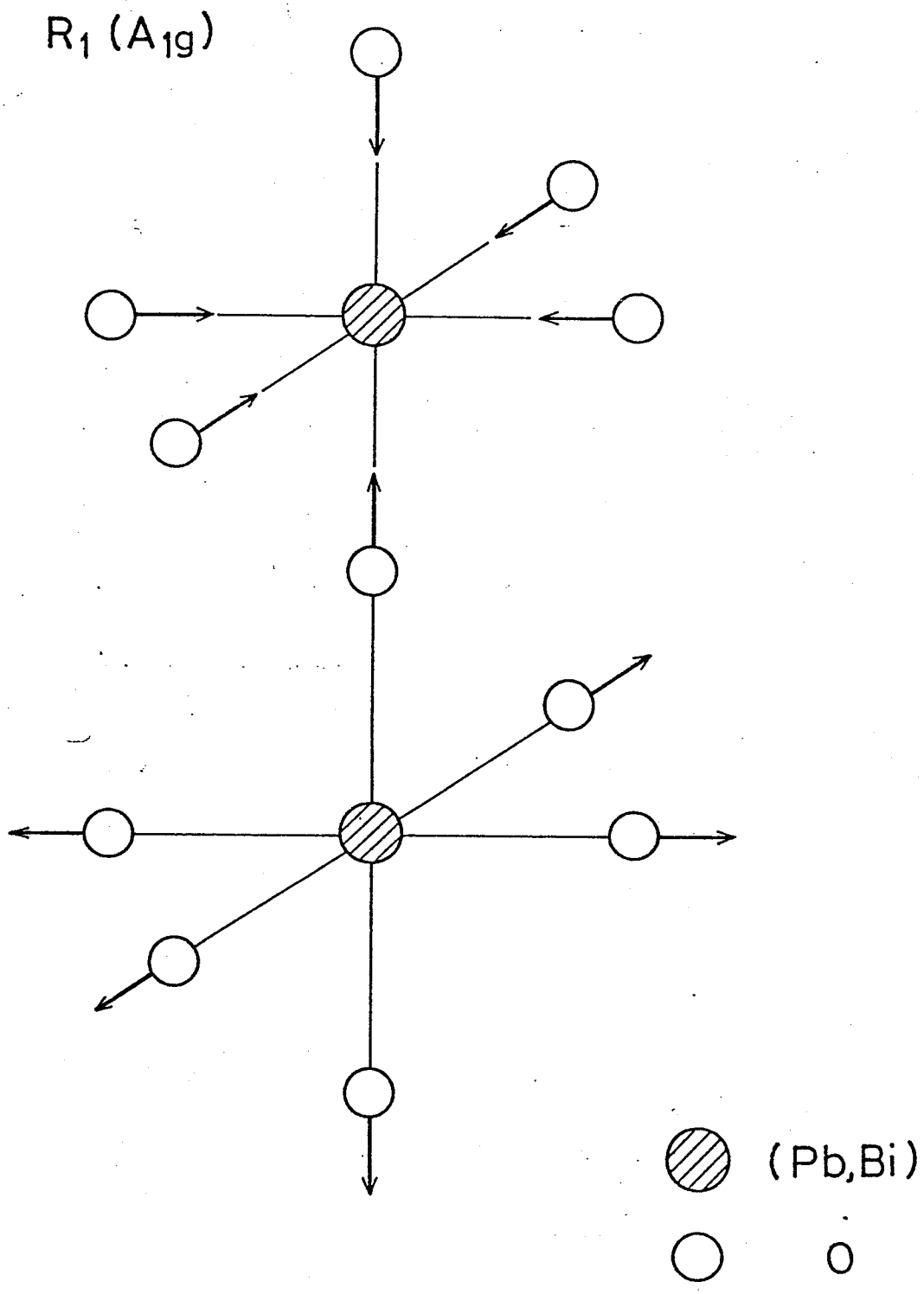

Fig.2-8.(a) Displacements illustrated for $R_1(A_{1g})$ normal mode. This is the so-called breathing mode.

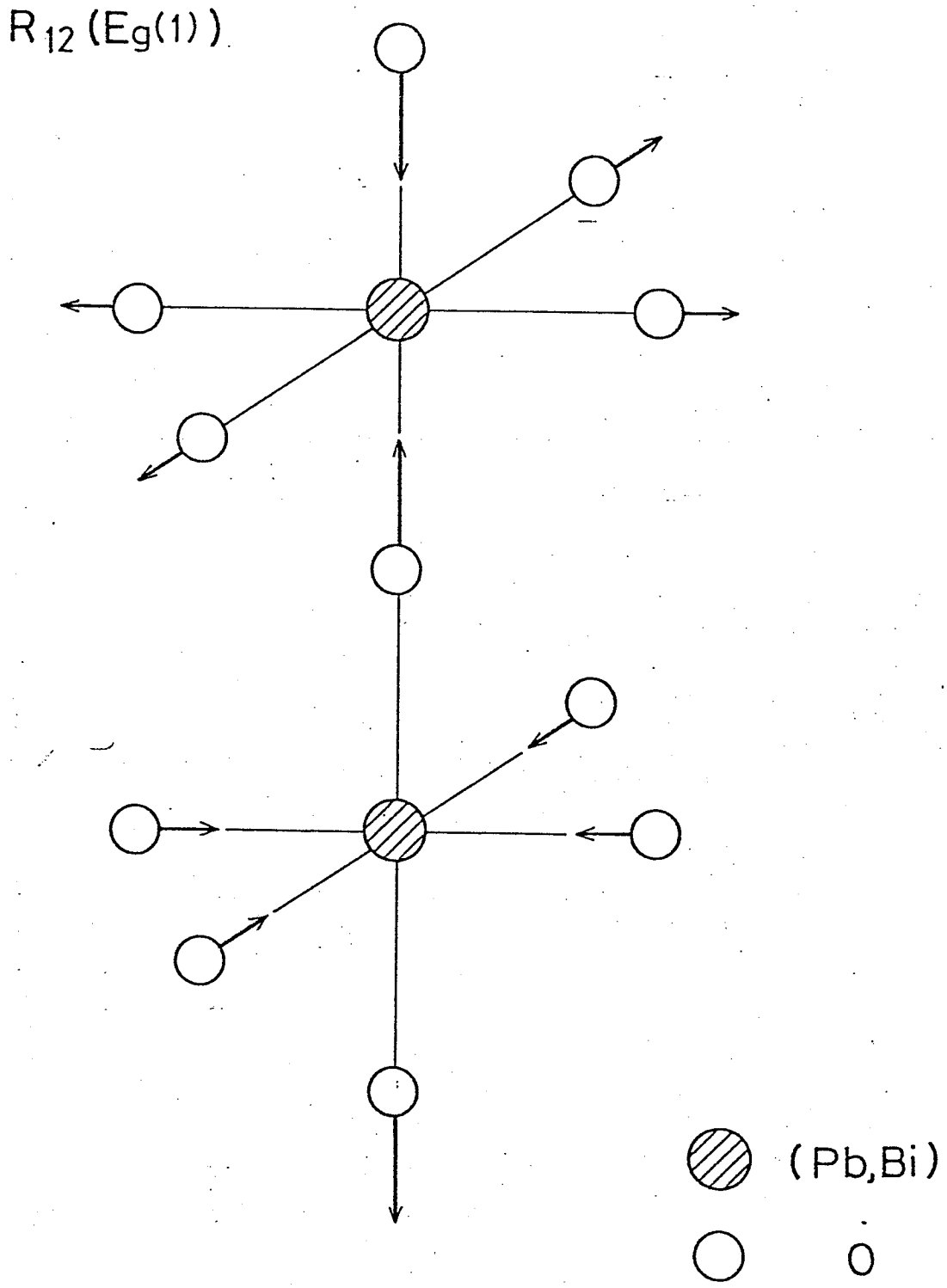

Fig.2-8.(b) Displacements illustrated for $R_{12}(E_g(1))$ normal mode.

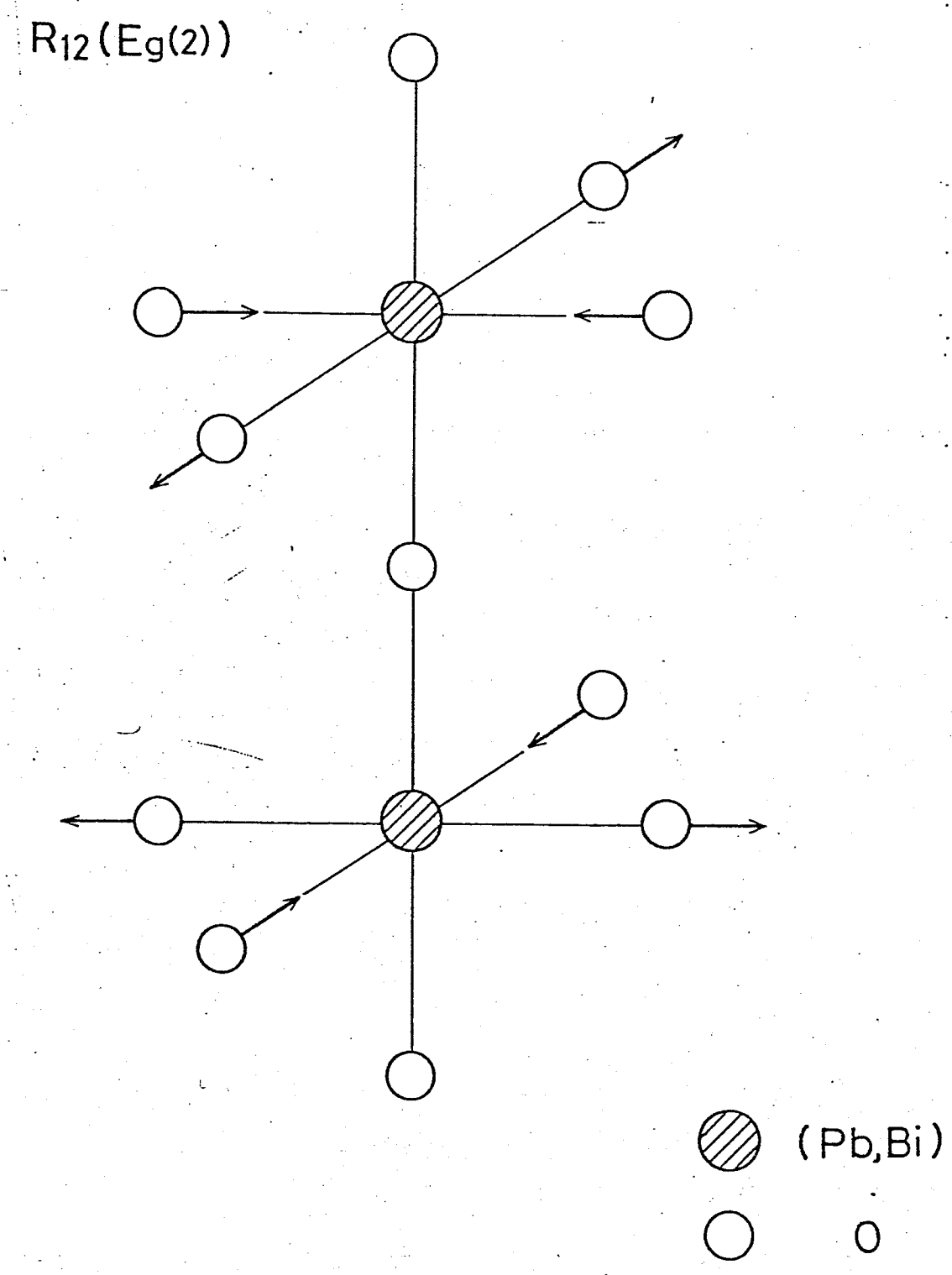

Fig.2-8.(c) Displacements illustrated for $R_{12}(E_g(2))$ normal mode.

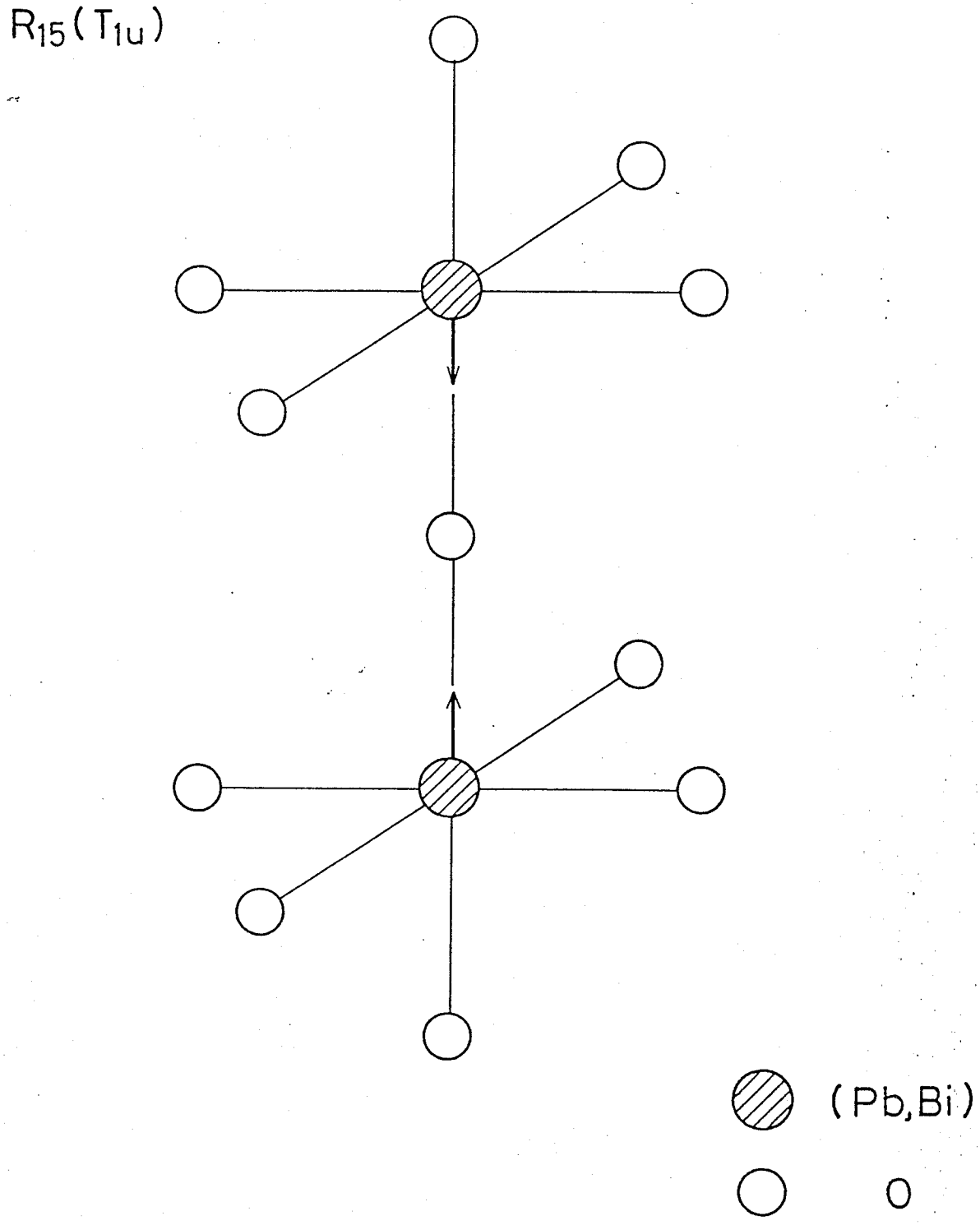

Fig.2-8.(d) Displacements illustrated for $R_{15}(T_{1u})$ normal mode. This is an antiferroelectric mode.

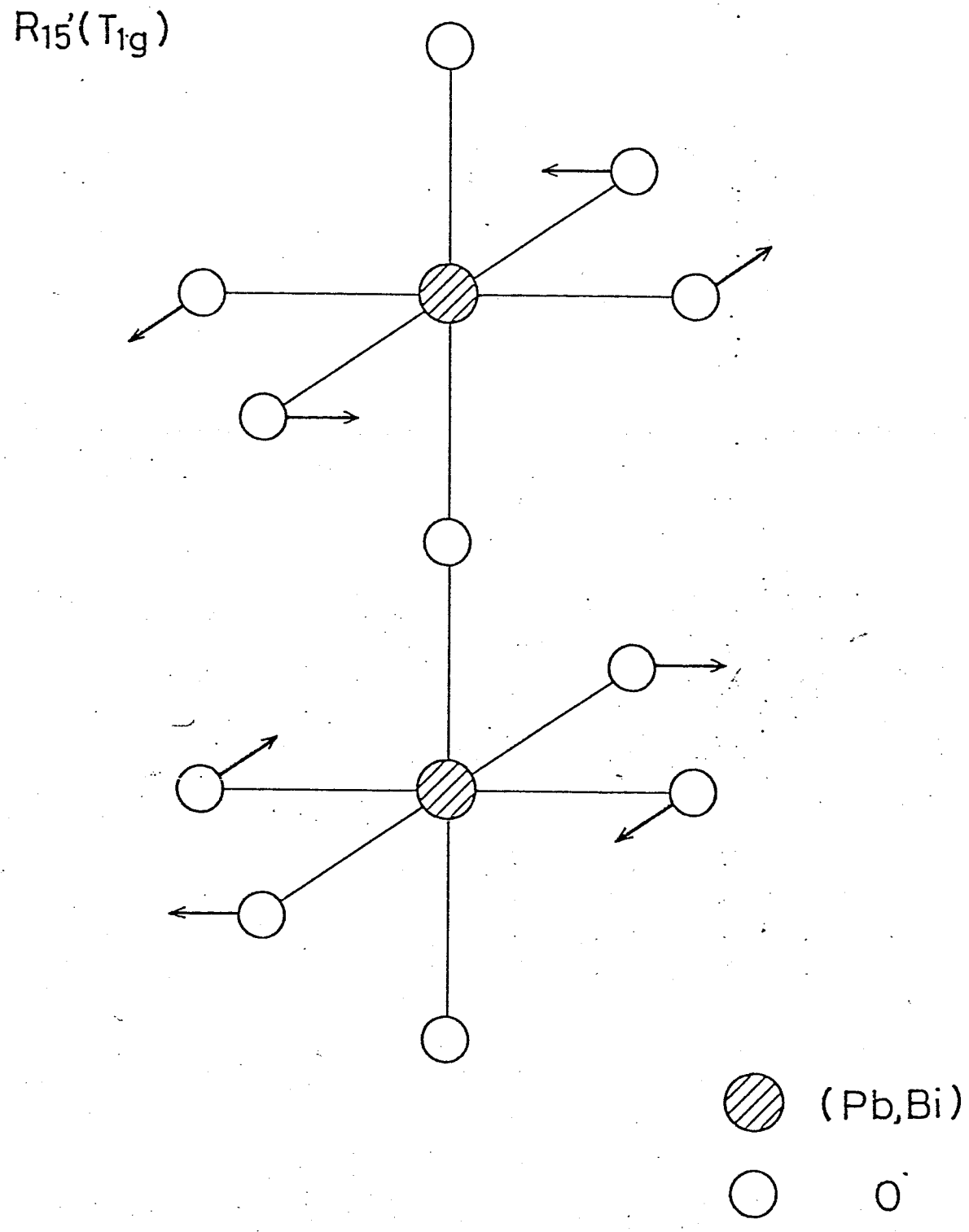

Fig.2-8.(e) Displacements illustrated for $R_{15}'(T_{1g})$ normal mode. This mode consists of the rotation of the (Pb,Bi)-O_6 octahedra.

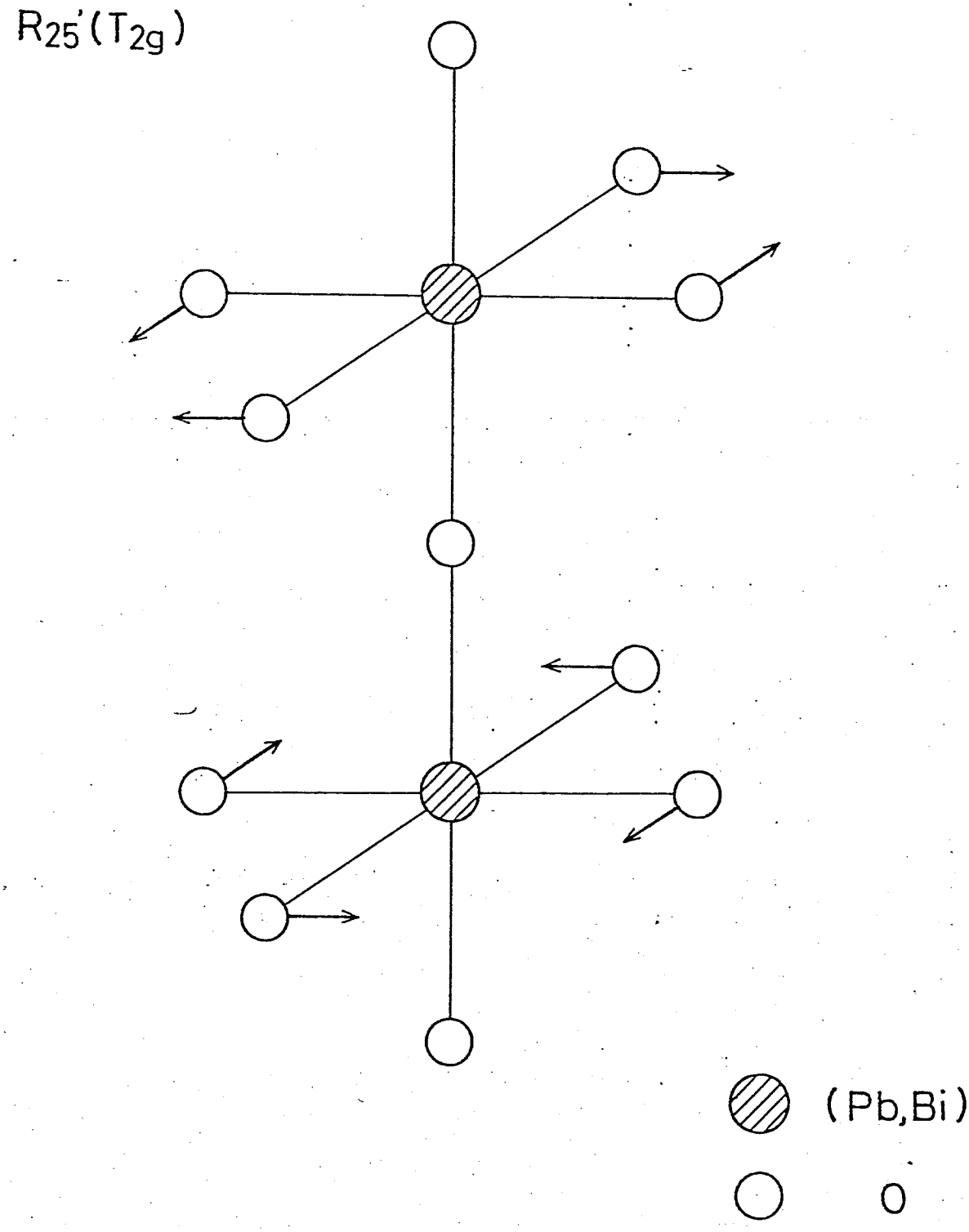

Fig.2-8.(f) Displacements illustrated for $R_{25}'(T_{2g})$ normal mode.

2-3. Estimation of derivatives of transfer integrals

In order to evaluate the strength of the electron-lattice coupling it is necessary to determine the value of derivatives of transfer integrals $t'(sp\sigma)$, $t'(pp\sigma)$ and $t'(pp\pi)$. These derivatives may be evaluated by a fit to the electronic band calculated self-consistently for distorted crystal structures which correspond to particular phonon symmetry modes. For BPB Mattheiss and Hamann[23] have carried out LAPW band calculation for some distorted crystal structures, suhc as a tetragonal phase for $BaPb_{0.7}Bi_{0.3}O_3$ and a monoclinic phase for $BaBiO_3$. For example, the monoclinic structure of $BaBiO_3$ is described as the frozen phonons which consist of a rigid-rotational mode of $(Pb,Bi)O_6$ octahedra about [110] axes as well as the so-called breathing mode at R point in the Brillouin zone. On the basis of the structure observed by the neutron diffraction measurement,[20] Mattheiss and Hamann[23] have obtained the electronic band structure of the monoclinic phase. However, it is pointed out that their results cannot reproduce the CDW energy gap observed by some experiments, such as electric resistivity measurement,[2] infra-red absorption spectroscopy,[29] and so on. We have estimated the derivatives of transfer integrals so as to reproduce overall features of the band structure obtained by Mattheiss and Hamann.

In the OTB approximation the electronic band structure for the distorted structure can be calculated in the following way.

When atomic displacements $\langle \delta R_{\ell\mu} \rangle$ which are modulated by a wave-vector Q:

$$\langle \delta R^{\alpha}_{\ell\mu} \rangle = \frac{1}{\sqrt{N}} \langle u^{\alpha}_{\mu}(Q) \rangle \, e^{iQ \cdot R_{\ell}} \quad , \tag{2-22}$$

are frozen, then the electronic states of wave-vector k couple with those of k-Q, and the k-Q states couple with the k-2Q states, and so on. When Q=G/2 (G represents a reciprocal lattice vector), which is just the present case, the series of coupling with the higher harmonics are decoupled so that the k states couple with only to the k-Q states exactly. Then, according to the results in Sec.2-2 the electronic band structure in distorted structure can be obtained by diagonalizing the following transfer matrix:

$$\underset{\sim}{T^{D}(k)} = \begin{pmatrix} T^{0}(k) & , & T'(k,k-Q) \\ T'(k-Q,k) & , & T^{0}(k-Q) \end{pmatrix} \quad , \tag{2-23}$$

where $T^{0}(k)$ is the transfer matrix of the undistorted phase which has the diagonal form as

$$[T^{0}(k)]_{n,n'} = E^{0}_{nk} \, \delta_{nn'} \quad , \tag{2-24}$$

and $T'(k,k-Q)$ is expressed as

$$[T'(k,k-Q)]_{n,n'} = \sum_{\mu\alpha} g^{\alpha}_{\mu}(nk,n'k-Q) \, \langle u^{\alpha}_{\mu}(Q) \rangle \quad . \tag{2-25}$$

Then, the energy eigenvalues are determined from the secular

determinant:

$$\det\left| \mathbf{T}^{D}(\mathbf{k}) - E^{D}_{n\mathbf{k}}\, 1 \right| = 0 \quad , \tag{2-26}$$

where 1 represents the unit matrix.

For $BaBiO_3$ the observed atomic displacement of O atoms from the equilibrium position of the undistorted structure is about 0.08 A [20] which corresponds to a few percents of the lattice constant. By using this value for the displacement $\langle \delta R \rangle$, the electronic band has been calculated. In order to reproduce the dispersion curves of the LAPW calculation, the derivatives of the transfer integrals should be taken as follows:

$$t'(sp\sigma) = -3.05 \text{ eV/A},$$

$$t'(pp\sigma) = -3.15 \text{ eV/A},$$

$$t'(pp\pi) = 2.85 \text{ eV/A}.$$

The calculated dispersion curves of the conduction bands for the distorted phase are shown in Fig.2-9 with those for the undistorted structure, which are folded into the half-size B.Z. of the distorted phase (see Fig.2-10). Most apparent change in the conduction band dispersion is found along the W-L line in the B.Z. The width of the splitting of the conduction band in the W-L line is about 1 eV in the case of t'=3.05 eV/A (where t' stands for the magnitude of the derivatives of the transfer integrals and is defined by $t' \equiv |t'(sp\sigma)|$). However, it is found in this case that the splitted bands have an indirect overlap of about 0.4 eV to each other.

In order to yield the complete energy gap in the conduction

band it is necessary that the derivatives of the transfer integrals are increased one and a half times larger than that of the previous value. As an example, the conduction band dispersion for t'=4.575 eV/A are shown in Fig.2-11. It is found that the indirect energy gap between an electron pocket at the L point and a hole pocket at the W point is about 0.05 eV. Sleight et al.[2] have found that $BaBiO_3$ shows semiconducting behavior with an activation energy of about 0.2 eV. On the other hand, Kahn et al.[29] reported that the optical absorption edge for $BaBiO_3$ was about 0.1 eV. The reason for this discrepancy is still unclear. However, it is common sence that $BaBiO_3$ is a semiconductor with a narrow energy gap. Thus, it is concluded that t' may be about 4.5 eV/A for $BaBiO_3$. However, it is noted that the estimation of t' is still somewhat uncertain, because the observed value of atomic displacements, $\langle\delta R\rangle$=0.08 A, is not always reliable. If $\langle\delta R\rangle$ includes the error of about 10 percent, then the estimated t' has also an uncertainty of 10 percent. Therefore, it can be only said that t' takes the value between 4 and 5 eV/A for $BaBiO_3$.

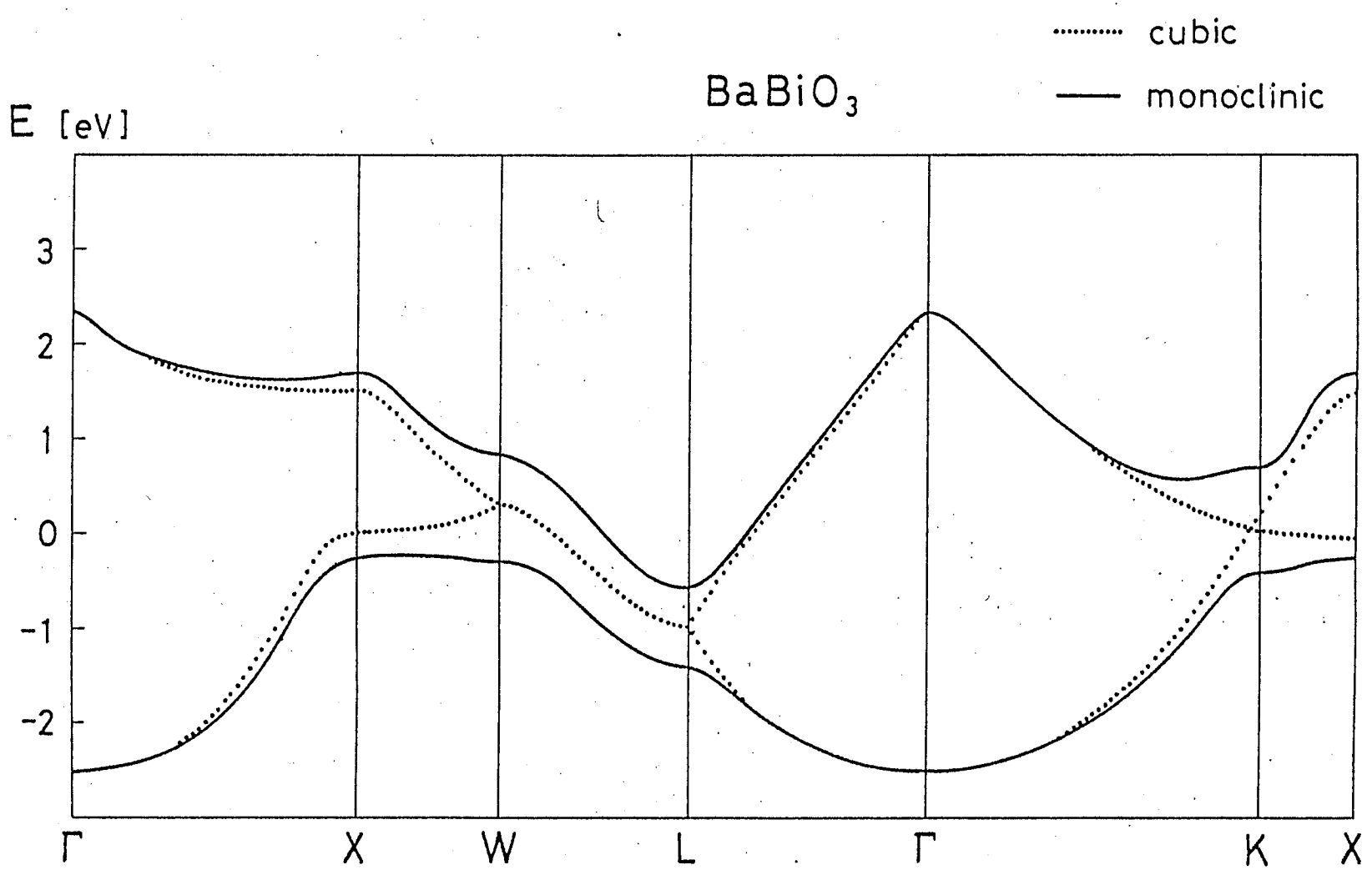

Fig.2-9. Dispersion curves of the electronic band calculated for the distorted (monoclinic) phase of $BaBiO_3$ with t'=3.05 eV/A. These for the undistorted (cubic) phase is also shown by dotted curves.

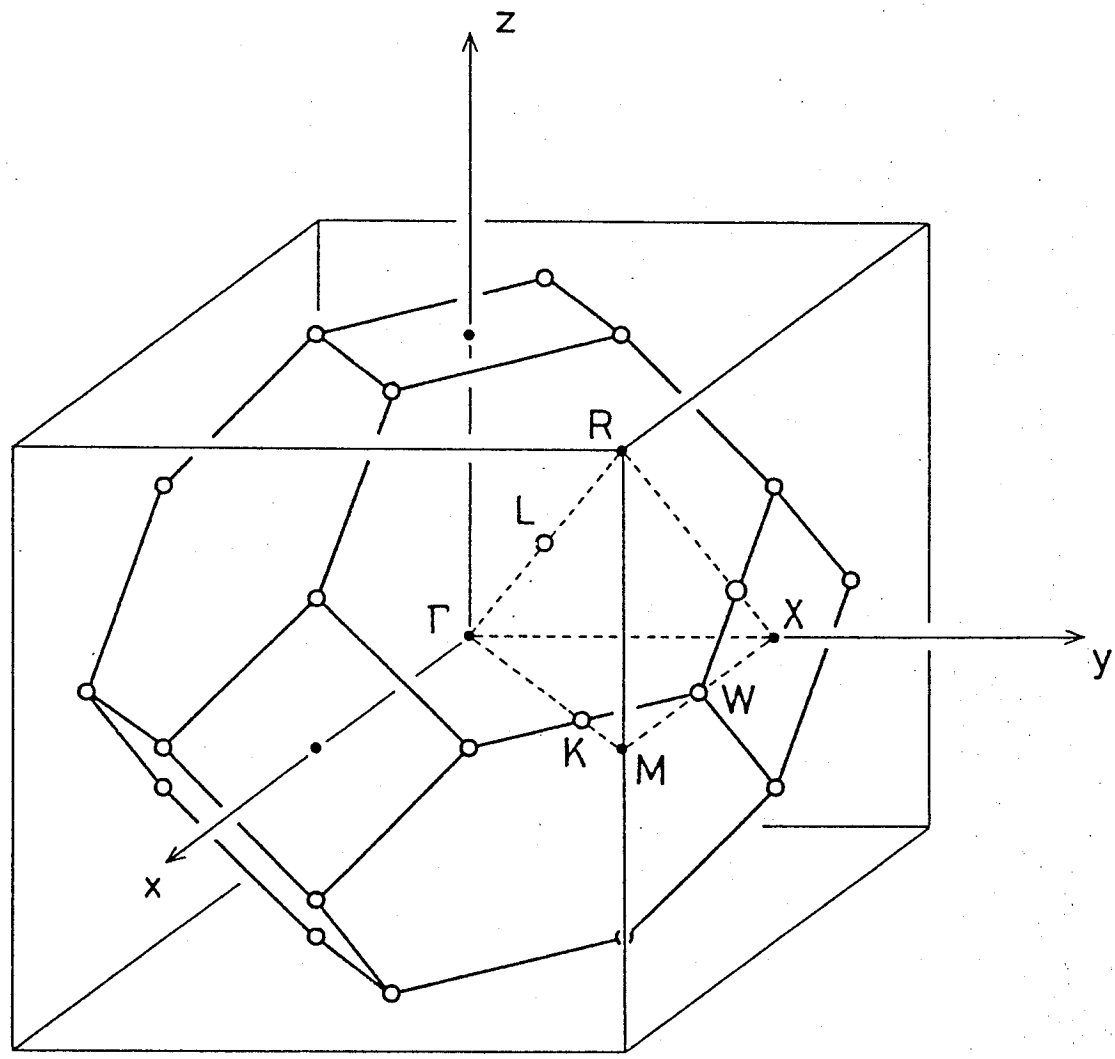

Fig.2-10. Brillouin zone for the distorted phase of $BaBiO_3$. That for the original cubic phase is also indicated.

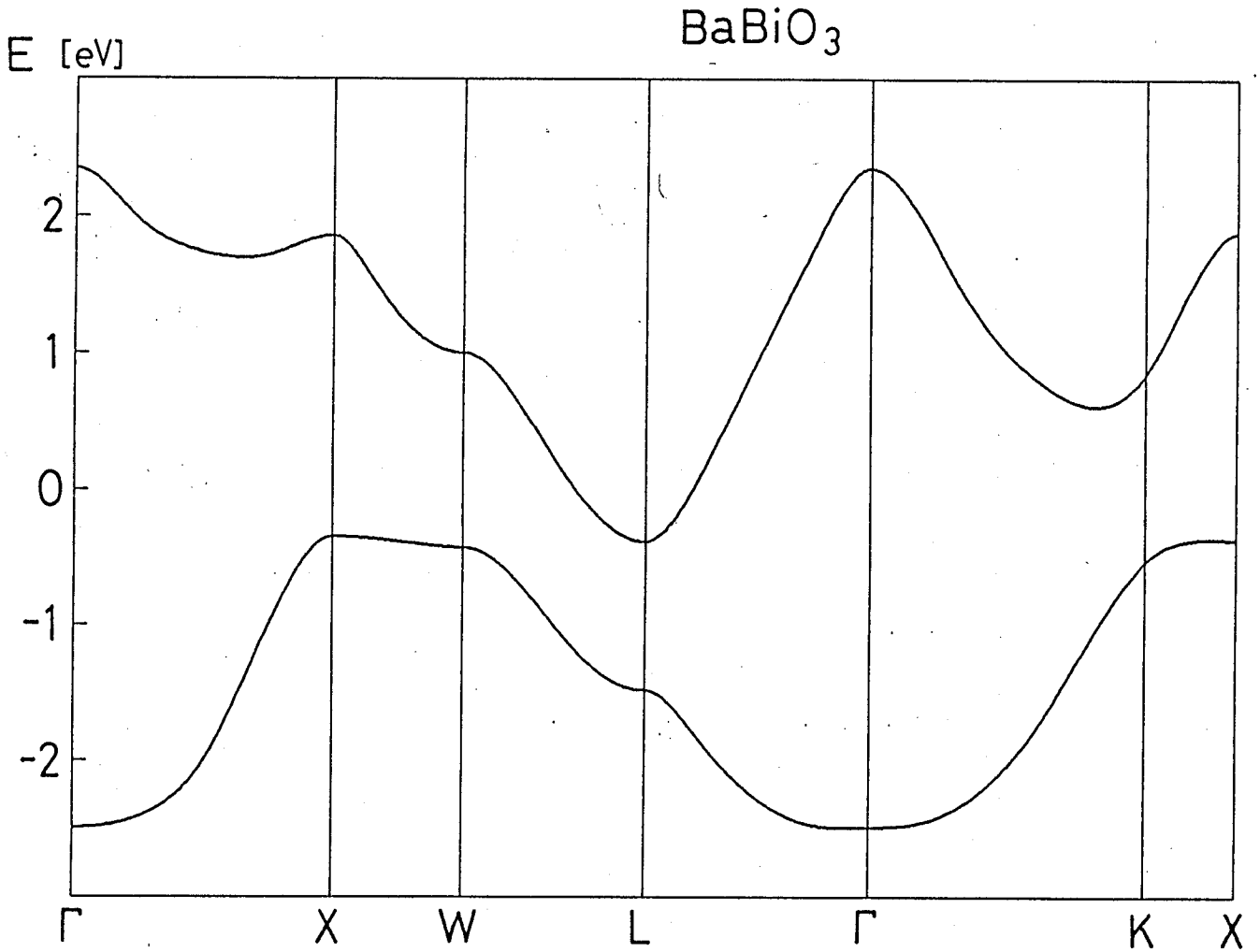

Fig.2-11. Dispersion curves of the electronic band calculated for the distorted (monoclinic) phase of $BaBiO_3$ with t'=4.575 eV/A.

§3. Lattice Dynamics

3-1. Short-range force constant model

In this section we investigate lattice dynamics of BPB, which gives an important information to understanding the role of the electron-lattice interaction in this system. We first summarize the formalism to investigate lattice dynamics. The displacement of an atom at the μ-th site in the ℓ-th unit cell from its equilibrium position $R_{\ell\mu}$ is denoted by $\delta R_{\ell\mu}$ hereafter. In the framework of the adiabatic (Born-Oppenheimer) approximation, the change in the potential energy caused by the atomic displacements $V(\{\delta R_{\ell\mu}\})$ can be expanded in a Taylor series of the displacements. The potential energy is assumed to be expressed within the harmonic approximation as follows:

$$V(\{\delta R_{\ell\mu}\}) = \frac{1}{2} \sum_{\ell\ell'\mu\nu} \sum_{\alpha\beta} F^{\alpha\beta}_{\ell\mu,\ell'\nu} \, \delta R^{\alpha}_{\ell\mu} \, \delta R^{\beta}_{\ell'\nu} \quad , \qquad (3\text{-}1)$$

where the second-order derivatives of the potential $F^{\alpha\beta}_{\ell\mu,\ell'\nu}$ is the interatomic force constant tensor between the ℓμ and ℓ'ν atoms. Clearly, $F^{\alpha\beta}_{\ell\mu,\ell'\nu}$ satisfies a condition

$$F^{\alpha\beta}_{\ell\mu,\ell'\nu} = F^{\beta\alpha}_{\ell'\nu,\ell\mu} \quad , \qquad (3\text{-}2)$$

and has a translational symmetry about the unit cell

$$F^{\alpha\beta}_{\ell\mu,\ell'\nu} = F^{\alpha\beta}_{\ell-\ell'\mu,0\nu} \quad . \qquad (3\text{-}3)$$

The Hamiltonian of the atomic vibrations is expressed in the following form:

$$H = \sum_{\ell\mu\alpha} \frac{1}{2M_\mu} (p^\alpha_{\ell\mu})^2 + \sum_{\ell\ell'\mu\nu} \sum_{\alpha\beta} F^{\alpha\beta}_{\ell\mu,\ell'\nu} \, \delta R^\alpha_{\ell\mu} \, \delta R^\beta_{\ell'\nu} \quad . \qquad (3\text{-}4)$$

The equation of motion for $\delta R^\alpha_{\ell\mu}$ is given by

$$M_\mu \, \ddot{\delta R}^\alpha_{\ell\mu} = - \sum_{\ell'\nu\beta} F^{\alpha\beta}_{\ell\mu,\ell'\nu} \, \delta R^\beta_{\ell'\nu} \quad , \qquad (3\text{-}5)$$

with use of the relation (3-2). If we assume the time dependence of $\delta R^\alpha_{\ell\mu}$ as $\exp(-i\omega t)$, then the eqation of motion becomes

$$M_\mu \omega^2 \, \delta R^\alpha_{\ell\mu} = - \sum_{\ell'\nu\beta} F^{\alpha\beta}_{\ell\mu,\ell'\nu} \, \delta R^\beta_{\ell'\nu} \quad . \qquad (3\text{-}6)$$

We introduce the Fourier transform of $\delta R^\alpha_{\ell\mu}$:

$$u^\alpha_{\mathbf{q}\mu} = \frac{1}{\sqrt{N}} \sum_{\ell} e^{-i\mathbf{q}\cdot\mathbf{R}_\ell} \, \delta R^\alpha_{\ell\mu} \quad , \qquad (3\text{-}7)$$

and rewrite eq.(3-6) as

$$M_\mu \omega^2 \, u^\alpha_{\mathbf{q}\mu} = \sum_{\nu\beta} D^{\alpha\beta}_{\mu\nu}(\mathbf{q}) \, u^\beta_{\mathbf{q}\nu} \quad , \qquad (3\text{-}7)$$

where

$$D^{\alpha\beta}_{\mu\nu}(\mathbf{q}) = \sum_{\ell-\ell'} F^{\alpha\beta}_{\ell\mu,\ell'\nu} \, e^{i\mathbf{q}\cdot(\mathbf{R}_\ell - \mathbf{R}_{\ell'})} \quad , \qquad (3\text{-}8)$$

which is the matrix element of the so-called dynamical matrix

D(q). Thus, the phonon freuency $\omega_{q\gamma}$ can be obtained by solving the secular determinant:

$$\det| \; D(q) - M \omega_{q\gamma}{}^2 | = 0 \quad , \tag{3-9}$$

or

$$\det| \; M^{-1/2} \; D(q) \; M^{-1/2} - \omega_{q\gamma}{}^2 | = 0 \quad , \tag{3-10}$$

where M is the diagonal matrix defined by

$$M_{\mu\nu}^{\alpha\beta} = M_{\mu} \; \delta_{\mu\nu} \; \delta_{\alpha\beta} \quad , \tag{3-11}$$

and here M_{μ} denotes the mass of the μ-th atom. It is noted that the eigen-vector of the matrix $M^{-1/2}D(q)M^{-1/2}$ corresponds to the polarization vector $\varepsilon_{\gamma,\mu\alpha}(q)$.

Usually, D(q) can be divided into two parts, χ(q) and $D^0(q)$. Here, χ(q) represents the generalized electronic susceptibility arising from the electron-lattice interaction and $D^0(q)$ denotes contributions other than χ(q). Matrix elements of $D^0(q)$ can be written in the form of the Fourier transform of short range forces. Matrix elements of χ(q) are given by

$$\chi_{\mu\nu}^{\alpha\beta}(q) = - 2 \sum_{k} g_{\mu}^{\alpha}(k,k-q) g_{\nu}^{\beta}(k,k-q)^* \; \frac{f(E_{k-q}^0) - f(E_k^0)}{E_k^0 - E_{k-q}^0} \quad , \tag{3-12}$$

where $g_{\mu}^{\alpha}(k,k-q)$ is the electron-lattice coupling coefficient which represents the strength of the coupling between the two

electronic states $\mathbf{k}$ and $\mathbf{k}-\mathbf{q}$ caused by displacement $u^{\alpha}_{\mathbf{q}\mu}$, $E^{0}_{\mathbf{k}}$ denotes the bare electronic energy and $f(E^{0}_{\mathbf{k}})$ is the Fermi distribution function. The Fourier transform of $\chi^{\alpha\beta}_{\mu\nu}(\mathbf{q})$ corresponds to the effective interatomic force:

$$F^{\alpha\beta}_{\ell\mu,\ell'\nu} = \frac{1}{N} \sum_{\mathbf{q}} \chi^{\alpha\beta}_{\mu\nu}(\mathbf{q}) \; e^{-i\mathbf{q}\cdot(R_{\ell} - R_{\ell'})} \quad , \tag{3-12}$$

which may be of long range.

First we have calculated phonon frequencies $\omega^{0}_{\mathbf{q}\gamma}$ with neglect of $\chi(\mathbf{q})$. The phonon dispersion curves calculated along the [100], [110] and [111] directions are shown in Fig.3-1(a) and the phonon density of states is shown in Fig.3-1(b). In obtaining these dispersion curves we have assumed stretching force for six kinds of nearest neighbouring (n.n.) atomic pair and tangential force for one kind of n.n. atomic pair. The seven force constants in total have been determined so as to reproduce seven phonon frequencies observed by inelastic scattering measurements[30] (closed circles in Fig.3-1(a)). The short range force constants thus determined are shown in Table 3-1 (in unit of eV/A^2).

By analyzing the phonon polarization vectors we have found that the frequencies of O-stretching vibration toward Pb or Bi atom lie near 60 meV and those of O-bending modes around 25 meV. The frequencies of phonon modes arising mainly from Ba atoms lie near 15 meV. Vibrations of Pb or Bi atoms are mainly included in acoustical branches near the Brillouin zone boundary. It also can be clearly seen in Fig.3-1(b) which gives the partial phonon

density of states $F_\mu(\omega)$ defined by:

$$F_\mu(\omega) = \frac{1}{N} \sum_{q\gamma\alpha} \sum \sum |\varepsilon_{\gamma,\mu\alpha}(q)|^2 \, \delta(\omega - \omega^0_{q\gamma}) \quad . \tag{3-14}$$

	stretching	bending
(Pb,Bi)-O	4.678	——
O-O	1.104	-0.055
(Ba,K)-O	0.309	——
(Ba,K)-(Pb,Bi)	1.426	——
(Ba,K)-(Ba,K)	0.129	——
(Pb,Bi)-(Pb,Bi)	0.968	——

Table 3-1. Short range force constants determined from the neutron scattering measurement in unit of eV/A^2.

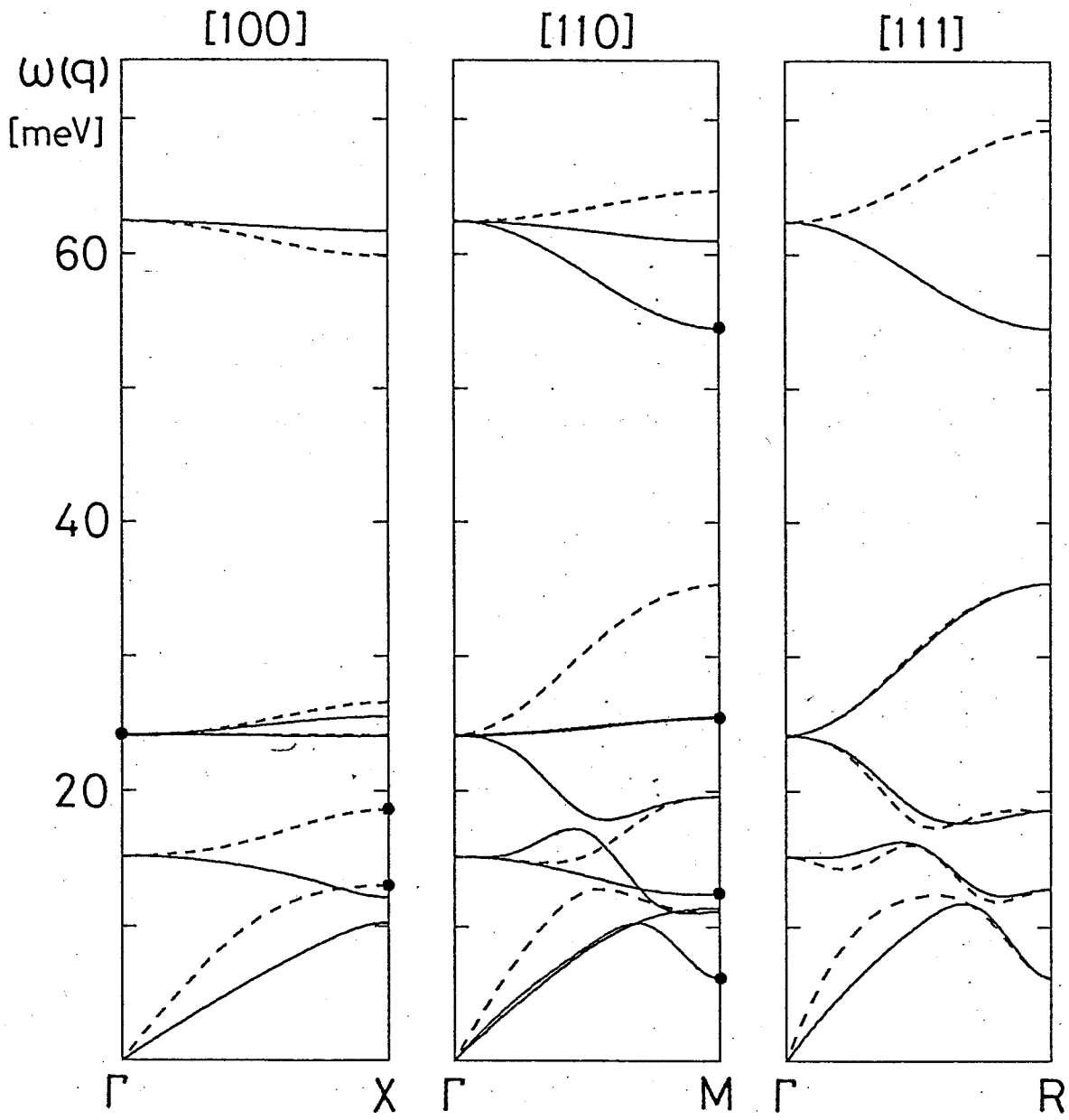

Fig.3-1.(a) Phonon dispersion curves calculated with only short range forces. The full curves denote the transverse mode and the broken curves the longitudinal mode. The closed circles represent the experimental data utilized in determining short-range force constants.

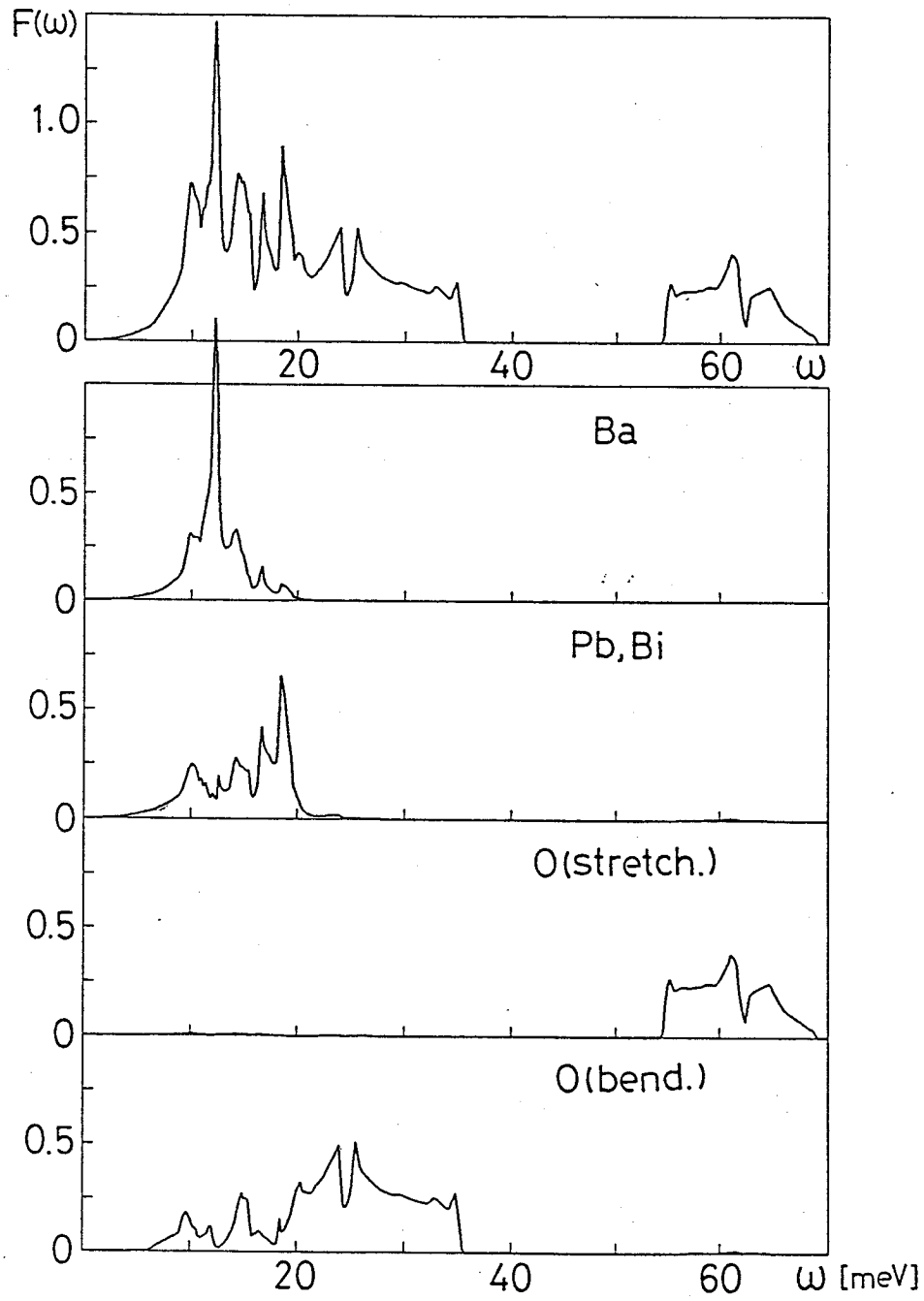

Fig.3-1.(b) Calulated phonon density of states (DOS) F(ω) corresponding to the case in Fig.3-1.(a). Four kinds of partial phonon DOS's are also shown. Unit of F(ω) and the partial one is $(\text{meV}\cdot\text{unit cell})^{-1}$.

3-2. Generalized electronic susceptibility and phonon energy renormalization

We have calculated the phonon dispersion curves by including the generalized electronic susceptibility $\chi(\mathbf{q})$ into the dynamical matrix $D(\mathbf{q})$. The dispersion curves and the density of states $F(\omega)$ calculated for $x=0.3$ are shown in Fig.3-2(a) and (b), respectively. In calculating $\chi(\mathbf{q})$ we have used $g_{\mu}^{\alpha}(\mathbf{k},\mathbf{k}')$ evaluated in Sec.2-2. by using $t'=4.05$ eV/A (t' represents the derivative of transfer integral). By compairing Figs.3-1(a) and 3-2(a) it is seen that the electron-lattice interaction causes a remarkable energy renormalization for only the longitudinal (L) mode of oxygen stretching and/or breathing vibrations whose bare frequencies lie near 60 meV. The phonon frequency renormalization shows remarkable wave-vector dependences. In this case large renormalization is found especially around the X-point in the Brillouin zone. It is originated from the nesting effect of the Fermi surface mentioned in Sec.2-1 as well as the remarkable wave-vector dependences of the electron-lattice coupling. If we neglect the wave-vector and mode dependences of the coupling coefficient $g_{\mu}^{\alpha}(\mathbf{k},\mathbf{k}-\mathbf{q})$, $\chi(\mathbf{q})$ becomes proportional to the bare electronic susceptibility given by

$$\chi^{0}(\mathbf{q}) = \sum_{\mathbf{k}} \frac{f(E^{0}_{\mathbf{k}-\mathbf{q}}) - f(E^{0}_{\mathbf{k}})}{E^{0}_{\mathbf{k}} - E^{0}_{\mathbf{k}-\mathbf{q}}} \quad . \tag{3-15}$$

The wave-vector dependence of $\chi^{0}(\mathbf{q})$ has been calculated in

several cases of x (see Fig.3-3). It is found that $\chi^0(q)$ has a broad hump around the X-point for x=0.3, however, its q-dependences are much calmer than that seen in the phonon frequency renormalization.

The magnitude of the renormalization of the L O-stretching/breathing mode increases with increasing the Bi concentration x and/or the strength of the electron-lattice interaction (i.e. value of t'). For an example, the phonon dispersion curves and $F(\omega)$ calculated for x=0.7 in case of the same value t'=4.05 eV/A are shown in Fig.3-4(a) and (b), respectively. It is clearly seen in this case that the L O-stretching/breathing phonon branch becomes soft around the M- and R-points besides the X-point. It is further noted that the O-breathing phonon at the R-point vanishes for $x \geqq 0.9$ in case of t'=4.05 eV/A and hence the lattice becomes unstable against formation of the distorted structure corresponding to that phonon. Experimentally the structure of $BaBiO_3$ at room temperatures has been confirmed to be described by a frozen state of the O- breathing phonon just at the R-point.[20)]

The phonon dispersion curves calculated above agree quite well with those observed by inelastic neutron scattering,[30)] except the L O-stretching/breathing mode. Mysteriously the energies of the L O-stretching/breathing mode have not been detected experimentally. Instead, rather broad peaks were observed near the B.Z. boundary in the energy region of 40~45 meV. In connection with this point the linewidth or the lifetime of phonon will be calculated in the next section, Sec.3-3.

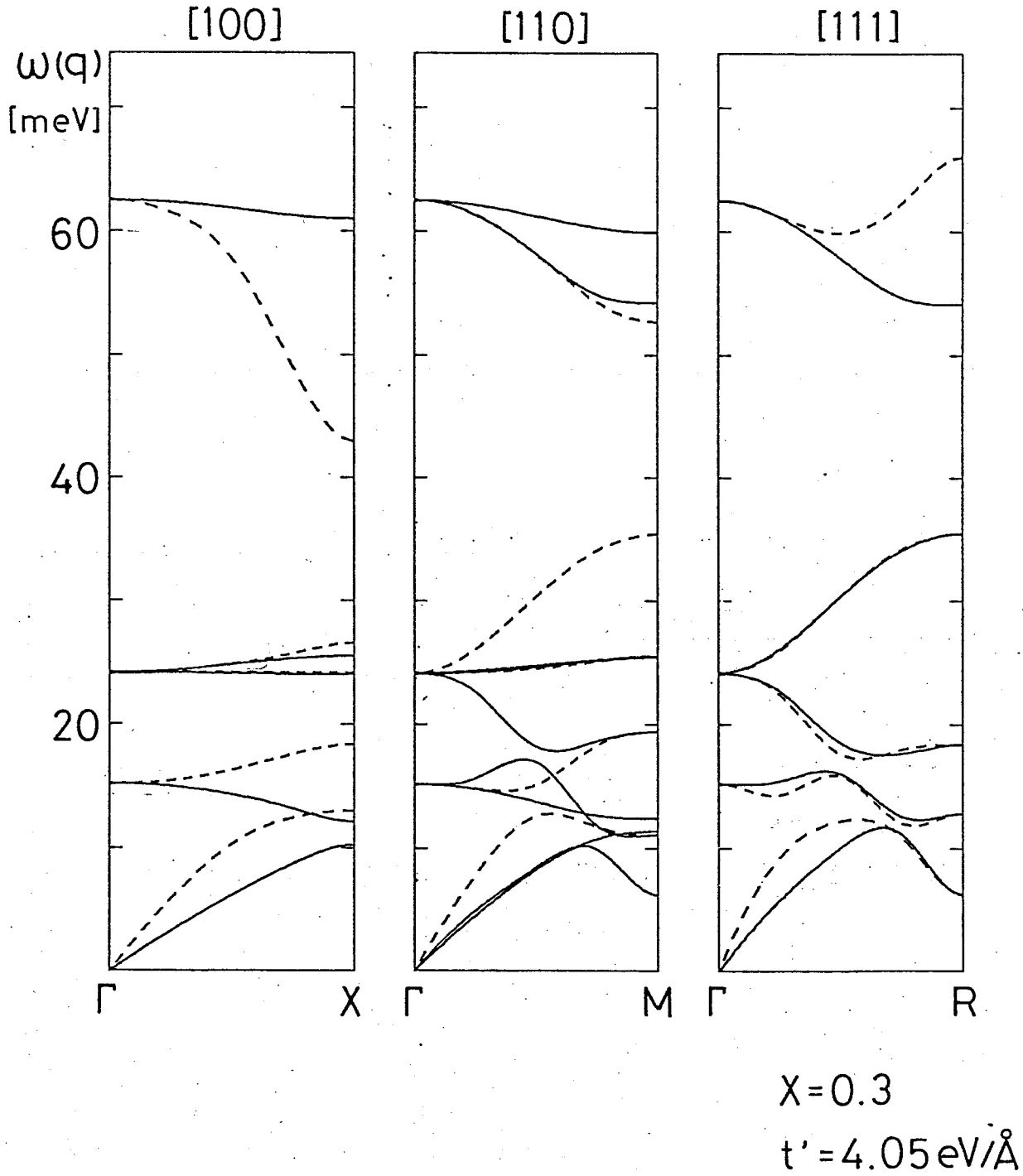

Fig.3-2.(a) Phonon dispersion curves calculated with including $\chi(q)$ for x=0.3 in case of t'=4.05 eV/A.

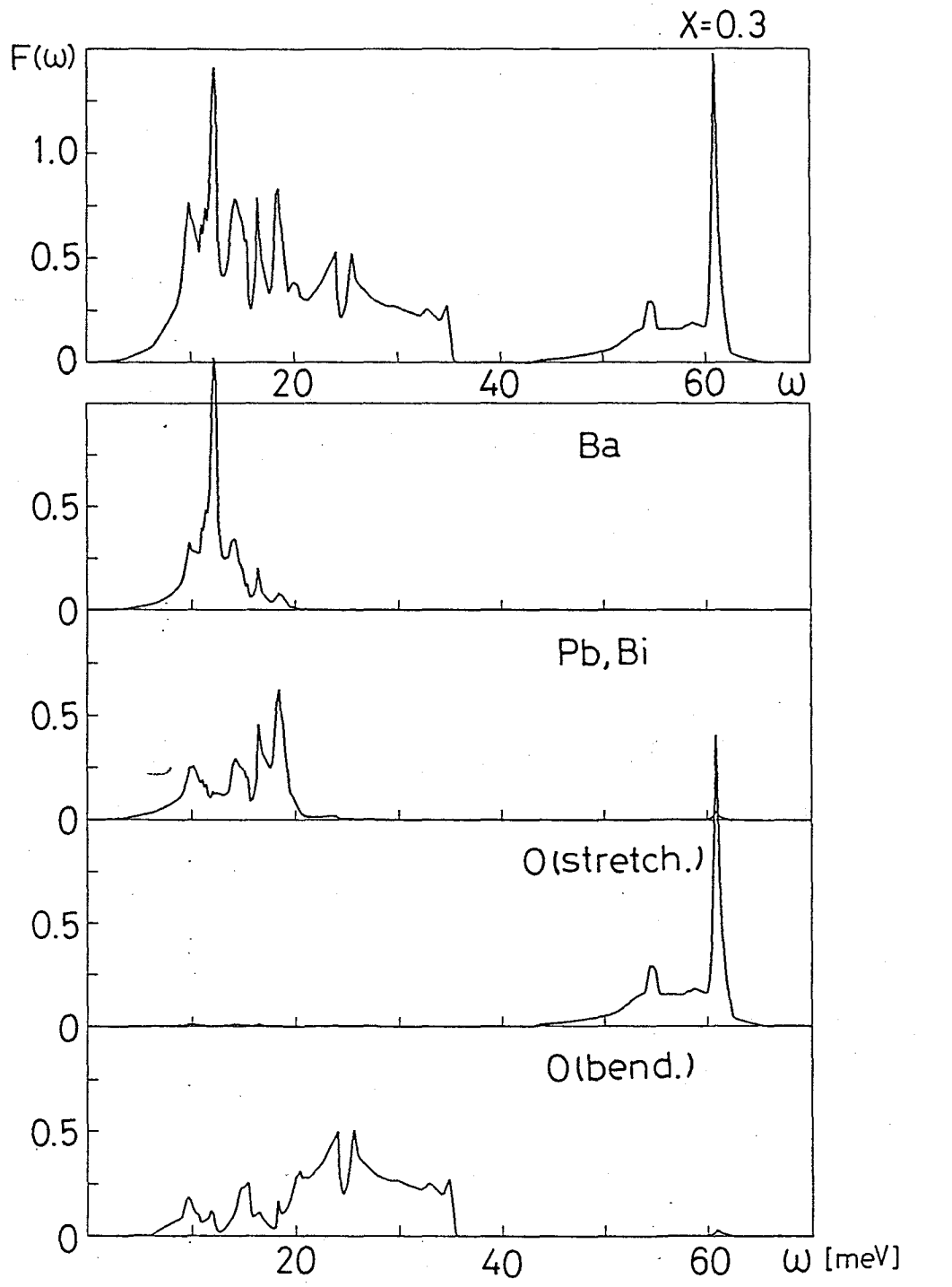

Fig.3-2.(b) Calculated F(ω) for x=0.3 in case of t'=4.05 eV/A.

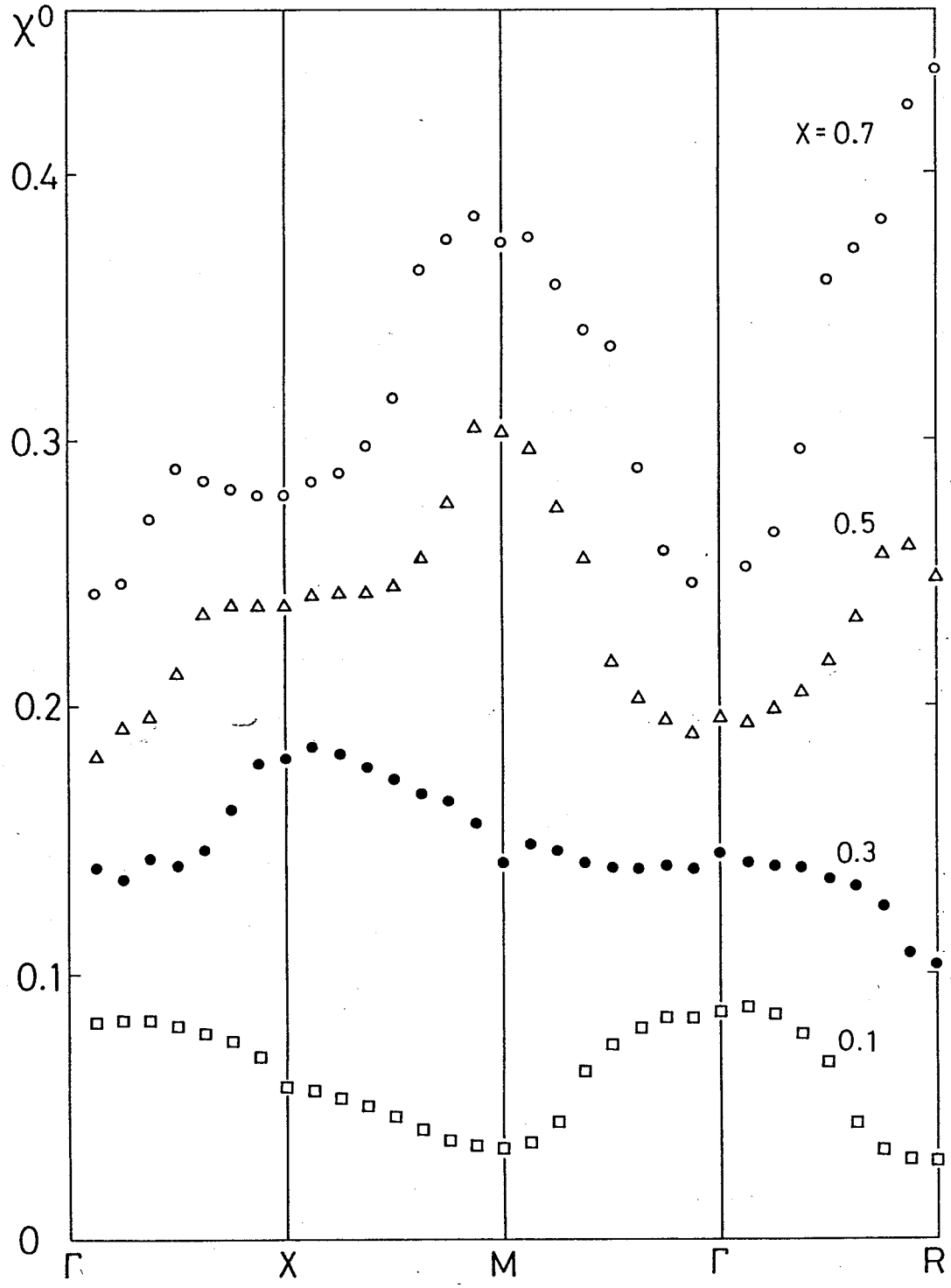

Fig.3-3. Bare electronic susceptibility $\chi^0(\mathbf{q})$ calculated for x=0.1 (□), 0.3 (●), 0.5 (△) and 0.7 (○).

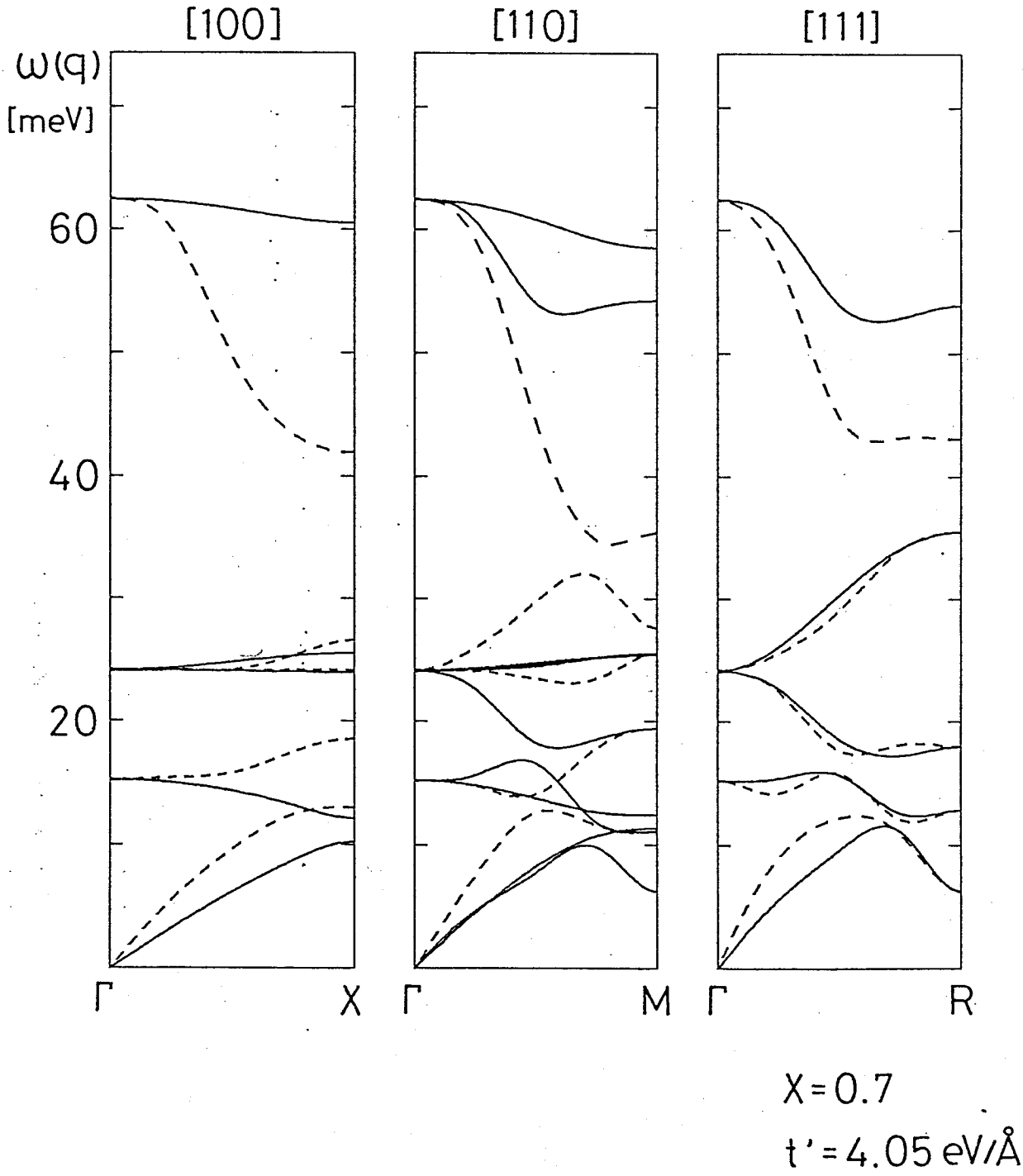

Fig.3-4.(a) Phonon dispersion curves for x=0.7 in case of t'=4.05 eV/A.

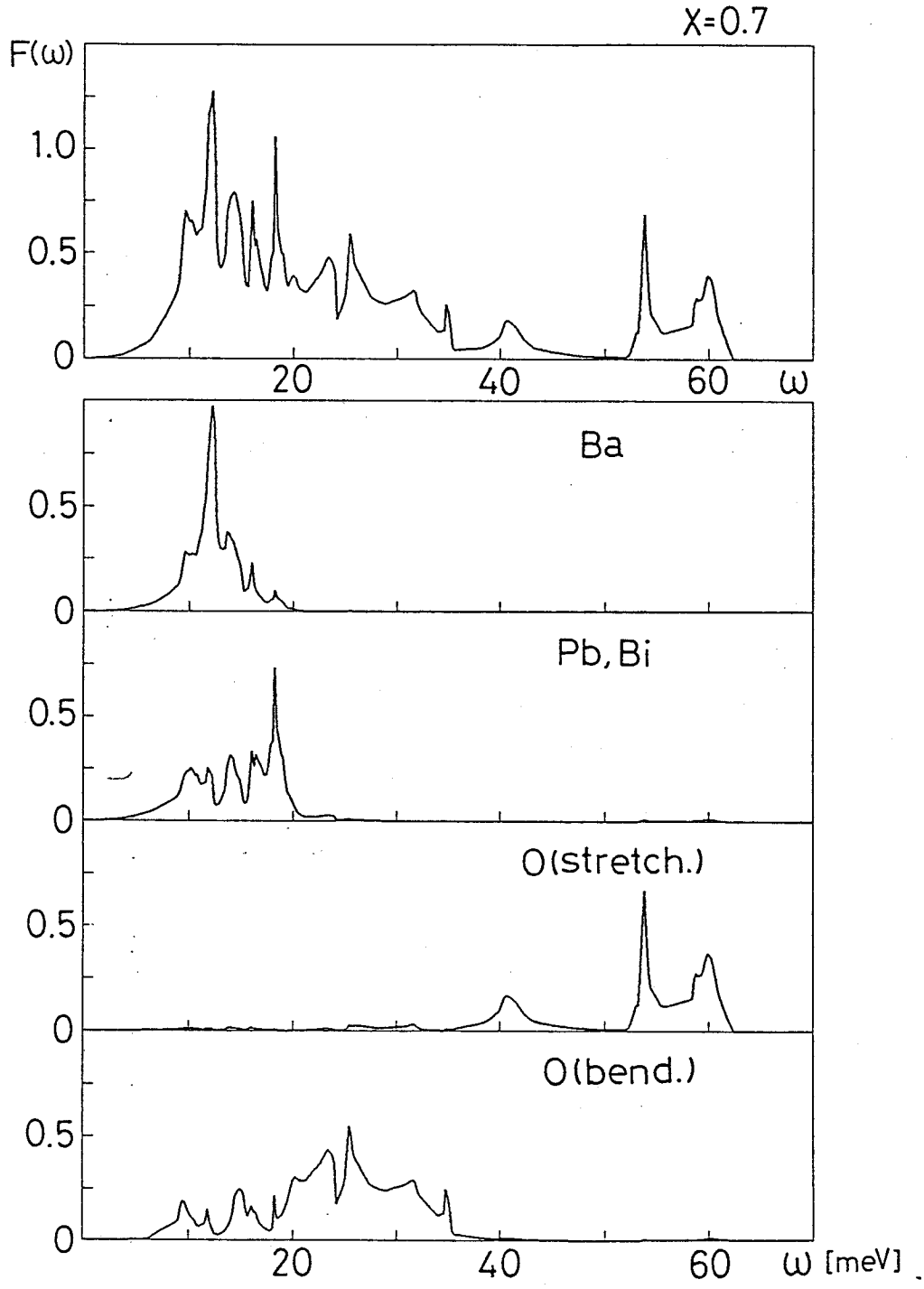

Fig.3-4.(b) Calculated F(ω) for x=0.7 in case of t'=4.05 eV/A.

3-3. Phonon linewidth

As we have mentioned in previous sections the longitudinal (L) O-stretching and/or breathing mode vibrations which may be strongly renormalized by the electron-lattice interaction have not been observed by the inelastic neutron scattering measurement.[30] A reason why the phonon mode can not be detected is considered as broadening of the phonon linewidth because of the strong electron-lattice interaction. Thus, in this section phonon linewidth or life-time caused by the electron-lattice interaction is calculated microscopically.[31]

In inelastic neutron scattering measurements the scattering intensity or the phonon spectral function $S(\mathbf{q},\omega)$ is proportional to the imaginary part of the phonon Green's function $D(\mathbf{q},\omega)$.[32] $D(\mathbf{q},\omega)$ is obtained by solving the Dyson's equation:

$$D(\mathbf{q},\omega) = D^0(\mathbf{q},\omega) + D^0(\mathbf{q},\omega)\,\Pi(\mathbf{q},\omega)\,D(\mathbf{q},\omega) \quad , \qquad (3\text{-}16)$$

where $\Pi(\mathbf{q},\omega)$ represents self-energy (or polarization function) for phonon Green's function and $D^0(\mathbf{q},\omega)$ the bare (or non-interacting) phonon Green's function defined as

$$D^0_\gamma(\mathbf{q},\omega) = -\frac{2\omega^0_{\mathbf{q}\gamma}}{\omega^2 - (\omega^0_{\mathbf{q}\gamma})^2} \quad , \qquad (3\text{-}17)$$

where $\omega^0_{\mathbf{q}\gamma}$ denotes the bare phonon frequency of mode γ. Then $D(\mathbf{q},\omega)$ is rewritten as follows:

$$D_\gamma(\mathbf{q},\omega) = \frac{1}{D_\gamma^0(\mathbf{q},\omega)^{-1} - \Pi_\gamma(\mathbf{q},\omega)}$$

$$= - \frac{2\omega_{\mathbf{q}\gamma}^0}{\omega^2 - (\omega_{\mathbf{q}\gamma}^0)^2 + 2\omega_{\mathbf{q}\gamma}^0 \Pi_\gamma(\mathbf{q},\omega)} \quad . \tag{3-18}$$

When we neglect the ω-dependence of $\Pi_\gamma(\mathbf{q},\omega)$, $D_\gamma(\mathbf{q},\omega)$ becomes

$$D_\gamma(\mathbf{q},\omega) = - \frac{2\omega_{\mathbf{q}\gamma}^0}{\omega^2 - (\omega_{\mathbf{q}\gamma})^2 - 2i\omega_{\mathbf{q}\gamma}\Gamma_{\mathbf{q}\gamma}} \quad , \tag{3-19}$$

where $\omega_{\mathbf{q}\gamma}$ is the phonon freuency renormalized by the electron-lattice interaction and is defined by

$$(\omega_{\mathbf{q}\gamma})^2 = (\omega_{\mathbf{q}\gamma}^0)^2 - 2\omega_{\mathbf{q}\gamma}^0 \, \mathrm{Re}[\Pi_\gamma(\mathbf{q},\omega_{\mathbf{q}\gamma})] \quad , \tag{3-20}$$

and $\Gamma_{\mathbf{q}\gamma}$ represents the phonon linewidth which has relation with the imaginary part of $\Pi_\gamma(\mathbf{q},\omega)$ as follows:

$$\Gamma_{\mathbf{q}\gamma} = - \frac{\omega_{\mathbf{q}\gamma}^0}{\omega_{\mathbf{q}\gamma}} \, \mathrm{Im}[\Pi_\gamma(\mathbf{q},\omega_{\mathbf{q}\gamma})] \quad . \tag{3-21}$$

For $\omega \simeq \omega_{\mathbf{q}\gamma}$, $D_\gamma(\mathbf{q},\omega)$ is approximately given by

$$D_\gamma(\mathbf{q},\omega) \simeq - \frac{\omega_{\mathbf{q}\gamma}^0}{\omega_{\mathbf{q}\gamma}} \cdot \frac{1}{\omega - \omega_{\mathbf{q}\gamma} - i\Gamma_{\mathbf{q}\gamma}} \quad , \tag{3-22}$$

and then the scattering intensity or the imaginary part of $D_\gamma(\mathbf{q},\omega)$ has a Lorentzian form:

$$S(\mathbf{q},\omega) \propto \mathrm{Im}\, D_\gamma(\mathbf{q},\omega) \simeq -\frac{\omega^0_{\mathbf{q}\gamma}}{\omega_{\mathbf{q}\gamma}} \cdot \frac{\Gamma_{\mathbf{q}\gamma}}{(\omega - \omega_{\mathbf{q}\gamma})^2 + (\Gamma_{\mathbf{q}\gamma})^2} \quad , \tag{3-23}$$

with a half-width of half-maximum $\Gamma_{\mathbf{q}\gamma}$.

In order to obtain the explicit expression for $\Gamma_{\mathbf{q}\gamma}$, $\Pi_\gamma(\mathbf{q},\omega)$ is evaluated within Migdal approximation (see Appendix.A).[33] A diagram which is taken for $\Pi_\gamma(\mathbf{q},\omega)$ in Migdal approximation is shown in Fig.3-5, where full curves denote the bare electronic Green's function. The diagram is evaluated as

$$\Pi_\gamma(\mathbf{q},\omega) = \frac{2}{N} \sum_{\mathbf{k}} |I^\gamma(\mathbf{k},\mathbf{k}-\mathbf{q})|^2 \frac{f(E^0_{\mathbf{k}-\mathbf{q}}) - f(E^0_{\mathbf{k}})}{E^0_{\mathbf{k}} - E^0_{\mathbf{k}-\mathbf{q}} - \omega - i\delta} \quad , \tag{3-24}$$

(for $\omega>0$)

where $f(E^0_{\mathbf{k}}) \equiv [\exp(\beta E^0_{\mathbf{k}})+1]^{-1}$ represents the Fermi distribution function. And the electron-phonon coupling coefficient $I^\gamma(\mathbf{k},\mathbf{k}-\mathbf{q})$ is related to $V^\gamma(\mathbf{k},\mathbf{k}-\mathbf{q})$ or $g^\alpha_\mu(\mathbf{k},\mathbf{k}-\mathbf{q})$, which appeared in previous sections, as follows:

$$I^\gamma(\mathbf{k},\mathbf{k}-\mathbf{q}) = \frac{V^\gamma(\mathbf{k},\mathbf{k}-\mathbf{q})}{(2\omega^0_{\mathbf{q}\gamma})^{1/2}} = \sum_{\mu\alpha} \frac{\varepsilon_{\gamma,\mu\alpha}(\mathbf{q})}{(2M_\mu \omega^0_{\mathbf{q}\gamma})^{1/2}} g^\alpha(\mathbf{k}.\mathbf{k}-\mathbf{q}) \quad . \tag{3-25}$$

where M_μ denotes the mass of the μ-th atom, and $\varepsilon_{\gamma,\mu\alpha}(\mathbf{q})$ is the polarization vector.

Then, from eqs.(3-21) and (3-24), the phonon linewidth is expressed as

$$\Gamma_{q\gamma} = 2\pi \frac{\omega^0_{q\gamma}}{\omega_{q\gamma}} \sum_{k} |I^{\gamma}(k,k-q)|^2 \, [f(E^0_k)-f(E^0_{k-q})] \, \delta(E^0_{k-q}-E^0_k-\omega_q) \ . \tag{3-26}$$

Since the summation for k in above equation is restricted to the electronic state near the Fermi level, we can replace approximately $[f(E^0_k)-f(E^0_{k-q})]$ to $\omega_{q\gamma}\delta(E^0_k-E_F)$, and neglect ω_q in the δ-function. Thus, the final expression is given by

$$\Gamma_{q\gamma} = 2\pi\omega^0_{q\gamma} \sum_{k} |I^{\gamma}(k,k-q)|^2 \, \delta(E^0_k-E_F) \, \delta(E^0_{k-q}-E_F) \ , \tag{3-27}$$

or

$$\Gamma_{q\gamma} = \pi \sum_{k} |V^{\gamma}(k,k-q)|^2 \, \delta(E^0_k-E_F) \, \delta(E^0_{k-q}-E_F) \ . \tag{3-28}$$

It is noted that the relation (3-25) has been used to obtain the final expression (3-28).

The calculated phonon linewidth for x=0.3 is shown in Fig.3-6. It is found that the L O-stretching/breathing mode phonons broaden significantly because of the electron-lattice interaction. The L O-stretching/breathing mode phonons have the linewidth several order of magnitude larger than that of the other modes. Especially near the X point, $(\pi/a,0,0)$, in the Brillouin zone, where the phonon frequencies are renormalized most significantly, the full-width becomes at most about 3 meV.

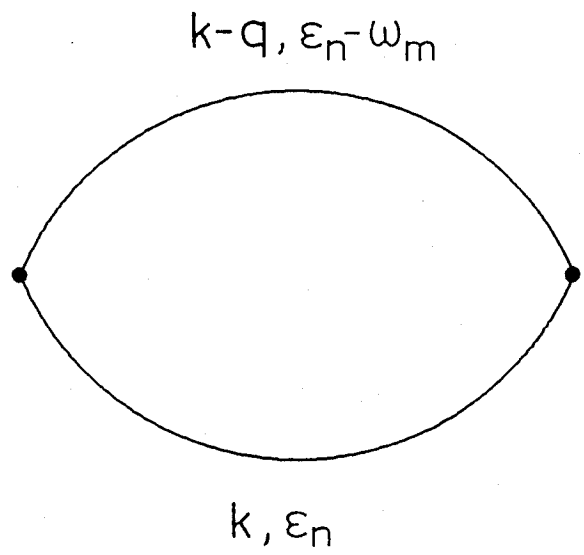

Fig.3-5. A Feynman diagram of the polarization function taken in the Migdal approximation. The full curves denote the bare electronic Green's function.

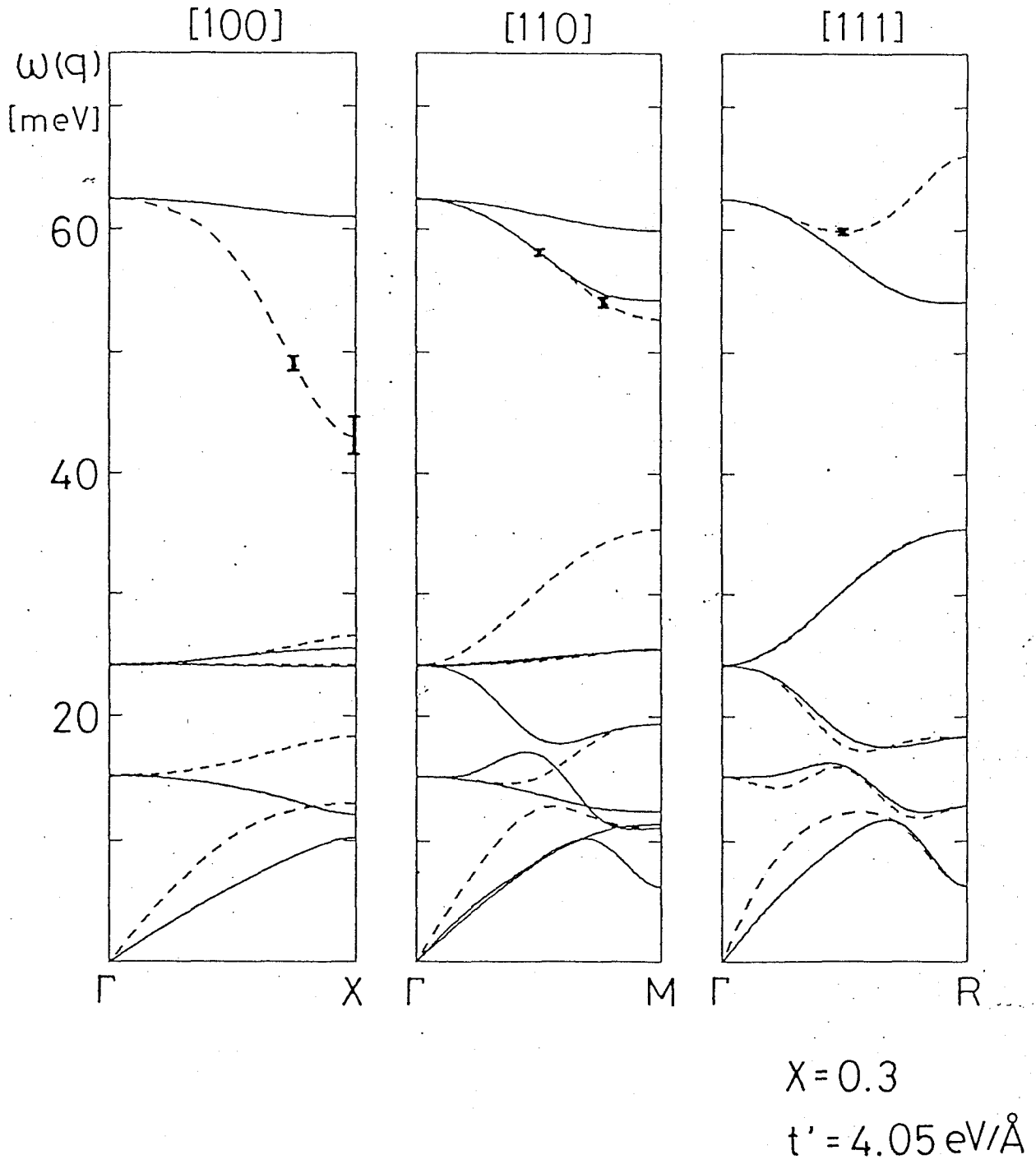

Fig.3-6. Phonon dispersion curves for x=0.3 in case of t'=4.05 eV/A. Calculated phonon line-width (full width of half maximum) of the longitudinal O-stretching/breathing mode is indicated by the vertical bars. The line-width of the other modes is invisible on this scale.

§4. Superconductivity

In this section the superconductivity in BPB and BKB is discussed on the basis of the strong coupling theory of phonon mechanism.[34] Prior to details of calculations, developments of the microscopic theory of the superconductivity are reviewed in Sec.4-1. In Sec.4-2 the spectral function of electron-phonon coupling $\alpha^2F(\omega)$ is calculated by using the phonon dispersion and the electron-lattice coupling which have been obtained in previous sections. The superconducting transition temperature T_c is calculated in Sec.4-3 by solving the Eliashberg equations.[35),36)] The calculated T_c shows the significant composition dependence and high T_c about 30 K in BKB is found to be possible in the framework of the phonon mechanism. Further, isotopic shift of T_c is evaluated by replacing ^{16}O with ^{17}O and ^{18}O. The apparent deviation from the BCS result,[37)] $T_c \propto M^{-1/2}$, can be obtained in the present system. Finally, in Sec.4-4 the Eliashberg equation for T=0 K [35),38)] is solved to evaluate the energy-dependent gap function $\Delta(\omega)$. The ratio $2\Delta_0/k_BT_c$ (where Δ_0 denotes the superconducting energy gap) is found to be about 3.5 in the case of T_c of about 30 K. This result agrees with the BCS result[37)] in spite of the strong electron-lattice interaction in this system. The tunneling spectrum for BKB is also predicted based on the calculated $\Delta(\omega)$.

4-1. Strong coupling theory

The first microscopic theory for superconductivity has been proposed by Bardeen-Cooper-Schrieffer (BCS) in 1957.[37] The BCS theory succeeded in the understanding of many properties of the superconducting states, such as the transition temperature T_c, energy gap Δ_0, critical field H_c, specific heat C_s, and so on. The essential idea in the BCS theory is that two electrons are condensed into a pairwise state, so-called Cooper pair, which is responsible for the superconductivity. The Cooper pair may be originated from an attractive interaction which is mediated by phonons or lattice vibrations in the crystal. However, the BCS theory has been found later to be applicable only for simple metal superconductors. Hence, Eliashberg[35] has extended the BCS theory to a rigorous form to deal with strong electron-phonon coupling systems with the aid of the Migdal theorem[33] in describing the normal state. In this section the developments of microscopic theories for the superconductivity are reviewed.

4-1-1. BCS theory

The essential features of the system which consists of electrons and phonons are described by Fröhlich Hamiltonian:[39]

$$H = H_{el} + H_{ph} + H_{el-ph} \quad , \tag{4-1}$$

where H_{el} and H_{ph} represent the Hamiltonians of non-interacting (or bare) electron and phonon systems, respectively. And H_{el-ph} represents the electron-phonon interaction.

The electronic Hamiltonian H_{el} is described as

$$H_{el} = \sum_{nk\sigma} E^0_{nk}\, c^\dagger_{nk\sigma}\, c_{nk\sigma} \quad , \tag{4-2}$$

where $c^\dagger_{k\sigma}$ (or $c_{k\sigma}$) is the creation (or annihilation) operator of a Bloch state with a wave-vector k and a spin σ of the n-th band, and E^0_{nk} is the bare electronic band energy of the Bloch state. Actually, E^0_{nk} may be calculated on the basis of the band theory which includes Coulomb interactions within the local-density-functional (LDF) approximation.

On the other hand H_{ph} is described as

$$H_{ph} = \sum_{q\gamma} \omega^0_{q\gamma}\, (a^\dagger_{q\gamma}\, a_{q\gamma} + \tfrac{1}{2}) \quad , \tag{4-3}$$

where $a^\dagger_{q\gamma}$ (or $a_{q\gamma}$) is the creation (or annihilation) operator of a phonon with a wave-vector q of the μ-th branch, and $\omega^0_{q\gamma}$ is its bare phonon energy with $\hbar = 1$, which is extracted from some experiments, such as Raman scattering, infrared absorption,

inelastic neutron scattering, and so on. On the other hand, $\omega^0_{q\gamma}$ can be calculated theoretically on the basis of the short range force constant model described in Sec.3-1.

Finally, the electron-phonon interaction is written as

$$H_{el\text{-}ph} = \sum_{nk\sigma} \sum_{q\gamma} I^{\gamma}(nk,n'k-q)\ c^{\dagger}_{nk\sigma}\ c_{n'k-q\sigma}\ (a_{q\gamma} + a^{\dagger}_{-q\gamma}) \quad , \tag{4-4}$$

where $I^{\gamma}(nk,n'k-q)$ denotes the matrix element of the electron scattering from a Bloch state $n'k-q$ to a state nk, which is caused by creating (or annihilating) a phonon with a wave-vector $-q$ (or q) of mode γ. It is noted that $I^{\gamma}(nk,n'k-q)$ can be related to the electron-lattice coupling coefficient $g^{\alpha}_{\mu}(nk,n'k-q)$ or $V^{\gamma}(nk,n'k-q)$, which has appeared in Sec.2-2.

The BCS theory starts from the Fröhlich Hamiltonian, but it does not treat them directly. Instead, an effective electronic Hamiltonian H^{eff} is constructed by performing the second-order perturbation with respect to the electron-phonon coupling $I^{\gamma}(nk,n'k-q)$ and H^{eff} is given in the following form:

$$H^{eff} = H_{el} + H_{int} \quad , \tag{4-5}$$

where

$$H_{int} = \frac{1}{2} \sum_{kk'\sigma\sigma'} \sum_{q\gamma} I^{\gamma}(k'-q,k')\ I^{\gamma}(k+q,k) \cdot \times \frac{2\,\omega^0_{q\gamma}}{(E^0_k - E^0_{k+q})^2 - (\omega^0_{q\gamma})^2}\ c^{\dagger}_{k'-q\sigma'}\ c_{k'\sigma'}\ c^{\dagger}_{k+q\sigma}\ c_{k\sigma} \quad . \tag{4-6}$$

Here band indices are omitted for brevity, and H_{int} indicates the effective electron-electron interaction which comes from virtual exchange of phonons (Bardeen-Pines interaction).[40] The form of H_{int} indicates that it is attractive (or negative) for excitation energies $|E^0_{\mathbf{k}} - E^0_{\mathbf{k}-\mathbf{q}}| < \omega^0_{\mathbf{q}\gamma}$.

In order to obtain the ground state of the effective Hamiltonian H^{eff}, BCS have produced a coherent state by introducing an idea of the Cooper pair. When the Bloch states are occupied in pairs, the matrix elements of the interaction Hamiltonian H_{int} are always negative between such electronic configrations. The best choice for pairing is found to be $(\mathbf{k}\uparrow, -\mathbf{k}\downarrow)$, i.e. the Cooper pair. Thus, the problem is reduced to a subset of configrations in which the states are occupied in Cooper pairs. Then, the Hamiltonian is also reduced to the form which connects Cooper pairs:

$$H_{red} = H_{el} + \tilde{H}_{int} \quad , \tag{4-7}$$

with

$$\tilde{H}_{int} = \sum_{\mathbf{k}\mathbf{k}'} V_{\mathbf{k}'\mathbf{k}} (c^{\dagger}_{-\mathbf{k}'\downarrow} c^{\dagger}_{\mathbf{k}'\uparrow})(c_{\mathbf{k}\uparrow} c_{-\mathbf{k}\downarrow}) \quad , \tag{4-8}$$

where $V_{\mathbf{k}'\mathbf{k}}$ is defined by

$$V_{\mathbf{k}'\mathbf{k}} = - \sum_{\gamma} \frac{2\,\omega^0_{\mathbf{k}-\mathbf{k}'\gamma} |I^{\gamma}(\mathbf{k},\mathbf{k}')|^2}{(\omega^0_{\mathbf{k}-\mathbf{k}'\gamma})^2 - (E^0_{\mathbf{k}} - E^0_{\mathbf{k}'})^2} \quad . \tag{4-9}$$

$V_{\mathbf{k}'\mathbf{k}}$ is time-independent attractive interaction for Cooper pairs in the vicinity of the Fermi surface.

BCS have obtained the ground state and excited states of the reduced Hamiltonian H_{red} by means of the conventional variational method. After the BCS theory many theorists have tried to describe the BCS solution in more convenient ways, such as a canonical transformation which diagonalizes H_{red} proposed by Bogolyubov,[41] a pseudo-spin representation by Anderson,[42] and a Green's function method by Gor'kov.[43]

Among these methods the Gor'kov's is reviewed hereafter, since the Green's functions are utilized also in the strong coupling theory. The thermal Green's function for electrons is defined in the range $-\beta<\tau<\beta$ as

$$G_\sigma(k,\tau) = - \langle T_\tau \, c_{k\sigma}(\tau) \, c^\dagger_{k\sigma}(0) \rangle \quad , \tag{4-10}$$

where T_τ denotes the Wick operator which reorders the operators in such a way that τ increases from right to left. In case of interchanging two fermion operators a factor of -1 is introduced. Thus,

$$G_\sigma(k,\tau) = - \langle c_{k\sigma}(\tau) \, c^\dagger_{k\sigma}(0) \rangle \, \theta(\tau) + \langle c^\dagger_{k\sigma}(0) \, c_{k\sigma}(\tau) \rangle \, \theta(-\tau) \quad , \tag{4-11}$$

where $\theta(\tau)$ is a step function defined by

$$\theta(\tau) = \begin{cases} 1 & ; \text{ for } \tau>0 \\ 0 & ; \text{ for } \tau<0 \quad , \end{cases} \tag{4-12}$$

And $c_{k\sigma}(\tau)$ is an annihilation operator for a Bloch state $k\sigma$ in the modified Heisenberg picture:

$$c_{k\sigma}(\tau) \equiv e^{\tau\hat{\mathcal{H}}} c_{k\sigma} e^{-\tau\hat{\mathcal{H}}} , \qquad (4\text{-}13)$$

and thermodynamic averages are defined by

$$\langle \cdots \rangle \equiv \frac{\mathrm{tr}(e^{-\beta\hat{\mathcal{H}}} \cdots)}{\mathrm{tr}(e^{-\beta\hat{\mathcal{H}}})} , \qquad (4\text{-}14)$$

where $\beta = 1/k_B T$ and

$$\hat{\mathcal{H}} = H - \mu N_e , \qquad (4\text{-}15)$$

with μ being the chemical potential of electrons and N_e the total number operator of electrons:

$$N_e = \sum_{k\sigma} c^{\dagger}_{k\sigma} c_{k\sigma} . \qquad (4\text{-}16)$$

Namely, $\langle \cdots \rangle$ means actually an average for a grand canonical ensemble.

It is found that the Green's function (4-10) has the anti-periodicity property for $-\beta < \tau < \beta$:

$$G_\sigma(k, \tau+\beta) = - G_\sigma(k, \tau) . \qquad (4\text{-}17)$$

By using this property the definition of $G_\sigma(k,\tau)$ is extended outside the range $-\beta < \tau < \beta$. Then, the Fourier expansion of $G_\sigma(k,\tau)$ is written in the form:

$$G_\sigma(k,\tau) = \frac{1}{\beta} \sum_{n=-\infty}^{\infty} e^{-i\omega_n \tau} G_\sigma(k,i\omega_n) \quad , \tag{4-18}$$

where

$$\omega_n = (2n+1)\pi k_B T \quad , \tag{4-19}$$

with n being an integer, which is called as "Matsubara frequency". The Fourier coefficients $G_\sigma(k,i\omega_n)$ are inversely given by:

$$G_\sigma(k,i\omega_n) = \frac{1}{2} \int_{-\beta}^{\beta} d\tau \; e^{i\omega_n \tau} G_\sigma(k,\tau) \quad . \tag{4-20}$$

For non-interacting electrons (where only Hamiltonian H_{el} should be taken) the Green's function (4-10) can be evaluated as

$$G_\sigma^0(k,\tau) = e^{-E_k^0 \tau}\{f(E_k^0)\theta(-\tau) - [1-f(E_k^0)]\theta(\tau)\} \quad , \tag{4-21}$$

where

$$f(E_k^0) = \langle c_{k\sigma}^\dagger c_{k\sigma} \rangle_0 = [\exp(\beta E_k^0) + 1]^{-1} \tag{4-22}$$

is the Fermi distribution function, and $\langle \cdots \rangle_0$ represents the thermodynamical average with the non-interacting Hamiltonian H_{el}. Then, the Fourier coefficients of $G_\sigma^0(k,\tau)$ can be calculated readily and obtained as

$$G_\sigma^0(k,i\omega_n) = \frac{1}{i\omega_n - (E_k^0 - \mu)} \quad . \tag{4-23}$$

It is proved that the analytic continuation of $G_\sigma(k,i\omega_n)$ to the complex plane, i.e. $G_\sigma(k,z)$, contains complete informations about quasi-particle excitations in the electronic system. The pole z_0 of $G_\sigma(k,z)$ represents the excitation energy ε (= Re z_0) and the life-time τ (or the damping $1/2\tau$ = Im z_0) of the quasi-particle.

In order to evaluate $G_\sigma(k,i\omega_n)$ one must solve the equation of motions in the modified Heisenberg representation:

$$-\frac{\partial}{\partial\tau} G_\sigma(k,\tau) = [H_{red} , G_\sigma(k,\tau)] \quad . \tag{4-24}$$

By carrying out the commutation relation in eq.(4-24) the equation of motions of $G_\sigma(k,\tau)$ is written in the explicit form:

$$-\frac{\partial}{\partial\tau} G_\sigma(k,\tau) = \delta(\tau) + (E_k^0 - \mu)\, G_\sigma(k,\tau) - \sum_{k'} V_{kk'} \langle T_\tau\, c^\dagger_{-k-\sigma}(\tau)\, c_{k'\sigma}(\tau)\, c_{-k'-\sigma}(\tau)\, c^\dagger_{k\sigma}(0)\rangle \quad . \tag{4-25}$$

The complicated thermal average on the right-hand side of eq.(4-25) is decoupled by using the extended Hartree-Fock approximation:

$$\langle T_\tau\, c^\dagger_{-k-\sigma}(\tau)\, c_{k'\sigma}(\tau)\, c_{-k'-\sigma}(\tau)\, c^\dagger_{k\sigma}(0)\rangle \rightarrow \langle T_\tau\, c_{k'\sigma}(\tau)\, c_{-k'-\sigma}(\tau)\rangle\langle T_\tau\, c^\dagger_{-k-\sigma}(\tau)\, c^\dagger_{k\sigma}(0)\rangle \quad . \tag{4-26}$$

It is noted that the pair amplitude $\langle c_{k\uparrow} c_{-k\downarrow}\rangle$ remains in this procedure. Other Hartree-Fock terms remain only for k=k', which

give unimportant contributions to $G_\sigma(\mathbf{k},\tau)$, i.e. small shifts of excitation energies.

Now, the Gor'kov's "anormalous" Green's function is introduced:

$$F_\sigma(\mathbf{k},\tau) = - \langle T_\tau \, c_{\mathbf{k}\sigma}(\tau) \, c_{-\mathbf{k}-\sigma}(0) \rangle \quad , \tag{4-27}$$

$$F_\sigma^\dagger(\mathbf{k},\tau) = - \langle T_\tau \, c_{-\mathbf{k}-\sigma}^\dagger(\tau) \, c_{\mathbf{k}\sigma}^\dagger(0) \rangle \quad . \tag{4-28}$$

Then, eq.(4-26) becomes

$$- \frac{\partial}{\partial \tau} G_\sigma(\mathbf{k},\tau) = \delta(\tau) + (E_{\mathbf{k}}^0 - \mu) \, G_\sigma(\mathbf{k},\tau) - \sum_{\mathbf{k}'} V_{\mathbf{k}\mathbf{k}'} \, F_\sigma(\mathbf{k}',0) \, F_\sigma^\dagger(\mathbf{k},\tau) \quad , \tag{4-29}$$

which couple with $F_\sigma^\dagger(\mathbf{k},\tau)$. Thus, an equation of motion for $F_\sigma^\dagger(\mathbf{k},\tau)$ is next produced in a similar way:

$$- \frac{\partial}{\partial \tau} F_\sigma^\dagger(\mathbf{k},\tau) = (E_{\mathbf{k}}^0 - \mu) \, F_\sigma^\dagger(\mathbf{k},\tau) - \sum_{\mathbf{k}'} V_{\mathbf{k}\mathbf{k}'} \, F_\sigma^\dagger(\mathbf{k}',0) \, G_\sigma(\mathbf{k},\tau) \quad . \tag{4-30}$$

It is noted that the coupled differential equations (4-29) and (4-30) are closed by themselves.

Next, these equations will be solved by defining first the BCS energy gap:

$$\Delta_{\mathbf{k}} \equiv \sum_{\mathbf{k}'} V_{\mathbf{k}\mathbf{k}'} F_\sigma(\mathbf{k}',0) \quad . \tag{4-31}$$

Furthermore, eqs.(4-29) and (4-30) are Fourier transformed by using eq.(4-20):

$$\begin{pmatrix} i\omega_n - E_k^0 + \mu & \Delta_k \\ \Delta_k^* & i\omega_n + E_k^0 - \mu \end{pmatrix} \begin{pmatrix} G_\sigma(k,i\omega_n) \\ F_\sigma^\dagger(k,i\omega_n) \end{pmatrix} = \begin{pmatrix} 1 \\ 0 \end{pmatrix} . \tag{4-32}$$

By solving the linear equations the results are obtained as

$$G_\sigma(k,i\omega_n) = - \frac{i\omega_n + E_k^0 - \mu}{\omega_n^2 + E_k^2} , \tag{4-33}$$

$$F^\dagger(k,i\omega_n) = \frac{\Delta_k^*}{\omega_n^2 + E_k^2} , \tag{4-34}$$

where

$$E_k \equiv (E_k^0 - \mu)^2 + |\Delta_k|^2 , \tag{4-35}$$

which denotes the quasi-particle energy in the BCS state, since the analytic continuation $G_\sigma(k,z)$ of eq.(4-33) has a pole at $z_0=\pm E_k$. It is noted that the energy spectrum E_k has an energy gap Δ_k at the Fermi level (or the chemical potential).

The BCS energy gap Δ_k must be determined in a self-consistent manner. The Fourier expansion form given by

$$F_\sigma(k,\tau=0) = \frac{1}{\beta} \sum_{n=-\infty}^{\infty} F(k,i\omega_n) \tag{4-36}$$

is substituted into eq.(4-31). Then, by using eq.(4-34) the BCS

gap equation is obtained as follows:

$$\Delta_{\mathbf{k}} = \frac{1}{\beta} \sum_{\mathbf{k}'} \sum_{n=-\infty}^{\infty} \frac{V_{\mathbf{k}\mathbf{k}'}\Delta_{\mathbf{k}'}}{\omega_n^2 + E_{\mathbf{k}'}^2} \quad . \tag{4-37}$$

With the aid of the Poisson sum formula

$$\sum_{n=-\infty}^{\infty} \frac{1}{(2n+1)^2\pi^2 + \alpha^2} = \frac{1}{2\alpha} \tanh \frac{\alpha}{2} \quad , \tag{4-38}$$

(α: real number)

the familiar expression of the gap equations are finally achieved:

$$\Delta_{\mathbf{k}} = \sum_{\mathbf{k}'} \frac{V_{\mathbf{k}\mathbf{k}'}\Delta_{\mathbf{k}'}}{2E_{\mathbf{k}'}} \tanh \frac{E_{\mathbf{k}'}}{2k_B T} \quad . \tag{4-39}$$

If neglecting the wave-vector dependence of the Bardeen-Pines interaction $V_{\mathbf{k}\mathbf{k}'}$ and replacing it with a simple model given by

$$V_{\mathbf{k}\mathbf{k}'} \rightarrow V\ \theta(\omega_D - |E_{\mathbf{k}}^0 - \mu|)\ \theta(\omega_D - |E_{\mathbf{k}'}^0 - \mu|) \quad , \tag{4-40}$$

where ω_D being the Debye frequency, the BCS energy gap $\Delta_{\mathbf{k}}$ also loses its k-dependences and becomes

$$\Delta_{\mathbf{k}} \rightarrow \begin{cases} \Delta & ; \text{ for } \mu-\omega_D < E_{\mathbf{k}}^0 < \mu+\omega_D \\ 0 & ; \text{ otherwise} \end{cases} \quad . \tag{4-41}$$

Then, the BCS gap equation is written in the simple form:

$$1 = V \sum_{k'} \frac{1}{2E_{k'}} \tanh \frac{E_{k'}}{2k_B T} \quad , \tag{4-42}$$

with $E_k^2 = (E_k^0 - \mu)^2 + \Delta^2$. Further, the summation of k is replaced by an energy integration by introducing the electronic density of states N(E) in the normal states as follows:

$$1 = N(E_F)V \int_{-\omega_D}^{\omega_D} dE \frac{1}{2(E^2+\Delta^2)^{1/2}} \tanh \frac{(E^2+\Delta^2)^{1/2}}{2k_B T} \quad . \tag{4-43}$$

Here, N(E) has been approximated to be a constant $N(E_F)$ in the region $\mu-\omega_D<E<\mu+\omega_D$. The transition temperature T_c can be derived easily from the gap equation (4-43). With temperatures approaching to T_c the gap Δ becomes to zero. Therefore, by setting $T\to T_c$ and $\Delta\to 0$ in eq.(4-43), T_c is determined by the following condition:

$$1 = N(E_F)V \int_0^{\omega_D} dE \frac{1}{E} \tanh \frac{E}{2k_B T_c} \quad . \tag{4-44}$$

By performing the integration on the right-hand side of eq.(4-44), the explicit expression for T_c , which is famous as the BCS result, is obtained as follows:

$$T_c = 1.13\ \Theta_D \exp\left[-\frac{1}{N(E_F)V}\right] \quad , \tag{4-45}$$

where $\Theta_D \equiv \omega_D / k_B$ denotes the Debye temperature.

4-1-2. Eliashberg theory

A failure of the BCS theory[37] which is discussed in the previous section may lie in the Bardeen-Pines interaction[40] which does not contain time-dependences. Therefore, the BCS theory cannot account any retardation (or dynamical) effects of the pairwise interaction which is mediated by phonons. In order to take into account the dynamical effects of the electron-phonon interaction phonons as well as electrons should be treated by using the Green's function method. Especially, renormalizations of electrons and/or phonons in the normal state should be considered accurately, since the renormalizations provide many important physical phenomena such as mass enhancements of electrons, Kohn anormalies in the phonon dispersion, finite life-time of quasi-particle states, and so on.

The theory of the superconductivity, which is also applicable to the strong electron-phonon coupled system, has been proposed first by Eliashberg in 1960.[35] In this section the Eliashberg theory for finite temperatures is reviewed, since the theory for T=0 K is derived essentially in a similar procedure which utilizes the causal Green's function for T=0 K in place of the thermal Green's function.

Now, we shall start again from the Fröhlich Hamiltonian,[39] eqs.(4-1)∿(4-4). In addition to the thermal Green's function for electrons, eq.(4-10), it is necessary to introduce that of phonons:

$$D_\gamma(\mathbf{q},\tau) = - \langle T_\tau \, \phi_{\mathbf{q}\gamma}(\tau) \, \phi_{-\mathbf{q}\gamma}(0) \rangle \quad , \tag{4-46}$$

with

$$\phi_{\mathbf{q}\gamma} \equiv a_{\mathbf{q}\gamma} + a^\dagger_{-\mathbf{q}\gamma} \quad , \tag{4-47}$$

which is related to the Fourier transform of atomic displacements $u^\alpha_\mu(\mathbf{q})$ (α=x,y,z) in the following way:

$$u^\alpha_\mu(\mathbf{q}) = \sum_\gamma \left(\frac{1}{2NM_\mu \omega_{\mathbf{q}\gamma}} \right)^{1/2} \varepsilon_{\mu\alpha,\gamma}(\mathbf{q}) \, \phi_{\mathbf{q}\gamma} \quad , \tag{4-48}$$

where M_μ is the mass of the μ-th atom, $\omega_{\mathbf{q}\gamma}$ and $\varepsilon_{\mu\alpha,\gamma}(\mathbf{q})$ denote the phonon frequency and the polarization vector of the wave-vector $\mathbf{q}$ and mode γ, respectively.

It is found that $D_\gamma(\mathbf{q},\tau)$ has the periodic property:

$$D_\gamma(\mathbf{q},\tau+\beta) = D_\gamma(\mathbf{q},\tau) \tag{4-49}$$

in the region $-\beta<\tau<\beta$. And the Fourier expansion form is given by

$$D_\gamma(\mathbf{q},\tau) = \frac{1}{\beta} \sum_{n=-\infty}^{\infty} e^{-i\omega_n \tau} \, D_\gamma(\mathbf{q},i\omega_n) \quad , \tag{4-50}$$

with

$$\omega_n = 2n\pi k_B T \quad , \tag{4-51}$$

which is the Matsubara frequency for bosons (n: integer). The inverse relation is the same with that of electrons:

$$D_\gamma(\mathbf{q},i\omega_n) = \frac{1}{2}\int_{-\beta}^{\beta} d\tau\ e^{i\omega_n\tau}\ D_\gamma(\mathbf{q},\tau) \quad . \tag{4-52}$$

When the electron-phonon interaction is neglected, i.e. in case of the "bare" phonon, the Green's function $D^0_\gamma(\mathbf{q},\tau)$ can be evaluated as

$$\begin{aligned} D^0_\gamma(\mathbf{q},\tau) = &- \exp(-\omega_{\mathbf{q}\gamma}\tau)\ \{[n(\omega_{\mathbf{q}\gamma})+1]\theta(\tau) + n(\omega_{\mathbf{q}\gamma})\theta(-\tau)\} \\ &- \exp(\omega_{\mathbf{q}\gamma}\tau)\ \{n(\omega_{\mathbf{q}\gamma})\theta(\tau) + [n(\omega_{\mathbf{q}\gamma})+1]\theta(-\tau)\} \quad . \end{aligned} \tag{4-53}$$

Also, the Fourier transform of $D^0_\gamma(\mathbf{q},\tau)$ is given by

$$\begin{aligned} D^0_\gamma(\mathbf{q},i\omega_n) &= \frac{1}{i\omega_n + \omega^0_{\mathbf{q}\gamma}} - \frac{1}{i\omega_n - \omega^0_{\mathbf{q}\gamma}} \\ &= \frac{2\omega^0_{\mathbf{q}\gamma}}{(i\omega_n)^2 - (\omega^0_{\mathbf{q}\gamma})^2} \quad , \end{aligned} \tag{4-54}$$

where $\omega^0_{\mathbf{q}\gamma}$ denotes the bare phonon energy.

Now, the equation of motion for $G_\sigma(\mathbf{k},\tau)$ is derived in analogy with that of previous section:

$$\begin{aligned} -\frac{\partial}{\partial\tau} G_\sigma(\mathbf{k},\tau) &= [H\ ,\ G_\sigma(\mathbf{k},\tau)] \\ &= \delta(\tau) + (E^0_{\mathbf{k}} - \mu)\ G_\sigma(\mathbf{k},\tau) \\ &\quad + \sum_{\mathbf{q}\gamma} I^\gamma(\mathbf{k}-\mathbf{q},\mathbf{k})^*\ \langle T_\tau\ \phi_{\mathbf{q}\gamma}(\tau)\ c_{\mathbf{k}-\mathbf{q}\sigma}(\tau)\ c^\dagger_{\mathbf{k}\sigma}(0)\rangle \quad . \end{aligned} \tag{4-55}$$

In order to evaluate the thermal average on the right-hand side of eq.(4-55) or the vertex function $\Gamma^{\gamma}_{\sigma'\sigma}(\mathbf{q}\tau;\mathbf{k}'\tau';\mathbf{k}0)$ which is defined by

$$\Gamma^{\gamma}_{\sigma'\sigma}(\mathbf{q}\tau;\mathbf{k}'\tau';\mathbf{k}0) \equiv - \langle T_{\tau}\ \phi_{\mathbf{q}\gamma}(\tau)\ c_{\mathbf{k}'\sigma'}(\tau')\ c^{\dagger}_{\mathbf{k}\sigma}(0)\rangle \quad , \tag{4-56}$$

the perturbation theory is usually employed for expanding the vertex function in a perturbation series (see Appendix.B).[44),45)] However, another procedure will be presented in the remaining part of this section. The equation of motion for the vertex function must be constructed. For this purpose the equation of motion for $\phi_{\mathbf{q}\gamma}(\tau)$ is first derived as

$$\frac{\partial^2}{\partial\tau^2}\phi_{\mathbf{q}\gamma}(\tau) = (\omega^0_{\mathbf{q}\gamma})^2\ \phi_{\mathbf{q}\gamma}(\tau) + 2\omega^0_{\mathbf{q}\gamma} \sum_{\mathbf{k}\sigma} I^{\gamma}(\mathbf{k}-\mathbf{q},\mathbf{k})\ c^{\dagger}_{\mathbf{k}-\mathbf{q}\sigma}(\tau)\ c_{\mathbf{k}\sigma}(\tau) \quad . \tag{4-57}$$

Here, a property of phonon frequencies $\omega^0_{\mathbf{q}\gamma}=\omega^0_{-\mathbf{q}\gamma}$ has been used. By utilizing eq.(4-57) the equation of motion for the vertex function $\Gamma^{\gamma}_{\sigma\sigma}(\mathbf{q}\tau;\mathbf{k}-\mathbf{q}\tau';\mathbf{k}0)$ can be written as

$$\frac{\partial^2}{\partial\tau^2}\Gamma^{\gamma}_{\sigma\sigma}(\mathbf{q}\tau;\mathbf{k}-\mathbf{q}\tau';\mathbf{k}0) = (\omega^0_{\mathbf{q}\gamma})^2\ \Gamma^{\gamma}_{\sigma\sigma}(\mathbf{q}\tau;\mathbf{k}-\mathbf{q}\tau';\mathbf{k}0) - 2\omega_{\mathbf{q}\gamma} \sum_{\mathbf{k}'\sigma'} I^{\gamma}(\mathbf{k}'-\mathbf{q},\mathbf{k}') \times \langle T_{\tau}\ c^{\dagger}_{\mathbf{k}'-\mathbf{q}\sigma'}(\tau)\ c_{\mathbf{k}'\sigma'}(\tau)\ c_{\mathbf{k}-\mathbf{q}\sigma}(\tau')\ c^{\dagger}_{\mathbf{k}\sigma}(0)\rangle \quad . \tag{4-58}$$

On the other hand, the equation of motion for the "dressed" phonon Green's function $D_\gamma(q,\tau)$ is expressed by

$$\frac{\partial^2}{\partial\tau^2} D_\gamma(q,\tau) = (\omega^0_{q\gamma})^2 D_\gamma(q,\tau) + 2\omega^0_{q\gamma} \delta(\tau) + 2\omega^0_{q\gamma} \sum_{k\sigma} I^\gamma(k-q,k) \langle T_\tau c^\dagger_{k-q\sigma}(\tau) c_{k\sigma}(\tau) \phi_{-q\gamma}(0)\rangle \quad . \tag{4-59}$$

By using eq.(4-59) with neglecting the third term on the right-hand side, which contains another vertex function, eq.(4-58) can be transformed to an integral representation:

$$\Gamma^\gamma_{\sigma\sigma}(q\tau;k-q\tau';k0) = -\int_0^\beta d\tau_1 \, D_\gamma(q,\tau-\tau_1) \sum_{k'\sigma'} I^\gamma(k'-q,k') \times \langle T_\tau c^\dagger_{k'-q\sigma'}(\tau_1) c_{k'\sigma'}(\tau_1) c_{k-q\sigma}(\tau') c^\dagger_{k\sigma}(0)\rangle \quad . \tag{4-60}$$

Substituting this expression into eq.(4-55), we obtain

$$-\frac{\partial}{\partial\tau} G_\sigma(k,\tau) = \delta(\tau) + (E^0_k - \mu) G_\sigma(k,\tau) - \sum_{q\gamma} I^\gamma(k-q,k)^* \int_0^\beta d\tau_1 \, D(q,\tau-\tau') \sum_{k'\sigma'} I^\gamma(k'-q,k') \times \langle T_\tau c^\dagger_{k'-q\sigma'}(\tau_1) c_{k'\sigma'}(\tau_1) c_{k-q\sigma}(\tau) c^\dagger_{k\sigma}(0)\rangle \quad . \tag{4-61}$$

Following the principle of the generalized Hartree-Fock approximation, the thermal average on the right-hand side of eq.(4-61) is decoupled as

$$\langle T_\tau \; c^\dagger_{k'-q\sigma'}(\tau_1) \; c_{k'\sigma'}(\tau_1) \; c_{k-q\sigma}(\tau) \; c^\dagger_{k\sigma}(0)\rangle$$

$$\rightarrow \langle T_\tau \; c_{k-q\sigma}(\tau) \; c^\dagger_{k-q\sigma}(\tau_1)\rangle\langle T_\tau \; c_{k\sigma}(\tau_1) \; c^\dagger_{k\sigma}(0)\rangle \; \delta_{k',k} \; \delta_{\sigma',\sigma}$$

$$- \langle T_\tau \; c_{k-q\sigma}(\tau) \; c_{-k+q-\sigma}(\tau_1)\rangle\langle T_\tau \; c^\dagger_{-k-\sigma}(\tau_1) \; c^\dagger_{k\sigma}(0)\rangle$$

$$\times \; \delta_{k',-k+q} \; \delta_{\sigma',-\sigma} \quad . \tag{4-62}$$

It is noted that the second term on the right-hand side in eq.(4-62) has been reserved for the Cooper pairs condensation. Then, the equation of motion (4-61) can be rewritten as

$$-\frac{\partial}{\partial\tau} G_\sigma(k,\tau) = \delta(\tau) + (E^0_k - \mu) \; G_\sigma(k,\tau)$$

$$- \int_0^\beta d\tau_1 \sum_{q\gamma} |I^\gamma(k-q,k)|^2 \; D_\gamma(q,\tau-\tau_1) \; G_\sigma(k-q,\tau-\tau_1) \; G_\sigma(k,\tau_1)$$

$$+ \int_0^\beta d\tau_1 \sum_{q\gamma} |I^\gamma(k-q,k)|^2 \; D_\gamma(q,\tau-\tau_1) \; F_\sigma(k-q,\tau-\tau_1) \; F^\dagger_\sigma(k,\tau_1) \quad , \tag{4-63}$$

where $F_\sigma(k,\tau)$ and $F^\dagger_\sigma(k,\tau)$ are the Gor'kov's anomalous Green's functions defined by eqs.(4-27) and (4-28), respectively. In deriving eq.(4-63), the conditions $I^\gamma(k,k') = I^\gamma(-k,-k')^* = I^\gamma(k',k)^*$ are used.

Now, the self-energies for the normal and anomalous Green's functions are defined by

$$\Sigma^G_\sigma(k,\tau) = \sum_{q\gamma} |I^\gamma(k-q,k)|^2 \; D_\gamma(q,\tau) \; G_\sigma(k-q,\tau) \quad , \tag{4-64}$$

$$\Sigma_\sigma^F(k,\tau) = \sum_{q\gamma} |I^\gamma(k-q,k)|^2 \; D_\gamma(q,\tau) \; F_\sigma(k-q,\tau) \quad . \qquad (4\text{-}65)$$

By using these self-energies, eq.(4-63) is rewritten as

$$-\frac{\partial}{\partial\tau} G_\sigma(k,\tau) = \delta(\tau) + (E_k^0 - \mu) \; G_\sigma(k,\tau)$$

$$+ \int_0^\beta d\tau_1 [\Sigma_\sigma^G(k,\tau-\tau_1) \; G_\sigma(k,\tau_1) + \Sigma_\sigma^F(k,\tau-\tau_1) \; F_\sigma^\dagger(k,\tau_1)] \quad . \qquad (4\text{-}66)$$

Then, eq.(4-66) can be transformed to the Fourier component as

$$[i\varepsilon_n - E_k^0 + \mu - \Sigma_\sigma^G(k,i\varepsilon_n)] \; G_\sigma(k,i\varepsilon_n) = 1 + \Sigma_\sigma^F(k,i\varepsilon_n) \; F_\sigma^\dagger(k,i\varepsilon_n) \quad , \qquad (4\text{-}67)$$

where the Fourier coefficients of self-energies are defined by

$$\Sigma_\sigma^G(k,i\varepsilon_n) \equiv \frac{1}{2} \int_{-\beta}^{\beta} d\tau \; e^{-i\varepsilon_n\tau} \; \Sigma_\sigma^G(k,\tau)$$

$$= \frac{1}{\beta} \sum_{m=-\infty}^{\infty} \sum_{k'\gamma} |I^\gamma(k',k)|^2 \; D_\gamma(k-k',i\varepsilon_n-i\varepsilon_m) \; G_\sigma(k',i\varepsilon_m) \quad , \qquad (4\text{-}68)$$

$$\Sigma_\sigma^F(k,i\varepsilon_n) \equiv \frac{1}{2} \int_{-\beta}^{\beta} d\tau \; e^{-i\varepsilon_n\tau} \; \Sigma_\sigma^F(k,\tau)$$

$$= \frac{1}{\beta} \sum_{m=-\infty}^{\infty} \sum_{k'\gamma} |I^\gamma(k',k)|^2 \; D_\gamma(k-k',i\varepsilon_n-i\varepsilon_m) \; F_\sigma(k',i\varepsilon_m) \quad . \qquad (4\text{-}69)$$

Similarly, the equation of motion for $F_\sigma^\dagger(\mathbf{k},\tau)$ can be derived as follows:

$$-\frac{\partial}{\partial\tau} F_\sigma^\dagger(\mathbf{k},\tau) = -(E_{\mathbf{k}}^0 - \mu) F_\sigma^\dagger(\mathbf{k},\tau) - \int_{-\beta}^{\beta} d\tau_1 [\Sigma_\sigma^G(\mathbf{k},\tau-\tau_1)^* F_\sigma^\dagger(\mathbf{k},\tau_1) - \Sigma_\sigma^F(\mathbf{k},\tau-\tau_1) G_\sigma(\mathbf{k},\tau_1)] \quad . \tag{4-70}$$

And its Fourier transform is given by

$$[i\varepsilon_n + E_{\mathbf{k}}^0 - \mu + \Sigma_\sigma^G(\mathbf{k},-i\varepsilon_n)] F_\sigma^\dagger(\mathbf{k},i\varepsilon_n) = \Sigma_\sigma^F(\mathbf{k},i\varepsilon_n) G_\sigma(\mathbf{k},i\varepsilon_n) \quad . \tag{4-71}$$

Eqs.(4-67) and (4-71) can be written in the matrix form as follows:

$$\begin{pmatrix} i\varepsilon_n - E_{\mathbf{k}}^0 + \mu - \Sigma_\sigma^G(\mathbf{k},i\varepsilon_n) & \Sigma_\sigma^F(\mathbf{k},i\varepsilon_n) \\ \Sigma_\sigma^F(\mathbf{k},i\varepsilon_n) & i\varepsilon_n + E_{\mathbf{k}}^0 - \mu + \Sigma_\sigma^G(\mathbf{k},-i\varepsilon_n) \end{pmatrix} \times \begin{pmatrix} G_\sigma(\mathbf{k},i\varepsilon_n) \\ F_\sigma^\dagger(\mathbf{k},i\varepsilon_n) \end{pmatrix} = \begin{pmatrix} 1 \\ 0 \end{pmatrix} \quad . \tag{4-72}$$

Thus, the Green's functions can be solved by inverting the matrix equation (4-72) in the following form:

$$G_\sigma(\mathbf{k},i\varepsilon_n) = [i\varepsilon_n + E^0_{\mathbf{k}} - \mu + \Sigma^G_\sigma(\mathbf{k},-i\varepsilon_n)] \;/\; \Xi_\sigma(\mathbf{k},i\varepsilon_n) \quad , \tag{4-73}$$

$$F^\dagger_\sigma(\mathbf{k},i\varepsilon_n) = \Sigma^F_\sigma(\mathbf{k},i\varepsilon_n) \;/\; \Xi_\sigma(\mathbf{k},i\varepsilon_n) \quad , \tag{4-74}$$

where $\Xi_\sigma(\mathbf{k},i\varepsilon_n)$ denotes the determinant of the coefficient matrix of eq.(4-72) and is given by

$$\Xi_\sigma(\mathbf{k},i\varepsilon_n) = [i\varepsilon_n - E^0_{\mathbf{k}} + \mu - \Sigma^G_\sigma(\mathbf{k},i\varepsilon_n)] \times [i\varepsilon_n + E^0_{\mathbf{k}} - \mu + \Sigma^G_\sigma(\mathbf{k},-i\varepsilon_n)] - [\Sigma^F_\sigma(\mathbf{k},i\varepsilon_n)]^2 \quad . \tag{4-75}$$

It is noted that the excitation spectrum and its damping are determined from the pole of the analytic continuation of $G_\sigma(\mathbf{k},i\varepsilon_n)$ on to the real axis $\varepsilon+i\delta$. In the normal limit, i.e. $\Sigma^F_\sigma(\mathbf{k},\varepsilon)\to 0$, the excitation spectrum is determined by solving the equation

$$G_\sigma(\mathbf{k},\varepsilon+i\delta)^{-1} = \varepsilon - E^0_{\mathbf{k}} + \mu - \Sigma^G_\sigma(\mathbf{k},\varepsilon+i\delta) = 0 \quad . \tag{4-76}$$

When the self-energy $\Sigma^G_\sigma(\mathbf{k},\varepsilon+i\delta)$ can be expanded around $\varepsilon=0$ in the form

$$\Sigma^G_\sigma(\mathbf{k},\varepsilon+i\delta) \simeq \Sigma^G_\sigma(\mathbf{k},0) - \lambda_{\mathbf{k}}\cdot\varepsilon + i\mathrm{Im}[\Sigma^G_\sigma(\mathbf{k},i\delta)] \quad , \tag{4-77}$$

with

$$\lambda_{\mathbf{k}} \equiv - \left. \frac{\partial \, \mathrm{Re}[\Sigma_\sigma^G(\mathbf{k},\varepsilon)]}{\partial \varepsilon} \right|_{\varepsilon=0} , \tag{4-78}$$

eq.(4-76) is solved in the following form:

$$\varepsilon = E_{\mathbf{k}}^N \equiv \frac{E_{\mathbf{k}}^0 - \tilde{\mu}_{\mathbf{k}}}{1 + \lambda_{\mathbf{k}}} - i\Gamma_{\mathbf{k}} , \tag{4-79}$$

with

$$\tilde{\mu}_{\mathbf{k}} \equiv \mu - \Sigma_\sigma^G(\mathbf{k},0) , \tag{4-80}$$

$$\Gamma_{\mathbf{k}} \equiv - \mathrm{Im}[\Sigma_\sigma^G(\mathbf{k},i\delta)]/(1 + \lambda_{\mathbf{k}}) , \tag{4-81}$$

where the small change in the chemical potential $\tilde{\mu}_{\mathbf{k}}-\mu$ and the damping $\Gamma_{\mathbf{k}}$ may be uninteresting quantities and negligible for usual metals. It is noted that the excitation energy $E_{\mathbf{k}}^N$ in the normal state is renormalized by a factor $(1+\lambda_{\mathbf{k}})^{-1}$, where $\lambda_{\mathbf{k}}$ is known as the mass enhancement factor.

On the other hand, in the superconducting state the excitation energy is determined by solving the equation

$$\Xi_\sigma(\mathbf{k},\varepsilon+i\delta) = [\varepsilon - E_{\mathbf{k}}^0 + \mu - \Sigma_\sigma^G(\mathbf{k},\varepsilon+i\delta)] \times [\varepsilon + E_{\mathbf{k}}^0 - \mu + \Sigma_\sigma^G(\mathbf{k},-\varepsilon-i\delta)] - [\Sigma_\sigma^F(\mathbf{k},\varepsilon+i\delta)]^2 = 0 . \tag{4-82}$$

When the self-energiy $\Sigma_\sigma^G(\mathbf{k},\varepsilon)$ is devided into the odd $\xi(\mathbf{k},\varepsilon)$ and

even $\eta(\mathbf{k},\varepsilon)$ parts relative for the energy ε, eq.(4-82) becomes

$$[\varepsilon - \xi(\mathbf{k},\varepsilon+i\delta)]^2 - [E_{\mathbf{k}}^0 - \mu + \eta(\mathbf{k},\varepsilon+i\delta)]^2 - [\Sigma_\sigma^F(\mathbf{k},\varepsilon+i\delta)]^2 = 0 \tag{4-83}$$

or

$$\varepsilon = \frac{E_{\mathbf{k}}^0 - \mu + \eta(\mathbf{k},\varepsilon+i\delta)}{Z(\mathbf{k},\varepsilon+i\delta)} + \Delta(\mathbf{k},\varepsilon+i\delta) \quad , \tag{4-84}$$

with

$$Z(\mathbf{k},z) \equiv 1 - \frac{\xi(\mathbf{k},z)}{z} \quad , \tag{4-85}$$

$$\Delta(\mathbf{k},z) \equiv \frac{\Sigma_\sigma^F(\mathbf{k},z)}{Z(\mathbf{k},z)} \quad , \tag{4-86}$$

where $Z(\mathbf{k},z)$ is called as the renormalization function, and $\Delta(\mathbf{k},z)$ as the gap function, respectively. By using the similar expansion as eq.(4-77) for $\xi(\mathbf{k},\varepsilon)$ and $\eta(\mathbf{k},\varepsilon)$, and neglecting the energy dependence of $\Sigma_\sigma^F(\mathbf{k},\varepsilon)$, we get

$$\varepsilon = E_{\mathbf{k}}^S \equiv \pm [(E_{\mathbf{k}}^N)^2 + \Delta(\mathbf{k},0)^2]^{1/2} \quad , \tag{4-87}$$

which corresponds to the BCS result.

It is convenient to solve the equation for the self-energies $\Sigma_\sigma^G(\mathbf{k},i\omega_n)$ and $\Sigma_\sigma^F(\mathbf{k},i\omega_n)$ in the self-consistent manner. For this purpose eqs.(4-73) and (4-74) are substituted into the right-hand side of eqs.(4-68) and (4-69), respectively. Then, we obtain

$$\Sigma_\sigma^G(\mathbf{k},i\varepsilon_n) = \frac{1}{\beta}\sum_{m=-\infty}^{\infty}\sum_{\mathbf{k}'\gamma}\sum |I^\gamma(\mathbf{k},\mathbf{k}')|^2 D_\gamma(\mathbf{k}-\mathbf{k}',i\varepsilon_n-i\varepsilon_m) \times \frac{i\varepsilon_m + E^0_{\mathbf{k}'} - \mu + \Sigma^G_\sigma(\mathbf{k}',-i\varepsilon_m)}{\Xi_\sigma(\mathbf{k}',i\varepsilon_m)} , \tag{4-88}$$

$$\Sigma_\sigma^F(\mathbf{k},i\varepsilon_n) = \frac{1}{\beta}\sum_{m=-\infty}^{\infty}\sum_{\mathbf{k}'\gamma}\sum |I^\gamma(\mathbf{k},\mathbf{k}')|^2 D_\gamma(\mathbf{k}-\mathbf{k}',i\varepsilon_n-i\varepsilon_m) \times \frac{\Sigma^F_\sigma(\mathbf{k}',i\varepsilon_m)}{\Xi_\sigma(\mathbf{k}',i\varepsilon_m)} . \tag{4-89}$$

Next, the spectral representation for the phonon Green's function $D_\gamma(\mathbf{q},i\omega_n)$ is introduced as

$$D_\gamma(\mathbf{q},i\omega_n) = -\frac{1}{\pi}\int_0^\infty d\Omega\ \mathrm{Im}\ D_\gamma(\mathbf{q},\Omega+i\delta)\ \frac{2\Omega}{(i\omega_n)^2 - \Omega^2} . \tag{4-90}$$

According to eq.(3-22), the imaginary part of the phonon Green's function can be approximately expressed in the Lorentzian form. If the phonon line-width $\Gamma_{\mathbf{q}\gamma}$ or the imaginary part of polarization function $\Pi''_\gamma(\mathbf{q})$ are assumed to be neglected, the spectral representation (4-90) becomes

$$D_\gamma(\mathbf{q},i\omega_n) = \frac{\omega^0_{\mathbf{q}\gamma}}{\omega_{\mathbf{q}\gamma}}\int_0^\infty d\Omega\ \delta(\Omega-\omega_{\mathbf{q}\gamma})\ \frac{2\Omega}{\omega_n^2 + \Omega^2} . \tag{4-91}$$

Substituting the spectral representation (4-91) into eqs.(4-88)

and (4-89), the self-consistent equations become

$$\Sigma_\sigma^G(\mathbf{k},i\varepsilon_n) = \frac{k_B T}{N(E_F)} \sum_{m=-\infty}^{\infty} \sum_{\mathbf{k}'} \int_0^\infty d\Omega\ \alpha^2 F(\mathbf{k},\mathbf{k}';\Omega)\ \frac{2\Omega}{(\varepsilon_n-\varepsilon_m)^2+\Omega^2} \times \frac{i\varepsilon_m + E^0_{\mathbf{k}'} - \mu + \Sigma_\sigma^G(\mathbf{k}',-i\varepsilon_m)}{\Xi_\sigma(\mathbf{k}',i\varepsilon_m)} \quad , \tag{4-92}$$

$$\Sigma_\sigma^F(\mathbf{k},i\varepsilon_n) = \frac{k_B T}{N(E_F)} \sum_{m=-\infty}^{\infty} \sum_{\mathbf{k}'} \int_0^\infty d\Omega\ \alpha^2 F(\mathbf{k},\mathbf{k}';\Omega)\ \frac{2\Omega}{(\varepsilon_n-\varepsilon_m)^2+\Omega^2} \times \frac{\Sigma_\sigma^F(\mathbf{k}',i\varepsilon_m)}{\Xi_\sigma(\mathbf{k}',i\varepsilon_m)} \quad . \tag{4-93}$$

$\alpha^2F(\mathbf{k},\mathbf{k}';\Omega)$ in eqs.(4-92) and (4-93) is the spectral function defined by

$$\alpha^2 F(\mathbf{k},\mathbf{k}';\Omega) \equiv N(E_F) \sum_\gamma \frac{\omega^0_{\mathbf{k}-\mathbf{k}'\gamma}}{\omega_{\mathbf{k}-\mathbf{k}'\gamma}} |I^\gamma(\mathbf{k},\mathbf{k}')|^2\ \delta(\Omega-\omega_{\mathbf{k}-\mathbf{k}'\gamma}) \quad , \tag{4-94}$$

and this function represents an intensity of the electron scattering between the Bloch states $\mathbf{k}$ and $\mathbf{k}'$ caused by phonons having an energy Ω.

Next step is a simplification of the self-consistent equations for the self-energies $\Sigma_\sigma^G(\mathbf{k},i\varepsilon_n)$ and $\Sigma_\sigma^F(\mathbf{k},i\varepsilon_n)$ to isotropic forms. The wave-vector dependence of the self-energy is assumed to be neglected (or averaged appropriately over the Fermi surfaces). This assumption may be justified for dirty

superconductors which lose the anisotropic character of crystallography. By using the eq.(4-92) and (4-93) the self-consistent equations are reduced in the following forms:

$$\Sigma_\sigma^G(i\varepsilon_n) = k_B T \sum_{m=-\infty}^{\infty} \lambda(\varepsilon_n-\varepsilon_m) \frac{1}{N(E_F)} \sum_{\mathbf{k}'} \frac{i\varepsilon_m + E_{\mathbf{k}}^0 - \mu + \Sigma_\sigma^G(-i\varepsilon_m)}{\Xi_\sigma(\mathbf{k}', i\varepsilon_m)} \quad , \tag{4-95}$$

$$\Sigma_\sigma^F(i\varepsilon_n) = k_B T \sum_{m=-\infty}^{\infty} \lambda(\varepsilon_n-\varepsilon_m) \frac{1}{N(E_F)} \sum_{\mathbf{k}'} \frac{\Sigma_\sigma^F(i\varepsilon_m)}{\Xi_\sigma(\mathbf{k}', i\varepsilon_m)} \quad , \tag{4-96}$$

with

$$\lambda(\varepsilon_n-\varepsilon_m) \equiv \int_0^\beta d\Omega \; \alpha^2F(\Omega) \frac{2\Omega}{(\varepsilon_n-\varepsilon_m)^2 + \Omega^2} \quad , \tag{4-97}$$

where $\alpha^2F(\Omega)$ denotes the spectral function averaged over the Fermi surface, which is expressed in terms of eq.(4-94) as

$$\begin{aligned} \alpha^2F(\Omega) &\equiv \frac{1}{N(E_F)^2} \sum\sum_{\mathbf{k}\mathbf{k}'} \alpha^2F(\mathbf{k},\mathbf{k}';\Omega) \; \delta(E_{\mathbf{k}}^0-E_F) \; \delta(E_{\mathbf{k}'}^0-E_F) \\ &= \frac{1}{N(E_F)} \sum\sum_{\mathbf{k}\mathbf{k}'\gamma} \sum \frac{\omega_{\mathbf{k}-\mathbf{k}'\gamma}^0}{\omega_{\mathbf{k}-\mathbf{k}'\gamma}} \left| I^\gamma(\mathbf{k},\mathbf{k}') \right|^2 \delta(\Omega-\omega_{\mathbf{k}-\mathbf{k}'\gamma}) \\ &\qquad \times \delta(E_{\mathbf{k}}^0-E_F) \; \delta(E_{\mathbf{k}'}^0-E_F) \quad . \end{aligned} \tag{4-98}$$

Again, the self-energy $\Sigma_\sigma^G(i\varepsilon_n)$ is devided into odd part $\xi(i\varepsilon_n)$ and even part $\eta(i\varepsilon_n)$, and $\eta(i\varepsilon_n)$ is included in the small change of the chemical potential, i.e. $\tilde{\mu}-\mu$. Then, eq.(4-95) becomes

$$\xi(i\varepsilon_n) = k_B T \sum_{m=-\infty}^{\infty} \lambda(\varepsilon_n-\varepsilon_m) \frac{1}{N(E_F)} \sum_{\mathbf{k}'} \frac{i\varepsilon_m - \xi(i\varepsilon_m)}{\Xi_\sigma(\mathbf{k}',i\varepsilon_m)} \quad , \tag{4-99}$$

with

$$\Xi_\sigma(\mathbf{k}',i\varepsilon_m) = [i\varepsilon_m - \xi(i\varepsilon_m)]^2 - [E^0_{\mathbf{k}'} - \tilde{\mu}]^2 - |\Sigma^F_\sigma(i\varepsilon_m)|^2 \quad . \tag{4-100}$$

With introducing the electronic density of states N(E), the $\mathbf{k}'$-summation is replaced by the energy integration as follows:

$$\sum_{\mathbf{k}'} \rightarrow \int_{-\infty}^{\infty} dE\ N(E) \simeq N(E_F) \int_{-\infty}^{\infty} dE$$

Then, the integration about E is performed by using the Cauchy's formula for complex integration:

$$\xi(i\varepsilon_n) = \pi i k_B T \sum_{m=-\infty}^{\infty} \lambda(\varepsilon_n-\varepsilon_m) \frac{i\varepsilon_m - \xi(i\varepsilon_m)}{\Omega_\sigma(i\varepsilon_m)} \text{ sign}[\text{Im } \Omega_\sigma(i\varepsilon_m)] \quad , \tag{4-101}$$

with

$$\Omega^2_\sigma(i\varepsilon_m) \equiv [i\varepsilon_m - \xi(i\varepsilon_m)]^2 - [\Sigma^F_\sigma(i\varepsilon_m)]^2 \quad . \tag{4-102}$$

By analogy with eqs.(4-85) and (4-86) the renormalization function $Z(i\varepsilon_n) \equiv 1-\xi(i\varepsilon_n)/i\varepsilon_n$ and the gap function $\Delta(i\varepsilon_n) \equiv \Sigma^F(i\varepsilon_n)/Z(i\varepsilon_n)$ are introduced so that eq.(4-102) becomes

$$\Omega_\sigma^2(i\varepsilon_m) = (i\varepsilon_m)^2 Z(i\varepsilon_m)^2 - [\Sigma_\sigma^F(i\varepsilon_m)]^2$$
$$= Z(i\varepsilon_m)^2 [(i\varepsilon_m)^2 - \Delta(i\varepsilon_m)^2] \quad . \qquad (4\text{-}103)$$

By taking this into account, eq.(4-101) becomes

$$\xi(i\varepsilon_n) = \pi i k_B T \sum_{m=-\infty}^{\infty} \lambda(\varepsilon_n - \varepsilon_m) \frac{i\varepsilon_m}{[(i\varepsilon_m)^2 - \Delta(i\varepsilon_m)^2]^{1/2}} \quad . \qquad (4\text{-}104)$$

It is readily found that eq.(4-96) can also be rewritten in the equation for the gap function $\Delta(i\varepsilon_n)$ as follows:

$$\Delta(i\varepsilon_n) = \frac{\pi i k_B T}{Z(i\varepsilon_n)} \sum_{m=-\infty}^{\infty} \lambda(\varepsilon_n - \varepsilon_m) \frac{\Delta(i\varepsilon_m)}{[(i\varepsilon_m)^2 - \Delta(i\varepsilon_m)^2]^{1/2}} \quad . \qquad (4\text{-}105)$$

In order to obtain complete informations in the superconducting state eqs.(4-104) and (4-105) should be solved in the self-consistent manner with $Z(i\varepsilon_n)=1-\xi(i\varepsilon_n)/i\varepsilon_n$. The coupled equation is nothing but the "Eliashberg" equation in the Matsubara's imaginary frequency version. On the other hand, real frequency version of that is given in Appendix.C.

4-2. Spectral function $\alpha^2F(\omega)$

To discuss the sperconductivity of BPB and BKB in the framework of the strong coupling theory based on the phonon mechanism we first calculate the spectral function $\alpha^2F(\omega)$ and the dimensionless electron-phonon coupling constant λ defined respectively by

$$\alpha^2F(\omega) = \frac{1}{N(E_F)} \sum_{\mathbf{k}\mathbf{k}'} \sum_{\gamma} \frac{|V^{\gamma}(\mathbf{k},\mathbf{k}')|^2}{2N\omega^{\gamma}_{\mathbf{k}'-\mathbf{k}}} \delta(E^0_{\mathbf{k}}-E_F)\ \delta(E^0_{\mathbf{k}'}-E_F)\ \delta(\omega-\omega^{\gamma}_{\mathbf{k}'-\mathbf{k}}) \ , \tag{4-106}$$

$$\lambda = 2\int_0^{\infty} \frac{\alpha^2F(\omega)}{\omega}\, d\omega \ , \tag{4-107}$$

where

$$V^{\gamma}(\mathbf{k},\mathbf{k}') = \sum_{\mu\alpha} \frac{1}{\sqrt{M_{\mu}}} \varepsilon_{\gamma,\mu\alpha}(\mathbf{k}-\mathbf{k}')g^{\alpha}_{\mu}(\mathbf{k},\mathbf{k}') \ , \tag{4-108}$$

with $\varepsilon_{\gamma,\mu\alpha}(\mathbf{k},\mathbf{k}')$ being the phonon polarization vector of mode γ.

We have calculated $\alpha^2F(\omega)$ for several values of x in the case of t'=4.05 eV/A, and the results are shown by full curves in Fig.4-1 with the phonon density of states $F(\omega)$ which is drawn by broken curves. It is found that $\alpha^2F(\omega)$ has a frequency dependence entirely different from that of $F(\omega)$. It should be noted that $\alpha^2F(\omega)$ has some prominent structures in the frequency range where O-stretching/breathing mode branches lie. Thus, this O-stretching/ breathing mode is expected to contribute dominantly

to the superconductivity. As x increases, some main peaks in $\alpha^2F(\omega)$ shift to lower energy side, reflecting the phonon frequency renormalisation, and the magnitude of $\alpha^2F(\omega)$ increases remamkably in the whole energy range up to 60 meV. This considerable change in $\alpha^2F(\omega)$ is expected to bring a remarkable x dependence of T_c.

In order to get rough estimate of T_c we have calculated also λ as a function of x. The results for t'=4.05 eV/A are shown in Fig.4-2. It is found that λ is enhanced significantly due to the renormalization of the L O-stretching/breathing mode, i.e. λ increases rapidly around x=0.5 and it exceeds 1.0 for x>0.7. Then, we may expect a high superconducting transition temperature such as $T_c \sim$ 30 K. However, to discuss the magnitude of T_c quantitatively, it is necessary to solve the Eliashberg equation[36] by using the calculated $\alpha^2F(\omega)$. It will be given in the next section, Sec.4-3.

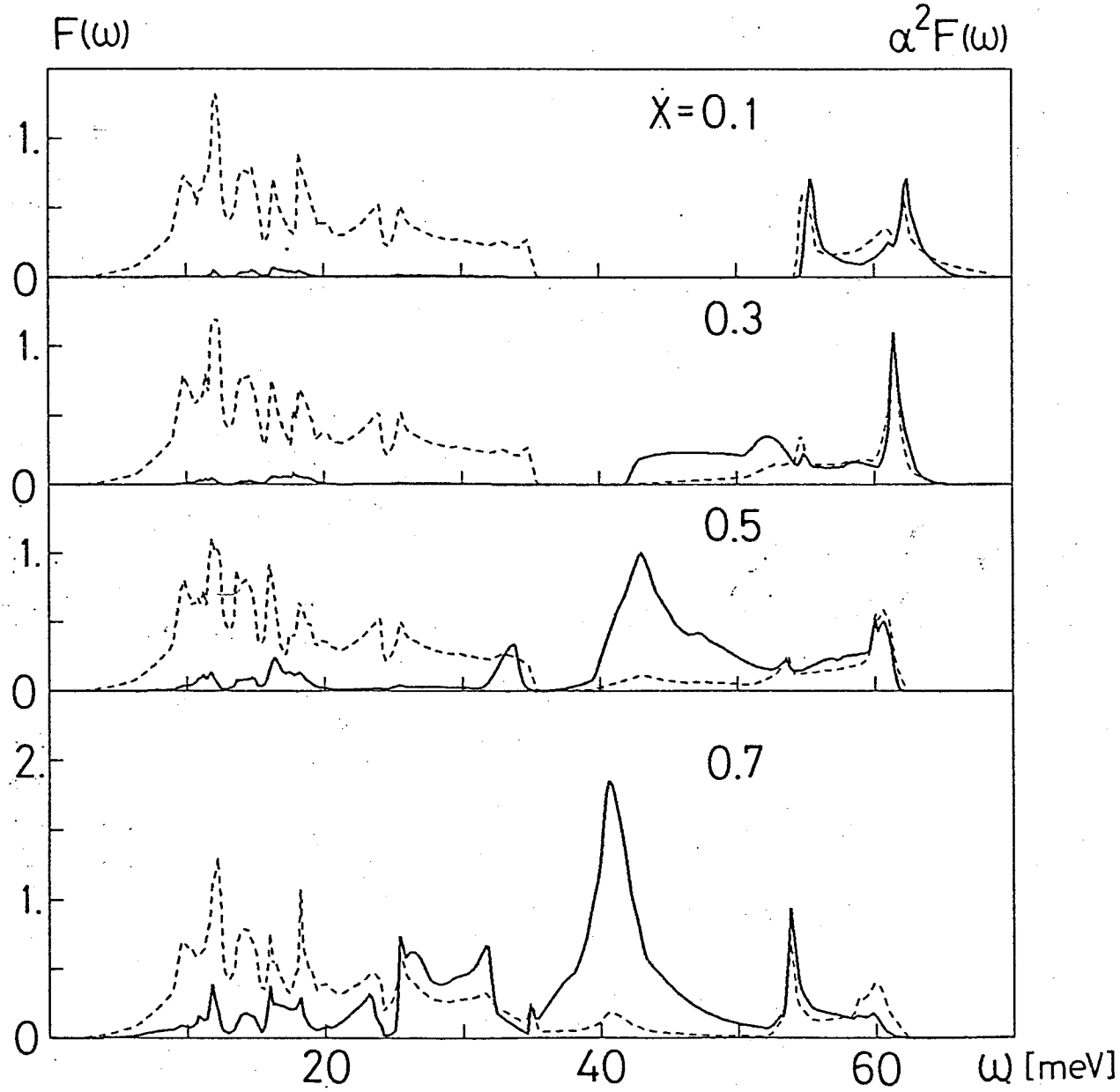

Fig.4-1. The spectral function $\alpha^2F(\omega)$ (full curves) calculated for x=0.1, 0.3, 0.5 and 0.7 in case of t'=4.05 eV/A. The calculated phonon density of states $F(\omega)$ are also shown by broken curves. Here, $\alpha^2F(\omega)$ is a dimensionless quantity and the unit of $F(\omega)$ is $(\text{meV}\cdot\text{unit cell})^{-1}$.

Fig.4-2. Dimensionless coupling constant λ calculated as a function of x in case of t'=4.05 eV/A. The shaded area denotes the region where the lattice becomes unstable.

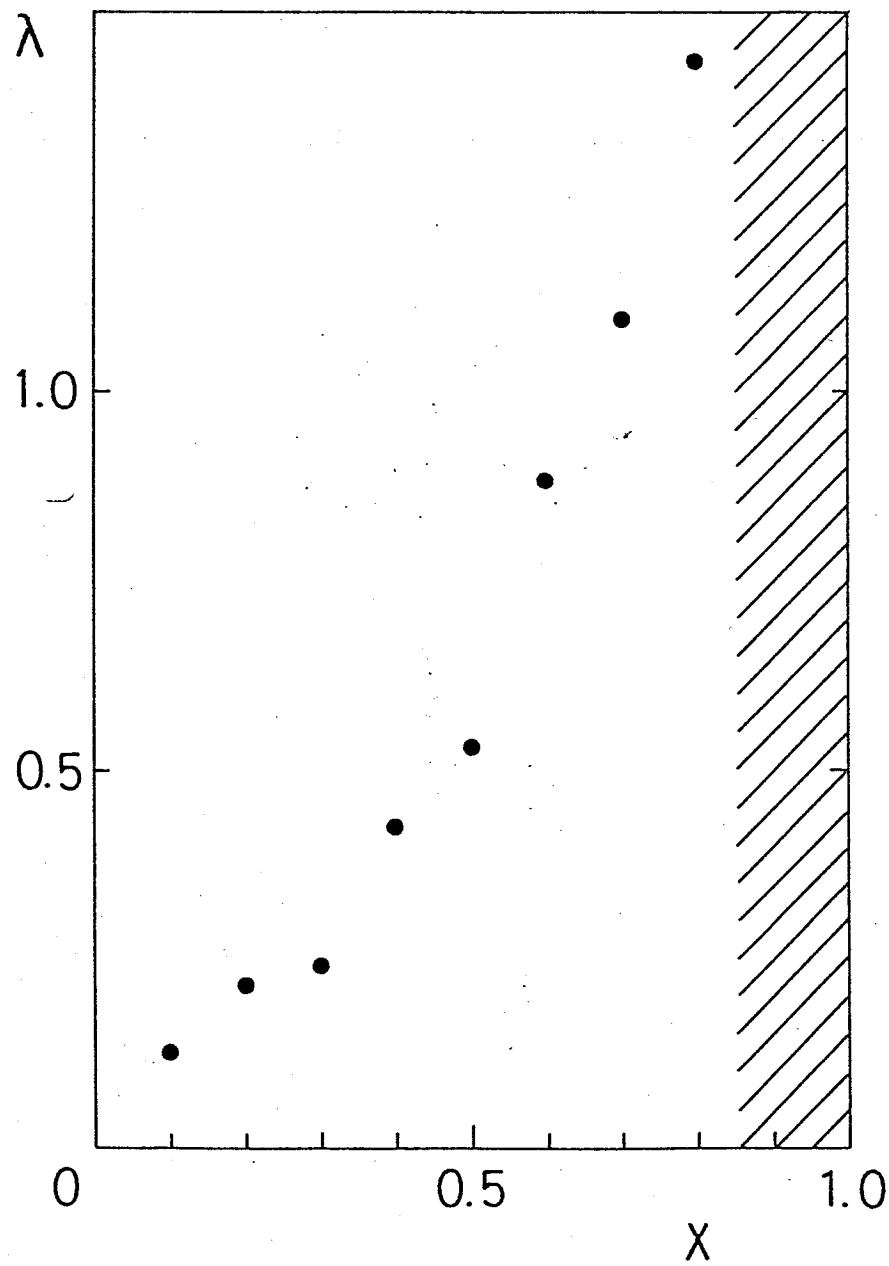

4-3. Transition temperature and isotope effect

Superconducting transition temperature T_c should be determined by solving linearlized Eliashberg equations at finite temperature.[35] It is much more convenient for numerical calculations to solve the "imaginary-axis" version of the Eliashberg equations which are defined on Matsubara imaginary frequencies $i\varepsilon_n=(2n+1)\pi i k_B T$ (n:integer), i.e. eqs.(4-104) and (4-105) in Sec.4-1-2. At any temperature $T<T_c$ the Eliashberg equations (4-104) and (4-105) are non-linear coupled equations.

When the temperature approaches to T_c, however, the coupled equations can be decoupled and expanded with respect to the self-energy for superconducting state (or the gap function $\Delta(i\varepsilon_n)$):[36]

$$\Delta(i\tilde{\varepsilon}_n) = \pi k_B T \sum_m \frac{\lambda(\varepsilon_n-\varepsilon_m) - \mu^*}{|\tilde{\varepsilon}_m|} \Delta(i\varepsilon_m) \quad , \tag{4-109}$$

where μ^* is the effective screened Coulomb repulsion constant,[46] and

$$\tilde{\varepsilon}_m = \varepsilon_m + \pi k_B T \sum_\ell \mathrm{sgn}(\varepsilon_\ell)\ \lambda(\varepsilon_m-\varepsilon_\ell) \quad , \tag{4-110}$$

$$\lambda(\varepsilon_n) = \int_0^\infty d\Omega\ \alpha^2F(\Omega)\ \frac{2\Omega}{\Omega^2 + \varepsilon_n^2} \quad , \tag{4-111}$$

which is related to the dimensionless electron-phonon coupling constant λ as $\lambda=\lambda(0)$.

The transition temperature T_c should be determined so that the linearlized gap equation (4-109) has any non-trivial solution at $T=T_c$:

$$\det\left| \pi k_B T_c \frac{\lambda(\varepsilon_n-\varepsilon_m) - \mu^*}{|\tilde{\varepsilon}_m|} - \delta_{mn} \right| = 0 \quad , \qquad (4\text{-}112)$$

There is an artificial method to reduce the above gap equation into a Hermitian form by introducing a pair-breaking parameter.[36] However, we need not such a method to calculate T_c, because the merit for the computation in the Hermitian form becomes less important with recent developments of numerical clculations. Thus, we use eq.(4-112) to determine T_c hereafter.

In calclating T_c we utilize the spectral function $\alpha^2F(\omega)$ calculated with t'=4.05 eV/A in the previous section. The obtained x-dependences of T_c are shown in Fig.4-3. For each x we have calculated T_c with four different values of μ^*, 0.0, 0.05, 0.1 and 0.15. In most superconductors μ^* has been taken empirically to be between 0.1 and 0.15. The calculated T_c increases rapidly with increasing x as long as the lattice instability dose not occur, and reaches 28 K at x=0.7 in case of λ=1.09 and μ^*=0.15. In the present case the lattice becomes unstable for x>0.9 (i.e. shaded region in Figs.4-2 and 4-3). Especially, it is confirmed that the frequency of the O-breathing phonon at the R-point vanishes in case of $BaBiO_3$ (x=1) and hence the lattice becomes unstable against formation of the distorted structure described by that phonon.

It should be noted here that one must be careful in using the McMillan's equation for T_c given by[47]

$$T_c = \frac{\Theta_D}{1.45} \exp\left[\frac{-1.04(1+\lambda)}{\lambda - \mu^*(1+0.62\lambda)}\right] , \qquad (4\text{-}113)$$

where Θ_D denotes the Debye temperature. For BPB Θ_D is estimated to be $\sim$ 190 K.[4] Then, if we use the above McMillan's equation to estimate T_c for λ=1.09 (μ^* is fixed at 0.15), we have T_c= 10.5 K. On the other hand, if we determine the value of λ from this McMillan's equation so as to get T_c= 28 K, we obtain a very large value of λ such as 3.0. Therefore, it is not justified to utilize the McMillan's equation with Θ_D for the evaluation of T_c in such a complex system as BPB or BKB. Our results for T_c agree well with observed T_c in BKB, but disagree with those in BPB. One of reasons for this discrepancy may be that the rigid-band model is insufficient to describe BPB, because in BPB the Pb atom, which is one of constitutive elements of the conduction band, is substituted randomly by the Bi atom.

Finally we have estimated the isotope shift of T_c by calculating T_c when ^{16}O is replaced with ^{17}O and ^{18}O. A characteristic exponent α, defined as $T_c \propto M_0^{-\alpha}$ (M_0: oxygen atomic mass), is evaluated from the slope of the $\ell n\ T_c$ vs. $\ell n\ M_0$ plots. A typical example for such plots is given in Fig.4-4 for t'=4.05 eV/A and x=0.7. The evaluated exponents α for x=0.5, 0.6 and 0.7 are listed in Table 4-1. It is found that α takes rather smaller values than the so-called BCS value (α=0.5).[37]

Experimentally the value of α is estimated to be 0.21 by Batlogg et al.,[48] 0.35 by Kondoh et al.[49] and 0.41 by Hinks et al.[50] The principal reason why α differs from the BCS value is that the vibration of atoms other than oxygens, such as Bi atoms, contribute appreciably to the superconductivity, particularly in case large phonon frequency renormalisation is caused by the electron-lattice interaction. Recently Barbee et al.[51] have carried out calculations of α in compound superconductors by using simplified model spectral function. They also have pointed out the possibility that the value of α can be much smaller than the BCS value in case of specific isotopic substitutions in compound superconductors.

		x		
		0.5	0.6	0.7
μ^*	0.	α = 0.42	0.43	0.45
	0.05	0.40	0.41	0.44
	0.10	0.39	0.40	0.43
	0.15	0.36	0.38	0.42

Table 4-1. Calculated oxygen isotope effect on T_c. The characteristic exponent α is defined by $T_c \propto M_0^{-\alpha}$ (M_0: mass of an oxygen atom).

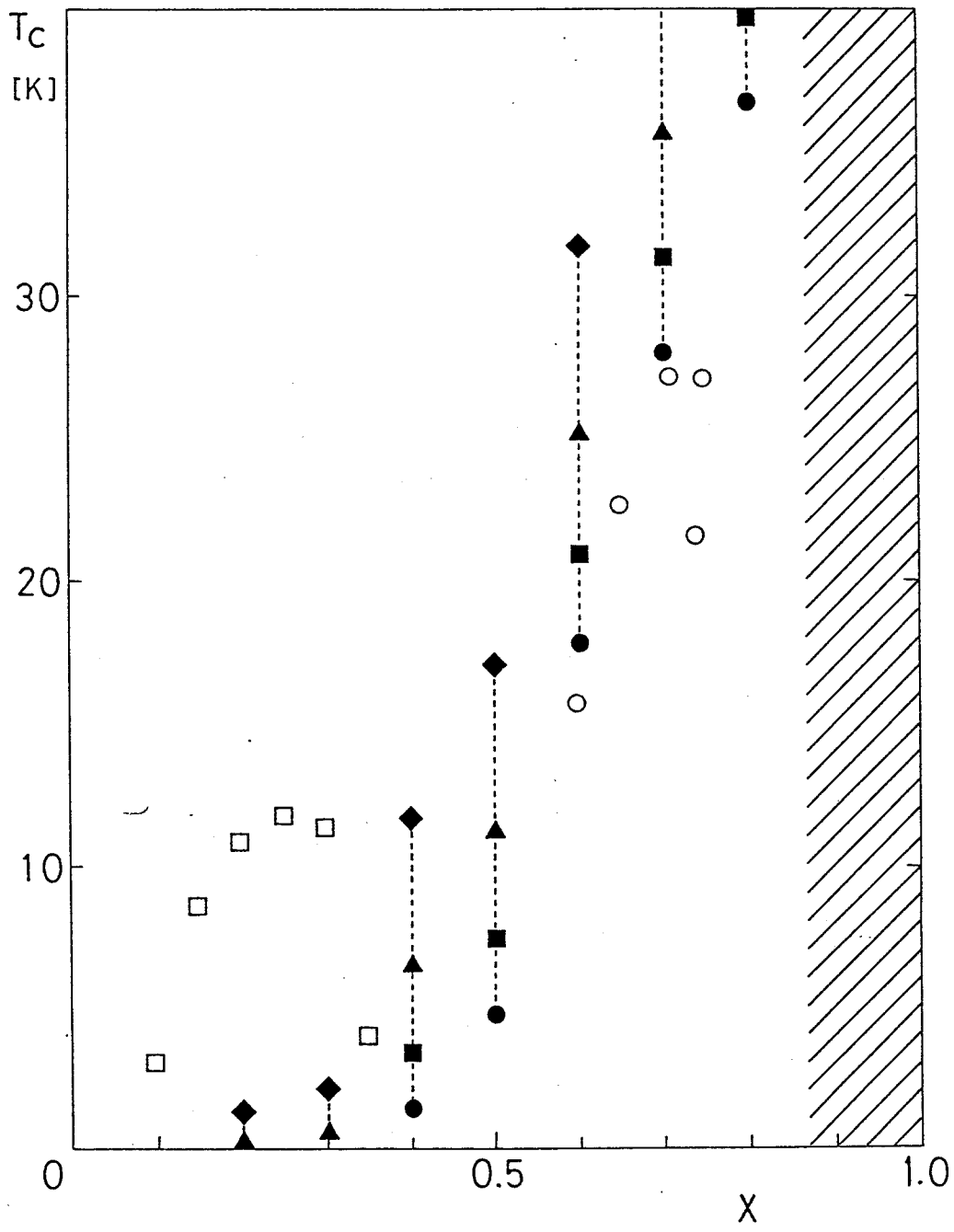

Fig.4-3. Superconducting transition temperature T_c as a function of x in case of t'=4.05 eV/A. The calculation of T_c is made for μ^* = 0.0 (◆), 0.05 (▲), 0.10 (■) and 0.15 (●), respectively. The shaded area denotes the region where the lattice instability occurs. The experimental data for BPB (□) and for BKB (○) are also shown.

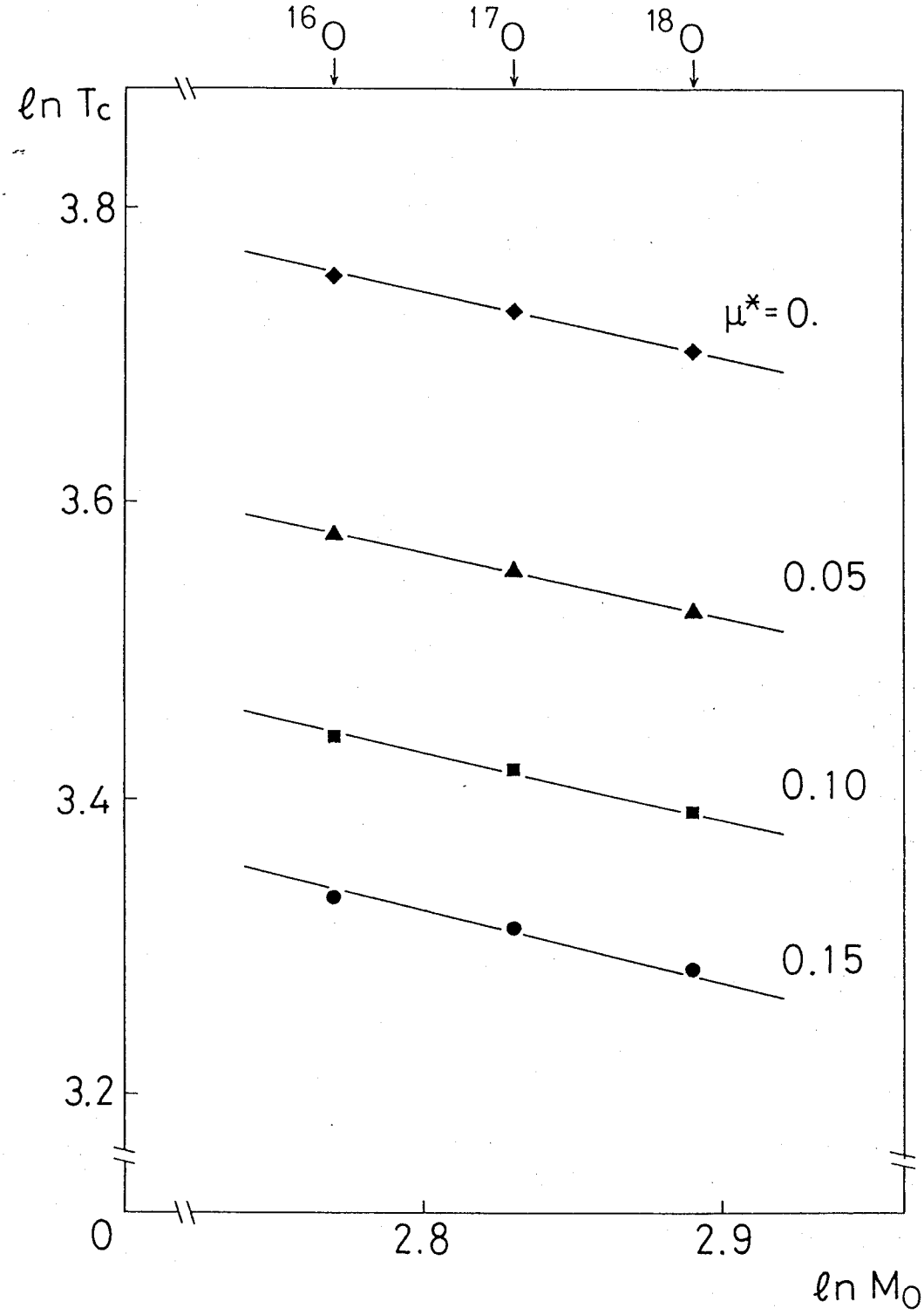

Fig.4-4. Isotopic shifts of T_c calculated for x=0.7. The characteristic exponent α defined by $T_c \propto M_0^{-\alpha}$ (M_0: mass of an oxigen atom) can be determined by the slope of the $\ell n\ T_c$ vs. $\ell n\ M_0$ plots.

4-4. Energy gap at T=0 K and tunneling experiment

Tunneling measurement is one of powerful methods which can observe directly the superconducting energy gap. An outline of the tunneling experiments is as follows. A superconducting specimen which is coverd by a thin (∿20 A) insulating oxide layer is attached to normal (or superconducting) metals. The tunneling current through the superconductor-insulator-normal (S-N) or superconductor-insulator-superconductor (S-S) junctions are measured as a function of applied voltage, I(V). Schrieffer-Scalapino-Wilkins[52] have shown that the differencial conductances dI/dV through the S-N junction is proportional to the electronic density of states $N_s(\varepsilon)$ in the superconducting state as

$$\left.\frac{dI}{dV}\right|_{eV=\varepsilon} \propto \frac{N_s(\varepsilon)}{N(E_F)} = \mathrm{Re}\left[\frac{|\varepsilon|}{[\varepsilon^2 - \Delta(\varepsilon)^2]^{1/2}}\right], \qquad (4\text{-}114)$$

where $N(E_F)$ denotes the electronic density of states at the Fermi level E_F in the normal state, and $\Delta(\varepsilon)$ represents the energy dependent gap function at T=0 K. Here, $\Delta(\omega)$ is determined by solving the Eliashberg equations for T=0 K and it is given by[38]

$$\xi(\varepsilon) = [1 - Z(\varepsilon)]\varepsilon$$

$$= \int_{\Delta_0}^{\infty} d\varepsilon' \ \mathrm{Re}\left\{ \frac{\varepsilon'}{[\varepsilon'^2 - \Delta(\varepsilon')^2]^{1/2}} \right\}$$

$$\times \int_0^{\infty} d\omega \ \alpha^2 F(\omega) \left\{ \frac{1}{\varepsilon' + \varepsilon + \omega - i\delta} - \frac{1}{\varepsilon' - \varepsilon + \omega - i\delta} \right\} \quad , \tag{4-115}$$

$$\Delta(\varepsilon) = \frac{1}{Z(\varepsilon)} \int_{\Delta_0}^{\infty} d\varepsilon' \ \mathrm{Re}\left\{ \frac{\varepsilon'}{[\varepsilon'^2 - \Delta(\varepsilon')^2]^{1/2}} \right\}$$

$$\times \int_0^{\infty} d\omega \ \alpha^2 F(\omega) \left\{ \frac{1}{\varepsilon' + \varepsilon + \omega - i\delta} + \frac{1}{\varepsilon' - \varepsilon + \omega - i\delta} \right\}$$

$$- \frac{\mu^*}{Z(\varepsilon)} \int_{\Delta_0}^{\varepsilon_c} d\varepsilon' \ \mathrm{Re}\left\{ \frac{\varepsilon'}{[\varepsilon'^2 - \Delta(\varepsilon')^2]^{1/2}} \right\} \quad , \quad (\delta \to +0) \tag{4-116}$$

where $\xi(\varepsilon)$ is the electronic self-energy of the normal state, $Z(\varepsilon) \equiv 1 - \xi(\varepsilon)/\varepsilon$ is called as the mass enhancement (or renormalization) function, and Δ_0 is the energy gap which appears in the electronic one-particle excitation spectrum or $N_s(\varepsilon)$. The gap Δ_0 is defined by

$$\Delta_0 = \Delta(\Delta_0) \quad , \tag{4-117}$$

(see also Appendix.C).

In deriving the gap equations (4-115) and (4-116) the

Coulomb interaction has been approximately replaced by the effective screened Coulomb repulsion constant μ^*, which is defined by[46)]

$$\mu^* = \frac{N(E_F)V_c}{1 + N(E_F)V_c \ell n(E_F/\varepsilon_c)} \quad , \tag{4-118}$$

where V_c is the static screened Coulomb interaction which is averaged over the Fermi surface, and ε_c is an appropriate cut-off energy.

In the week coupling limit (or the BCS result) $N_s(\varepsilon)$ can be written as

$$N_s(\varepsilon) = \sum_{\mathbf{k}} \delta(E_{\mathbf{k}} - \varepsilon)$$

$$\simeq N(E_F)\ \mathrm{Re}\left[\frac{|\varepsilon|}{[\varepsilon^2 - \Delta_0{}^2]^{1/2}} \right] \quad , \tag{4-118}$$

where $E_{\mathbf{k}} \equiv [(E^0_{\mathbf{k}})^2 + \Delta_0{}^2]^{1/2}$ represents the one-particle excitation energy in the superconducting state, and $E^0_{\mathbf{k}}$ is the electronic band energy in the normal state. The BCS energy gap Δ_0 is essentially the same quantity with that of the strong coupling theory, which is defined by eq.(4-117).

Once the spectral function $\alpha^2F(\omega)$ and μ^* are given, $\xi(\varepsilon)$ and $\Delta(\varepsilon)$ are calculated by utilizing eqs.(4-115) and (4-116) in a self-consistent manner. In actual calculation $\Delta(\varepsilon)$ has sufficiently converged in iteration of several times. The obtained $Z(\varepsilon)$ and $\Delta(\varepsilon)$ in case of $x=0.7$ and $\mu^*=0.1$ are shown in

Figs.4-5 and 4-6, respectively. Here, $\alpha^2F(\omega)$ obtained for t'=4.05 eV/A has been used in the present calculation. It is found that the real part of the renormalization function $Z(\varepsilon)$ has some little humps up to 60 meV, which indicates the electronic mass enhancement due to the strong coupling with relevalent phonons. The mass enhancement factor $Z(0)=1+\lambda$ is found to be 2.09 in the present case.

On the other hand, $\Delta(\varepsilon)$ has sharp and prominent structures reflecting the peaks in $\alpha^2F(\omega)$, and the structures are extended to higher energy range above 60 meV. The superconducting energy gap Δ_0 is found to be 4.8 meV. Since T_c has been evaluated to be 31.3 K in case of x=0.7 and $\mu^*=0.1$ in the previous section, the ratio $2\Delta_0/k_BT_c$ is found to be about 3.6, which is accidentally close to that predicted by the BCS theory ($2\Delta_0/k_BT_c=3.5$). Direct observation of Δ_0 has not been carried out for BKB yet, however, for BPB Akimitsu et al.[53] observed $2\Delta_0=1.69$ meV ($2\Delta_0/k_BT_c=3.45$ with $T_c=11.2$ K) from the tunneling measurement. In usual strong coupling superconductor the ratio $2\Delta_0/k_BT_c$ often deviates from the BCS value to larger side,[54] for example, 4.6 for Hg [55] and 4.3 for Pb.[56] It is still unresolved why the ratio agrees with the BCS one for BPB or BKB in spite of the strong electron-lattice coupling in these systems.

Further, such a prominent structures in $\Delta(\varepsilon)$ would be observed by the tunneling experiments.[38] Hence, we have also calculated the differential conductance dI/dV by making use of eq.(4-114). The result is shown by the full curve in Fig.4-7

together with the BCS result calculated by (4-118) (broken curve). The apparent deviation from the BCS reult is clearly seen whereas the deviation is about a few percent of the conductance in the normal state. Tunneling measurements with high resolution are desired in order to obtain the experimental evidence for strong coupling superconductivity in BKB.

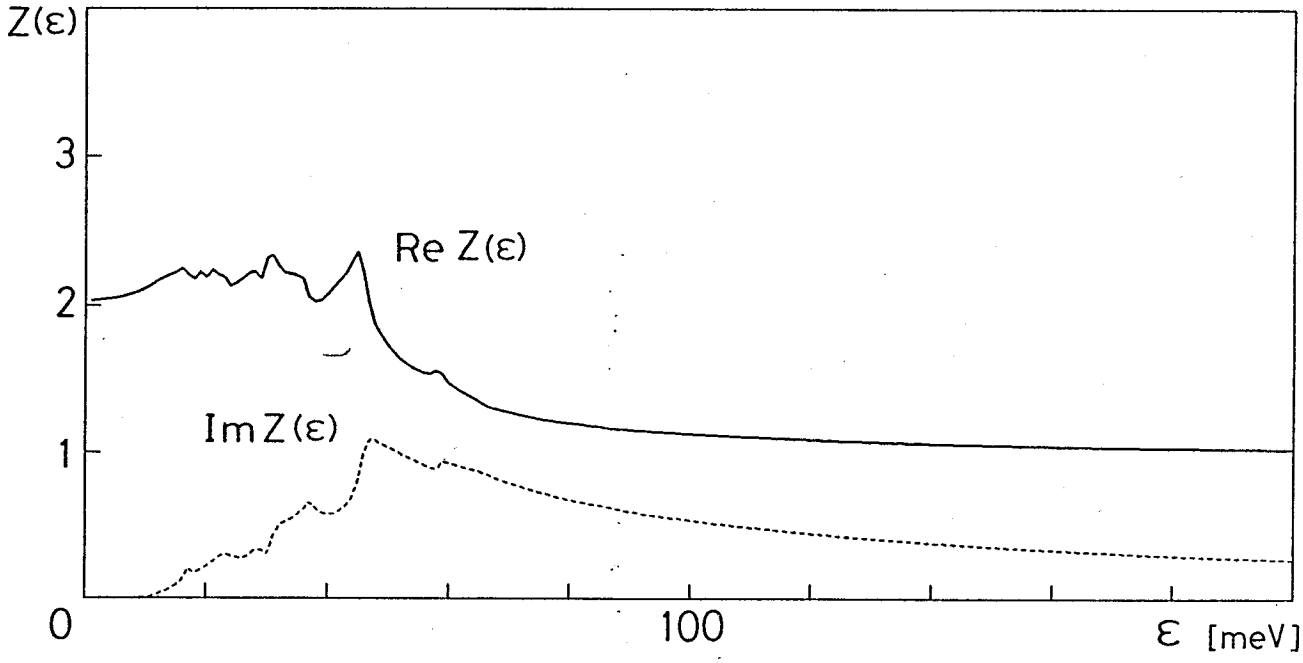

Fig.4-5. Renormalization function $Z(\varepsilon)$ determined by solving the Eliashberg equation for $x=0.7$ in case of $\mu^{*}=0.1$.

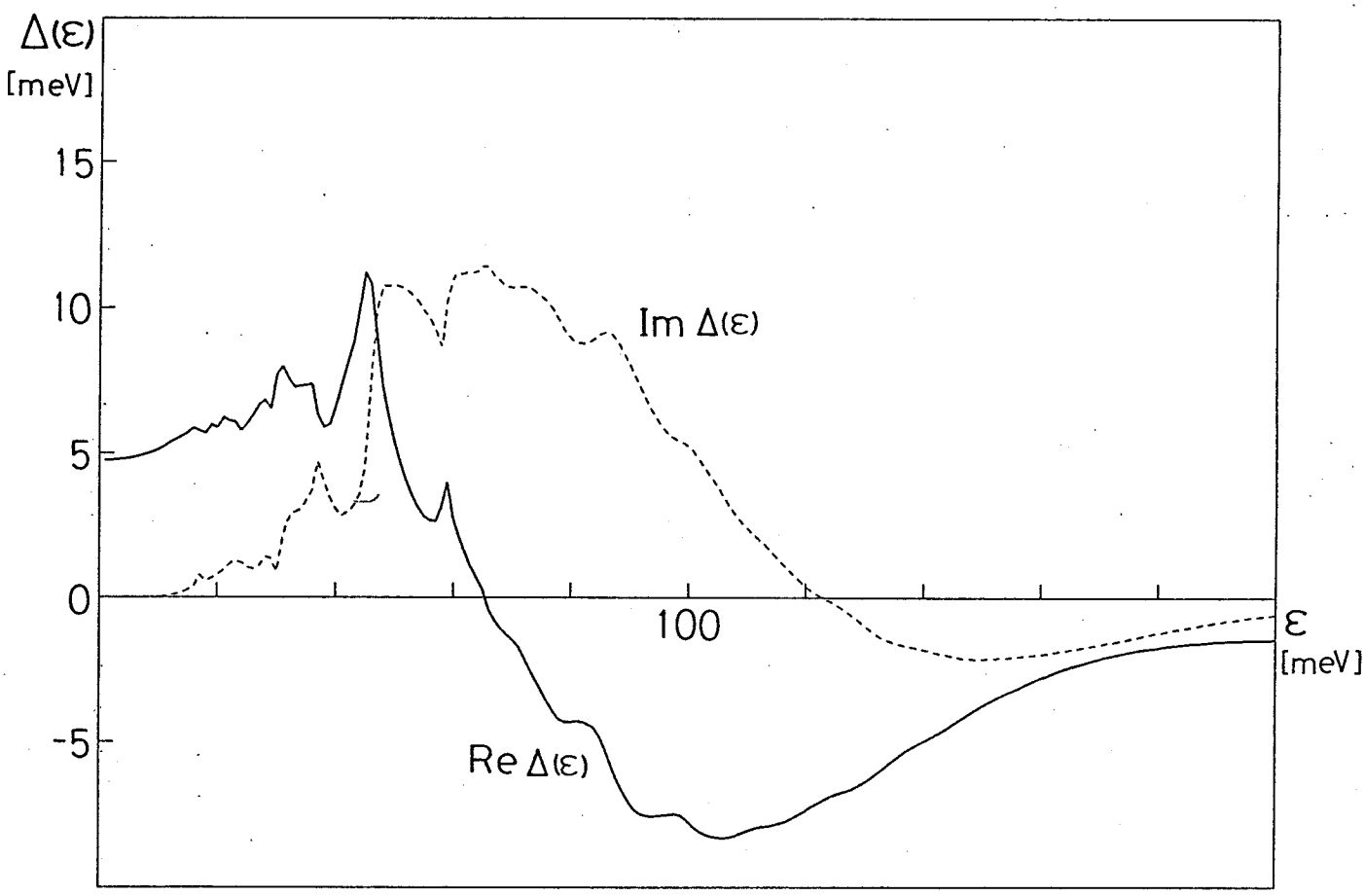

Fig.4-6. Calculated gap function $\Delta(\varepsilon)$ for x=0.7 in case of $\mu^{*}=0.1$.

Fig.4-7. Density of states (DOS) $N_s(\varepsilon)$ in the superconducting states. Here, $N_s(\varepsilon)$ is normalized by the DOS $N(E_F)$ at the Fermi level in the normal state. This quantity is identical with the tunneling differential conductance dI/dV through the normal(N)-superconducting(S) junction, which is measured in the unit of dI/dV through the N-N junction.

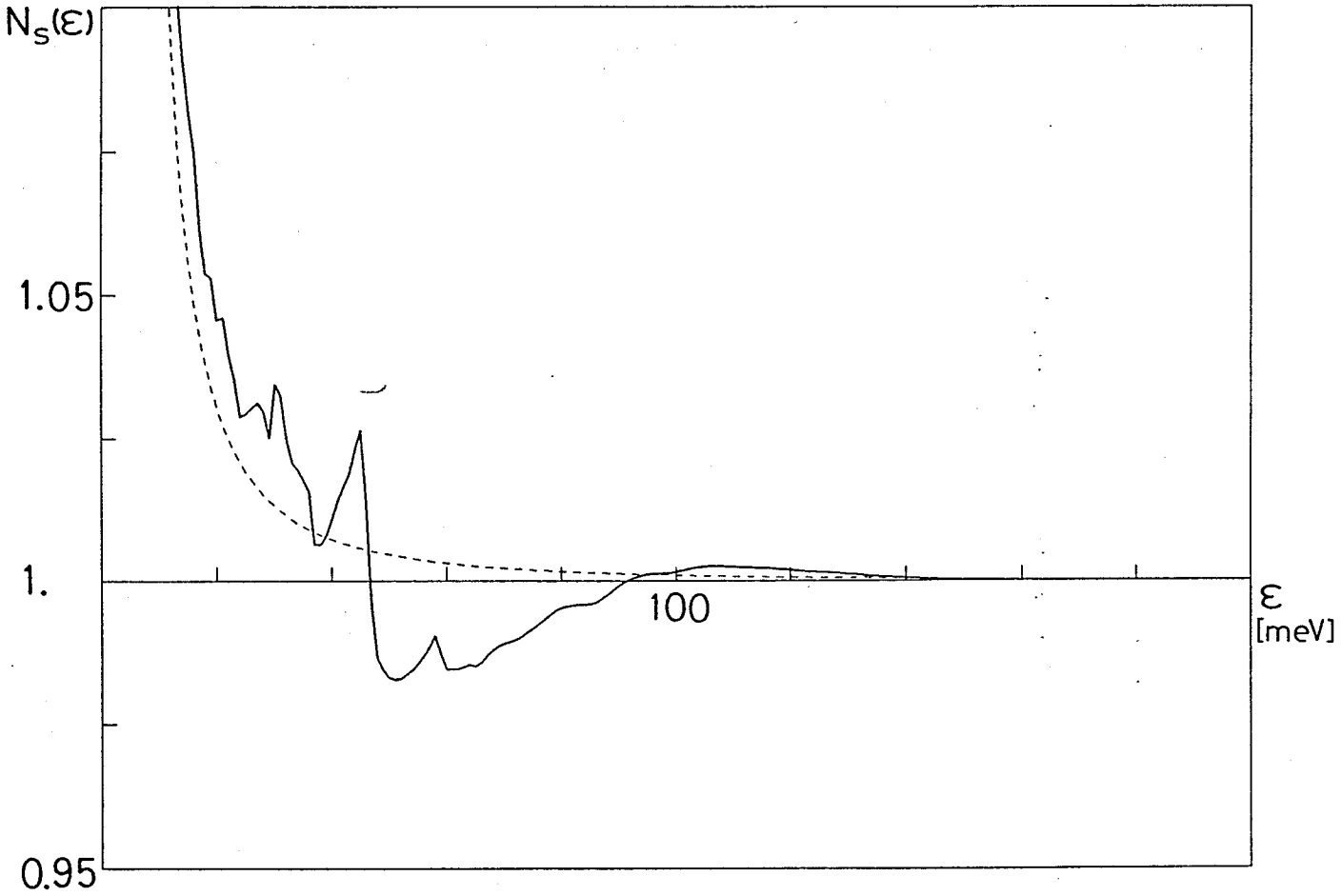

§5. Summary

First, the electron-lattice interaction of BPB and BKB has been calculated microscopically by using the realistic electronic band structure obtained by the orthogonal tight-binding approximation. We have confirmed that the vibrations of O atoms along the direction toward the nearest neighbouring Pb or Bi atoms have strong coupling with the conduction band states. This property of the electron-lattice coupling arises from the nature of the conduction band states, i.e. the conduction band states consist mainly of the 6s and 6p orbitals of Pb or Bi atoms and the 2p orbitals of O atoms.

Next, we have investigated the lattice dynamics of BPB and BKB by taking account of the effect of the electron-lattice interaction. It is found that the electron-lattice interaction causes the remarkable renormalization of the longitudinal (L) O-stretching and/or breathing mode phonons especially near the Brillouin zone boundary. The phonon frequencies of those modes become lower and lower with increasing the number of the conduction electrons or the composition x. And finaly the lattice instability occurs accompanied with vanishing of those phonons. The broadening of the renormalized phonons is also found from the calculation, which might be related with the absence of those phonon modes in the neutron scattering measurement.

Further, the superconductivity of BPB and BKB has been

discussed in the framework of the strong coupling theory of the phonon mechanism. We have obtained the following results.

(1) The spectral function $\alpha^2F(\omega)$ takes large values in the frequency range where the L O-stretching/breathing mode phonons lie, which implies the importance of those phonons.

(2) The transition temperature T_c has been calculated by solving the Eliashberg equation. It is found that T_c increases rapidly with increasing x, and reaches 30 K around x=0.7. The obtained x dependence of T_c agrees well with that observed in BKB.

(3) The isotope effect on T_c has been investigated by calculating T_c , when ^{16}O is replacing with ^{17}O and ^{18}O. The characteristic exponent α defined by $T_c \propto M_0^{-\alpha}$ has rather small value between 0.35 and 0.45 compaired with that predicted by the BCS theory (α=0.5). The results agree well with the experimental data obtained by Kondoh et al.(0.35) and/or by Hinks et al.(0.41).

(4) The gap function $\Delta(\varepsilon)$ has been calculated for T=0 K. The ratio $2\Delta_0/k_BT_c$ (Δ_0: superconducting energy gap) is found to have the value close to that predicted by the BCS (week coupling) theory ($2\Delta_0/k_BT_c$=3.5). However, the tunneling differential conductance dI/dV is turn out to show the behavior which is characteristic to the strong coupling superconductor.

Our results suggest that the superconducting properties in BKB, such as the magnitude of T_c and the isotope effect on T_c, can be

understood within the phonon mechanism. It is particularly emphasized that the significant renormalization of the L O-stretching/breathing mode phonons plays an important role for the high T_c in BKB. On the other hand, it is a further problem whether the superconductivity in BPB can be explained within the phonon mechanism. It seems that effects of random substitution of Bi for Pb have to be taken into account.

References

1. J.G. Bednortz and K.A. Müller: Z. Physik B 64 (1986) 189.
2. A.W. Sleight, J.L. Gilson and P.E. Bierstedt: Solid State Commun. 17 (1975) 27.
3. T.D. Thanh, A. Koma and S. Tanaka: Appl. Phys 22 (1980) 205.
4. T. Itoh, K. Kitazawa and S. Tanaka: J. Phys. Soc. Jpn. 53 (1984) 2668.
5. H. Takagi, M. Naito, S. Uchida, K. Kitazawa, S. Tanaka and A. Katsui: Solid State Commun. 55 (1985) 1019.
6. S. Tajima, S. Uchida, A. Masaki, H. Takagi, K.Kitazawa, S. Tanaka and A. Katsui: Phys. Rev. B 32 (1985) 6302.
7. E. Jurczek and T.M. Rice: Europhys. Lett. 1 (1986) 225.
8. W. Weber: Jpn. J. Appl. Phys. 26, Suppl. 3 (1987) 981.
9. L.F. Mattheiss, E.M. Gyorgy and D.W. Johnson, Jr.: Phys. Rev. B 37 (1988) 3745.
10. D.G.Hinks, B.Dabrowski, J.D.Jorgensen, A.W.Mitchell, D.R. Richards, S.Pei and D.Shi: Nature (London) 333 (1988) 836.
11. B. Batlogg, R.J. Cava, A. Jayaraman, R.B. van Dover, G.A. Kourouklis, S. Sunshine, D.W. Murphy, L.W. Rupp, H.S. Chen, A. White, K.T. Short, L.M. Mujsce and E.A. Rietman: Phys. Rev. Lett. 58 (1987) 2333.
12. L.C. Bourne, M.F. Crommie, A. Zettl, H.C. zur Loye, S.W. Keller, K.L. Leary, A.M. Stacy, K.J. Chang, M.L. Cohen and D.E. Morris: Phys. Rev. Lett. 58 (1987) 2337.

13. B. Batlogg, G. Kourouklis, W. Weber, R.J. Cava, A. Jayaraman, A.E. White, K.T. Short, L.W. Rupp and E.A. Rietman: Phys. Rev. Lett. 59 (1987) 912.

14. T.A. Faltens, W.K. Ham, S.W. Keller, K.J.Leary, J.N. Michaels, A.M. Stacy, H.C. zur Loye, T.W. Barbee,III, L.C. Bourne, M.L. Cohen, S. Hoen and A. Zettl: Phys. Rev. Lett. 59 (1987) 915.

15. K.J. Leary, H.C. zur Loye, S.W. Keller, T.A. Faltens, W.K. Ham, J.N. Michaels and A.M. Stacy: Phys. Rev. Lett. 59 (1987) 1236.

16. H. Katayama-Yoshida, T. Hirooka, A.J. Mascarenhas, Y. Okabe, T. Takahashi, T. Sasaki, A. Ochiai, T. Suzuki, J.I.Pankove, T. Ciszek and S.K. Deb: Jap. J. Appl. Phys. 26 (1987) L2085.

17. T. Ekino, J. Akimitsu, M. Sato and S. Hosoya: Solid State Commun. 62 (1987) 535.

18. A.P. Felin, J.R. Kirtley and M.W. Shafer: Phys. Rev. B 37 (1988) 9738.

19. H. Ikuta, A. Maeda, K. Uchinokura and S. Tanaka: Jpn. J. Appl. Phys. 27 (1988) L1038.

20. D.E. Cox and A.W. Sleight: Solid State Commun. 19 (1976) 969.; Proceedings of Conference on Neutron Scattering, Gatlinburg,Tennessee, 1976, ed. by R.M. Moon.

21. M. Oda, Y. Hidaka, A. Katsui and T. Murakami: Solid State Commun. 55 (1985) 423.

22. S. Uchida, K. Kitazawa and S. Tanaka: Phase Transitions 8 (1987) 95 and references cited herein.

23. L.F. Mattheiss and D.R. Hamann: Phys. Rev. B 26 (1982) 2686.; ibid. B 28 (1983) 4227.
24. J.C. Slater and G.F. Koster: Phys. Rev. 94 (1954) 1498.
25. K. Kitazawa, S. Uchida and S. Tanaka: Physica 126 B (1984) 275.
26. L.F. Mattheiss and D.R. Hamann: Phys. Rev. Lett. 60 (1988) 2681.
27. G. Lehmann and M. Taut: Phys. Stat. Sol.(b) 54 (1972) 469.
28. K. Motizuki and N. Suzuki: Structural Phase Transitions in Layered Transition-Metal Compounds, ed. by K. Motizuki (D. Reidel Publishing Co., 1986) p.1.
29. Y. Kahn, K. Nahm, M. Rosenberg and H. Willner: Phys. Stat. Sol.(a) 39 (1977) 79.
30. W. Reichardt and W. Weber: Jpn. J. Appl. Phys. 26, Suppl. 3 (1987) 1121.
31. P.B. Allen: Phys. Rev. B 6 (1972) 2577.
32. W. Marshall and S.W. Lovesey: Theory of Thermal Neutron Scattering, (Oxford Univ. Press, London, 1971) p.64.
33. A.B. Migdal: Soviet Phys. JETP 7 (1958) 996.
34. D.J. Scalapino: Superconductivity, ed. by R.D. Parks (Marcel Dekker, New York, 1969) p.449.
35. G.M. Eliashberg: Soviet Phys. JETP 11 (1960) 696.; ibid. 12 (1961) 1000.
36. G. Bergmann and D. Rainer: Z. Physik 263 (1973) 59.
37. J. Bardeen, L.N. Cooper and J.R. Schrieffer: Phys. Rev. 108 (1957) 1175.
38. W.L. McMillan and J.M. Rowell: Phys. Rev.Lett. 14 (1965) 108.

39. H. Fröhlich: Proc. R. Soc. (London) A **215** (1952) 291.

40. J. Bardeen and D. Pines: Phys Rev. **99** (1955) 1140.

41. N.N. Bogoliubov: Soviet Phys. JETP **7** (1958) 41.

42. P.W. Anderson: Phys. Rev. **112** (1958) 1900.

43. L.P. Gor'kov: Soviet Phys. JETP **7** (1958) 505.

44. A.L. Fetter and J.D. Walecka: Quantum Theory of Many Particle Systems (McGraw-Hill, New York, 1971).

45. A.A. Abrikosov, L.P. Gor'kov and I.E. Dzyaloshinski: Methods of Quantum Field Theory in Stastical Physics (Prentice-Hill, Englewood Cliffs, New Jersey, 1963).

46. P. Morel and P.W. Anderson: Phys. Rev. **125** (1962) 1263.

47. W.L. McMillan: Phys. Rev. **167** (1968) 331.

48. B. Batlogg, R.J. Cava, L.W. Rupp, Jr., A.M. Mujsce, J.J. Krajewski, J.P. Remeika,, W.F. Peck, Jr., A.S. Cooper and G.P. Espinoza: Phys. Rev. Lett. **61** (1988) 1670.

49. S. Kondoh, M. Sera, Y. Ando and M. Sato: to be bublished.

50. D.G. Hinks, D.R. Richards, B. Dabrowski, D.T. Marx and A.W. Mitchell: Nature (London) **335** (1988) 419.

51. T.W. Barbee III, M.L. Cohen, L.C. Bourne and A. Zettl: J. Phys. C **22** (1988) 5977.

52. J.R. Schrieffer, D.J. Scalapino and J.W. Wilkins: Phys. Rev. Lett. **10** (1963) 336.

53. J. Akimitsu, T. Ekino and K. Kobayashi: Jpn. J. Appl. Phys. **26**, Suppl. 3 (1987) 995.

54. S. Berman and D.M. Ginsberg: Phys. Rev. A **135** (1964) 306.

55. I. Giaever, H.R. Hart, Jr. and K. Megerle: Phys. Rev. **126** (1962) 941.

Appendix.A. Migdal theorem

A criterion of the applicability of perturbation theory to electron-phonon problems has been developed by Migdal in 1958. Based on quantum field theoretical methods Migdal has evaluated the vertex part of the electron-phonon interaction and found that the vertex part can be expanded in a perturbation series with a small parameter $M^{-1/2}$, where M is the mass of an atom. The result enables one to apply the perturbation theory without assuming the weak electron-phonon coupling. The Eliashberg theory owes to this guiding principle in constructing the self-energy equations for strong coupling superconductors. In this Appendix we will review the process of deriving the Migdal theorem and discuss the efficiency of the theorem.

Starting from the Fröhlich Hamiltonian (4-1)∿(4-4), equations of motion for thermal Green's functions of electron $G(\mathbf{k},\tau)$ and phonon $D(\mathbf{q},\tau)$ can be constructed. Here, indeces for the electronic band and the phonon branch shall be omitted for brevity. Introducing self-energies $\Sigma(\mathbf{k},\tau)$ for electrons and polarization functions $\Pi(\mathbf{q},\tau)$ for phonons, the equations of motion can be transformed to that of the Fourier components defined on the Matsubara frequencies. That is the so-called Dyson's equation:

$$G(\mathbf{k},i\varepsilon_n) = G^0(\mathbf{k},i\varepsilon_n) + G^0(\mathbf{k},i\varepsilon_n)\,\Sigma(\mathbf{k},i\varepsilon_n)\,G(\mathbf{k},i\varepsilon_n) \quad , \tag{A-1}$$

$$D(\mathbf{q},i\omega_m) = D^0(\mathbf{q},i\omega_m) + D^0(\mathbf{q},i\omega_m)\,\Pi(\mathbf{q},i\omega_m)\,D(\mathbf{q},i\omega_m) \quad , \tag{A-2}$$

where $i\varepsilon_n \equiv (2n+1)\pi i k_B T$ and $i\omega_m \equiv 2m\pi i k_B T$ with n and m being integers, and $G^0(\mathbf{k},i\varepsilon_n)$ and $D^0(\mathbf{q},i\omega_m)$ is the non-interacting Green's function for electrons and phonons, respectively:

$$G^0(\mathbf{k},i\varepsilon_n) = \frac{1}{i\varepsilon_n - E^0_{\mathbf{k}}} \quad , \tag{A-3}$$

$$D^0(\mathbf{q},i\omega_m) = -\frac{2\omega^0_{\mathbf{q}}}{(i\omega_m)^2 - (\omega^0_{\mathbf{q}})^2} \quad . \tag{A-4}$$

where the chemical potential has been set to zero for brevity.

By using the usual Feynman's diagramatic techniques, $\Sigma(\mathbf{k},i\varepsilon_n)$ and $\Pi(\mathbf{q},i\omega_n)$ is written in terms of the vertex function $\Gamma(\mathbf{q},i\omega_m;\mathbf{k},i\varepsilon_n)$ as follows:

$$\Sigma(\mathbf{k},i\varepsilon_n) = -\frac{1}{N\beta}\sum_{\mathbf{q}} |I(\mathbf{k},\mathbf{k}-\mathbf{q})|^2 \times \sum_{m=-\infty}^{\infty} D(\mathbf{q},i\omega_m)\; G(\mathbf{k}-\mathbf{q},i\varepsilon_{n-m})\; \Gamma(\mathbf{q},i\omega_m;\mathbf{k},i\varepsilon_n) \quad , \tag{A-5}$$

$$\Pi(\mathbf{q},i\varepsilon_m) = \frac{1}{N\beta}\sum_{\mathbf{k}} |I(\mathbf{k}.\mathbf{k}-\mathbf{q})|^2 \times \sum_{n=-\infty}^{\infty} G(\mathbf{k},i\varepsilon_n)\; G(\mathbf{k}-\mathbf{q},i\varepsilon_{m-n})\; \Gamma(\mathbf{q},i\omega_m;\mathbf{k},i\varepsilon_n)^* \quad . \tag{A-6}$$

The vertex function $\Gamma(\mathbf{q},i\omega_m;\mathbf{k},i\varepsilon_n)$, which is the Fourier

transform of eq.(4-56), should be evaluated diagramatically. The perturbation series of the vertex function, $\Gamma=\Gamma_0+\Gamma_1+\cdots$, is presented in Fig.A-1, where the full and wavy curves denote the non-interacting Green's function for electrons $G^0(\mathbf{k},i\varepsilon_n)$ and phonons $D^0(\mathbf{q},i\omega_m)$, respectively.

The first-order correction to the vertex function, $\Gamma_1(\mathbf{q},i\omega_m;\mathbf{k},i\varepsilon_n)$, is obtained by

$$\Gamma(\mathbf{q},i\omega_m;\mathbf{k},i\varepsilon_n) = -\frac{1}{N\beta}\sum_{\mathbf{k}'}|I(\mathbf{k},\mathbf{k}')|^2 \times \sum_{n'=-\infty}^{\infty} D^0(\mathbf{k}-\mathbf{k}',i\varepsilon_{n-n'})\, G^0(\mathbf{k}',i\varepsilon_{n'})\, G^0(\mathbf{k}'-\mathbf{q},i\varepsilon_{n'}-i\omega_m) \quad . \tag{A-7}$$

It is difficult to evaluate eq.(A-7) accurately based on the realistic electron-phonon systems. However, it is easilly confirmed that the main contribution to eq.(A-7) arises in case of $E^0_{\mathbf{k}} \simeq E^0_{\mathbf{k}'} \simeq E_F$. Then, eq.(A-7) has an order of $|I(\mathbf{k},\mathbf{k}')|^2/\omega_{\mathbf{k}-\mathbf{k}'}$ which proportional to $M^{-1/2}$.

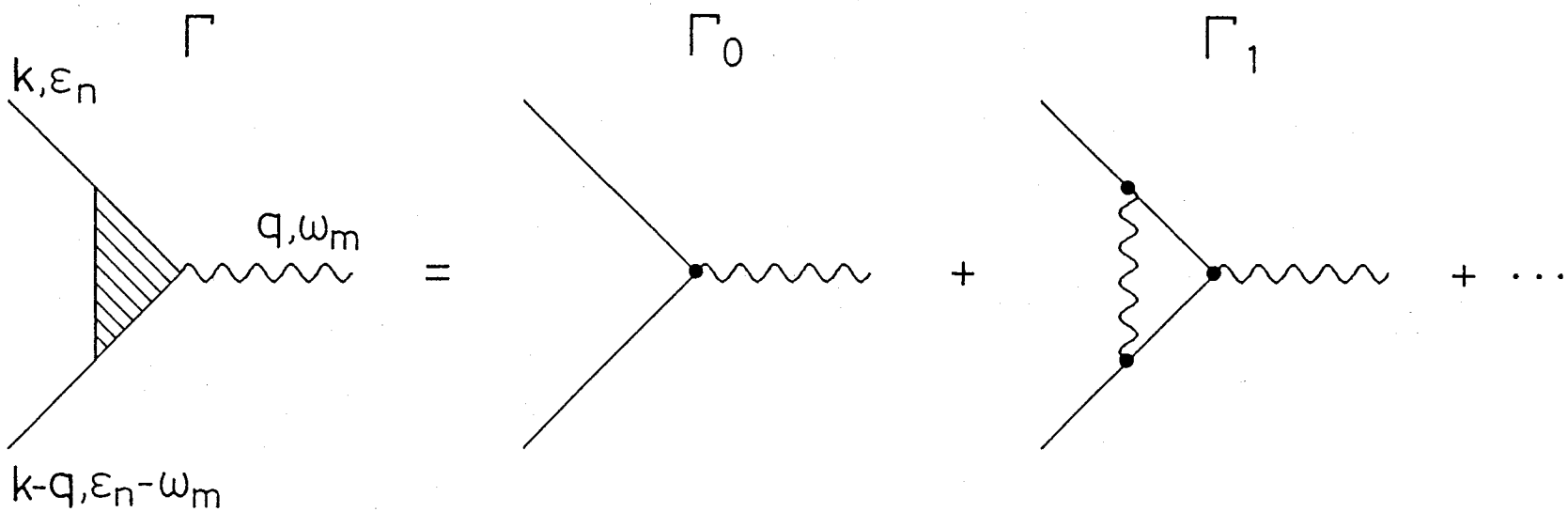

Fig.A-1. Feynman diagrams for the vertex part of the electron-phonon interaction with the external lines. The full and wavy lines denote the Green's function for electron and phonon, respectively.

Appendix.B. Nambu formalism

In order to derive the Eliashberg equation the equation of motion for the electronic Green's function has been constructed and decoupled in the Gor'kov's manner. However, it is also convenient to utilize the usual quantum field-theoretical method. In this context Nambu representation will be introduced to simplify the notation of the formalism. First, two-component field operator $\Psi_{\mathbf{k}}$ and its Hermite conjugate are defined as

$$\Psi_{\mathbf{k}} = \begin{pmatrix} c_{\mathbf{k}\uparrow} \\ c^{\dagger}_{-\mathbf{k}\downarrow} \end{pmatrix} , \qquad \Psi^{\dagger}_{\mathbf{k}} = [c^{\dagger}_{\mathbf{k}\uparrow} , c_{-\mathbf{k}\downarrow}] \quad . \tag{B-1}$$

It is found from above expressions that the Nambu formalism is only concerning itself with formation of the Cooper (i.e. singlet) pairs. If one wants to deal with triplet pairs, the Eliashberg's four-components field operator must be used instead of Nambu's operator.

The commutation relation of these operators are formally given by

$$\{\Psi_{\mathbf{k}} , \Psi^{\dagger}_{\mathbf{k}'}\}_{+} = \delta_{\mathbf{k},\mathbf{k}'}\tau_0 \quad , \tag{B-2a}$$

$$\{\Psi_{\mathbf{k}} , \Psi_{\mathbf{k}'}\}_{+} = \{\Psi^{\dagger}_{\mathbf{k}} , \Psi^{\dagger}_{\mathbf{k}'}\}_{+} = 0 \quad . \tag{B-2b}$$

where τ_0 denotes the unit matrix of dimension 2×2:

$$\tau_0 = \begin{pmatrix} 1 & 0 \\ 0 & 1 \end{pmatrix} \quad . \tag{B-3}$$

In order to write down the Hamiltonian in terms of these operators Pauli matrices τ_i (i=1,2,3) shall be used. The Pauli matrices are defined by

$$\tau_1 = \begin{pmatrix} 0 & 1 \\ 1 & 0 \end{pmatrix} \quad , \quad \tau_2 = \begin{pmatrix} 0 & -i \\ i & 0 \end{pmatrix} \quad , \quad \tau_3 = \begin{pmatrix} 1 & 0 \\ 0 & -1 \end{pmatrix} \quad . \tag{B-4}$$

By using these notations, it is readily found that

$$\Psi_{\mathbf{k}}^{\dagger} \tau_1 \Psi_{\mathbf{k}} = c_{\mathbf{k}\uparrow}^{\dagger} c_{-\mathbf{k}\downarrow}^{\dagger} + c_{-\mathbf{k}\downarrow} c_{\mathbf{k}\uparrow} \quad , \tag{B-5a}$$

$$\Psi_{\mathbf{k}}^{\dagger} \tau_2 \Psi_{\mathbf{k}} = -i[c_{\mathbf{k}\uparrow}^{\dagger} c_{-\mathbf{k}\downarrow}^{\dagger} + c_{-\mathbf{k}\downarrow} c_{\mathbf{k}\uparrow}] \quad , \tag{B-5b}$$

$$\Psi_{\mathbf{k}}^{\dagger} \tau_3 \Psi_{\mathbf{k}} = c_{\mathbf{k}\uparrow}^{\dagger} c_{\mathbf{k}\uparrow} + c_{-\mathbf{k}\downarrow}^{\dagger} c_{-\mathbf{k}\downarrow} - 1 \quad , \tag{B-5c}$$

$$\Psi_{\mathbf{k}}^{\dagger} \tau_0 \Psi_{\mathbf{k}} = c_{\mathbf{k}\uparrow}^{\dagger} c_{\mathbf{k}\uparrow} - c_{-\mathbf{k}\downarrow}^{\dagger} c_{-\mathbf{k}\downarrow} + 1 \quad . \tag{B-5d}$$

Then, the Fröhlich Hamiltonian can be rewritten in the form as

$$H_{el} = \sum_{\mathbf{k}} E_{\mathbf{k}}^{0} (\Psi_{\mathbf{k}}^{\dagger} \tau_3 \Psi_{\mathbf{k}}) \quad , \tag{B-6}$$

$$H_{el\text{-}ph} = \sum_{\mathbf{kq}} \sum I(\mathbf{k},\mathbf{k}-\mathbf{q}) (\Psi_{\mathbf{k}} \tau_3 \Psi_{\mathbf{k}}) (b_{\mathbf{q}} + b_{-\mathbf{q}}^{\dagger}) \quad . \tag{B-7}$$

The thermal Green's function for electrons is also generalized in the Nambu reperesentation, which is defined by

$$\mathbf{G}(\mathbf{k},\tau) \equiv - \langle T_\tau \; \Psi_{\mathbf{k}}(\tau) \; \Psi^\dagger_{\mathbf{k}}(0) \rangle$$

$$= - \begin{pmatrix} \langle T_\tau \; c_{\mathbf{k}\uparrow}(\tau) \; c^\dagger_{\mathbf{k}\uparrow}(0) \rangle & \langle T_\tau \; c_{\mathbf{k}\uparrow}(\tau) \; c_{-\mathbf{k}\downarrow}(0) \rangle \\ \langle T_\tau \; c^\dagger_{-\mathbf{k}\downarrow}(\tau) \; c^\dagger_{\mathbf{k}\uparrow}(0) \rangle & \langle T_\tau \; c^\dagger_{-\mathbf{k}\uparrow}(\tau) \; c_{-\mathbf{k}\downarrow}(0) \rangle \end{pmatrix} \tag{B-8}$$

and its Fourier expansion form is given by

$$\mathbf{G}(\mathbf{k},\tau) = k_B T \sum_{n=-\infty}^{\infty} e^{-i\varepsilon_n \tau} \; \mathbf{G}(\mathbf{k}, i\varepsilon_n) \tag{B-9}$$

The component $G_{11}(\mathbf{k},\tau)$ corresponds to the "normal" Green's function for spin-up electrons:

$$G_{11}(\mathbf{k},\tau) = G_\uparrow(\mathbf{k},\tau) \quad , \tag{B-10}$$

and $G_{22}(\mathbf{k},\tau)$ can be thought as that for spin-down holes. On the other hand, the off-diagonal matrix elements of $\mathbf{G}(\mathbf{k},\tau)$ are nothing but the Gor'kov's "anormalous" Green's functions:

$$G_{12}(\mathbf{k},\tau) = F_\uparrow(\mathbf{k},\tau) \quad , \tag{B-11a}$$

$$G_{21}(\mathbf{k},\tau) = F^\dagger_\uparrow(\mathbf{k},\tau) \quad , \tag{B-11b}$$

As long as the system with the spin independent interaction is under consideration, the diagonal matrix elements have the following relation each other:

$$G_{11}(\mathbf{k},\tau) = - G_{22}(-\mathbf{k},-\tau) \quad , \tag{B-12a}$$

$$G_{11}(\mathbf{k},i\varepsilon_n) = - G_{22}(-\mathbf{k},-i\varepsilon_n) \quad . \tag{B-12b}$$

The quantum-field theory will be applied to the superconductors from now on. However, it is noted that the superconducting (or pairing) state cannot be obtained from the normal state, which is the ground state of the non-interacting electron-phonon system, by applying the electron-phonon interaction adiabatically. Thus, the unperturbed Hamiltonian H_0 should be rearranged as

$$H_0 = H_{el} + H_{ph} + H_{int}^{HF} \quad , \tag{B-13}$$

where H_{int}^{HF} is the reduced interaction Hamiltonian (4-8) in the generalized Hartree-Fock approximation, which is of the form:

$$H_{int}^{HF} = \sum_{\mathbf{k}} [\Delta_{\mathbf{k}}^{*} \, c_{\mathbf{k}\uparrow}^{\dagger} \, c_{-\mathbf{k}\downarrow}^{\dagger} + \Delta_{\mathbf{k}} \, c_{\mathbf{k}\uparrow} \, c_{-\mathbf{k}\downarrow}] \quad . \tag{B-14}$$

Then the perturbed term of the Hamiltonian should be

$$H' = H_{int} - H_{int}^{HF} \quad . \tag{B-15}$$

The rearrangement of the Hamiltonian shall ensure one to apply the usual perturbation theory, since the symmetry breaking term is already included in the zero-th Hamiltonian H_0. However, it is complicated that one performs actually the perturbation expansion based on the Hamiltonian (B-13), (B-14) and (B-15). Thus, we make the added term H_{int}^{HF} go to zero, after applying the

perturbation theory. Standing on the concepts described above, the complicated treatment can be avoided and the results may be identical with that based on the original Hamiltonian.

By making use of the usual perturbation theory, the true Green's function $G(\mathbf{k},i\varepsilon_n)$ should be determined by the Dyson's equation:

$$G(\mathbf{k},i\varepsilon_n) = G^0(\mathbf{k},i\varepsilon_n) + G^0(\mathbf{k},i\varepsilon_n)\ \Sigma(\mathbf{k},i\varepsilon_n)\ G(\mathbf{k},i\varepsilon_n) \quad , \tag{B-16}$$

where the self-energy $\Sigma(\mathbf{k},i\varepsilon_n)$ is also the matrix of the dimension 2×2, and $G^0(\mathbf{k},i\varepsilon_n)$ denotes the non-interactiong Green's function for electrons, which is given by

$$\begin{aligned} G^0(\mathbf{k},i\varepsilon_n) &= \begin{pmatrix} [i\varepsilon_n - E_{\mathbf{k}}^0]^{-1} & 0 \\ 0 & [i\varepsilon_n + E_{\mathbf{k}}^0]^{-1} \end{pmatrix} \\ &= [i\varepsilon_n\,\tau_0 - E_{\mathbf{k}}^0\,\tau_3]^{-1} \\ &= \frac{i\varepsilon_n\,\tau_0 + E_{\mathbf{k}}^0\,\tau_3}{(i\varepsilon_n)^2 - (E_{\mathbf{k}}^0)^2} \quad . \end{aligned} \tag{B-17}$$

The most general form of $\Sigma(\mathbf{k},i\varepsilon_n)$ can be written as

$$\begin{aligned} \Sigma(\mathbf{k},i\varepsilon_n) = \xi(\mathbf{k},i\varepsilon_n)\ \tau_0 + \eta(\mathbf{k},i\varepsilon_n)\ \tau_3 \\ + \phi_1(\mathbf{k},i\varepsilon_n)\ \tau_1 + \phi_2(\mathbf{k},i\varepsilon_n)\ \tau_2 \quad , \end{aligned} \tag{B-18}$$

where $\xi(\mathbf{k},i\varepsilon_n)$, $\eta(\mathbf{k},i\varepsilon_n)$, $\phi_1(\mathbf{k},i\varepsilon_n)$ and $\phi_2(\mathbf{k},i\varepsilon_n)$ are independent

functions which may be arbitrary so far. Then, from eqs.(B-16), (B-17) and (B-18), the Green's function can be written as

$$\begin{aligned} G(\mathbf{k},i\varepsilon_n)^{-1} &= G^0(\mathbf{k},i\varepsilon_n)^{-1} - \Sigma(\mathbf{k},i\varepsilon_n) \\ &= [i\varepsilon_n - \xi(\mathbf{k},i\varepsilon_n)]\,\tau_0 - [E_{\mathbf{k}}^0 + \eta(\mathbf{k},i\varepsilon_n)]\,\tau_3 \\ &\quad - \phi_1(\mathbf{k},i\varepsilon_n)\,\tau_1 - \phi_2(\mathbf{k},i\varepsilon_n)\,\tau_2 \quad . \end{aligned} \tag{B-19}$$

By inverting this equation, the Green's function $G(\mathbf{k},i\varepsilon_n)$ is expressed as

$$\begin{aligned} G(\mathbf{k},i\varepsilon_n) = \{&[i\varepsilon_n - \xi(\mathbf{k},i\varepsilon\ )]\,\tau_0 + [E_{\mathbf{k}}^0 + \eta(\mathbf{k},i\varepsilon_n)]\,\tau_3 \\ &+ \phi_1(\mathbf{k},i\varepsilon_n)\,\tau_1 + \phi_2(\mathbf{k},i\varepsilon_n)\,\tau_2\} \,/\, \Xi(\mathbf{k},i\varepsilon_n) \quad , \end{aligned} \tag{B-20}$$

with

$$\begin{aligned} \Xi(\mathbf{k},i\varepsilon_n) &\equiv \det\left|G(\mathbf{k},i\varepsilon_n)^{-1}\right| \\ &= [i\varepsilon_n - \xi(\mathbf{k},i\varepsilon_n)]^2 - [E_{\mathbf{k}}^0 + \eta(\mathbf{k},i\varepsilon_n)]^2 \\ &\quad + \phi_1(\mathbf{k},i\varepsilon_n)^2 - \phi_2(\mathbf{k},i\varepsilon_n)^2 \quad . \end{aligned} \tag{B-21}$$

The above expression is nothing but eqs.(4-73), (4-74) and (4-75) in the Nambu representation. To hold the property (B-12b) the following relation must be satisfied:

$$\xi(\mathbf{k},i\varepsilon_n) = -\xi(\mathbf{k},-i\varepsilon_n) \quad , \tag{B-22}$$

$$\eta(\mathbf{k},i\varepsilon_n) = \eta(\mathbf{k},i\varepsilon_n) \quad , \tag{B-23}$$

$$\phi_1(\mathbf{k},i\varepsilon_n)^2 + \phi_2(\mathbf{k},i\varepsilon_n)^2 = \phi_1(\mathbf{k},-i\varepsilon_n)^2 + \phi_2(\mathbf{k},-i\varepsilon_n)^2 \quad , \tag{B-24}$$

where the inversion symmetry of the system has been assumed so that any function is to be even about the wave-vector $\mathbf{k}$.

By using the usual Feynman's diagram method, it is found that the self-energy $\Sigma(\mathbf{k},i\varepsilon_n)$ can be expanded in the perturbation series. With use of the Migdal theorem only the lowest order diagram should be taken, which is given in Fig.B-1 and evaluated to be as

$$\Sigma(\mathbf{k},i\varepsilon_n) = -\frac{1}{N\beta}\sum_{\mathbf{k}'}\sum_{\gamma}|I^{\gamma}(\mathbf{k},\mathbf{k}')|^2\sum_{m=-\infty}^{\infty}D^{\gamma}(\mathbf{k}-\mathbf{k}',i\varepsilon_n-i\varepsilon_m) \times \tau_3\, G(\mathbf{k}',i\varepsilon_m)\,\tau_3 \quad , \tag{B-25}$$

which is nothing but the Eliashberg equation in the Nambu representation.

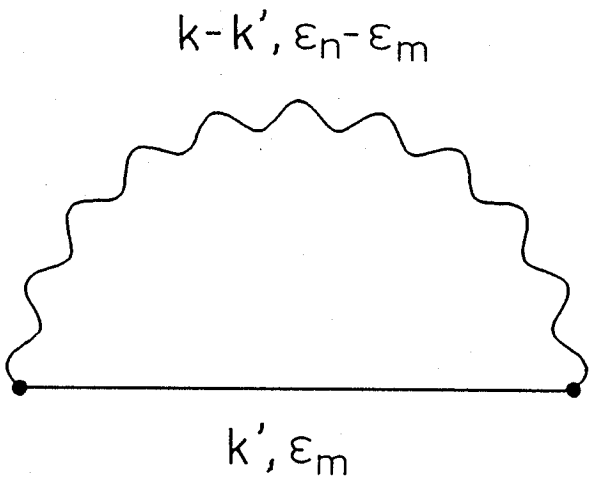

Fig.B-1. A Feynman diagram taken for the self-energy for the electronic Green's function. The full line denotes the electronic Green's function in the Nambu representation, and the wavy line that of phonon within the Migdal approximation.

Appendix.C. Eliashberg equation on real-axis

In order to obtain a familiar expression for the Eliashberg equation an analytic continuation on to the real-axis shall be carried out in this Appendix. For this purpose we will start from the self-energies, eqs.(4-92) and (4-93), or their original form:

$$\Sigma^{G}(\mathbf{k},i\varepsilon_n) = \frac{k_B T}{N(E_F)} \sum_{m=-\infty}^{\infty} \sum_{\mathbf{k}'} \int_0^{\infty} d\omega\ \alpha^2 F(\mathbf{k},\mathbf{k}';\omega)\ \frac{2\omega}{(\varepsilon_n-\varepsilon_m)^2+\omega^2} \times G(\mathbf{k}',i\varepsilon_m) \quad , \tag{C-1}$$

which have been obtained by utilizing the spectral representation for $D_\gamma(\mathbf{q},i\omega_n)$, eq.(4-90). A similar expression for $\Sigma^{F}(\mathbf{k},i\varepsilon_n)$ is given by replacing $G(\mathbf{k}',i\varepsilon_m)$ with $F(\mathbf{k}',i\varepsilon_m)$ on the right-hand side of eq.(C-1). Here, the spin index σ in the self-energies as well as the electron Greeen's functions has been omitted since they are independent of σ as far as the magnetic interaction has not been concerned, such as the effects of the paramagnetic impurities or the spin fluctuations.

By utilizing the Cauchy's theorem of complex integration the following equality can hold:

$$\int_{C_1} dz\ f(z)\ G(\mathbf{k}',z) \left\{ \frac{1}{i\varepsilon_n - z + \omega} - \frac{1}{i\varepsilon_n - z - \omega} \right\}$$

$$= 2\pi i k_B T \sum_{m=-\infty}^{\infty} G(\mathbf{k}', i\varepsilon_m) \frac{2\omega}{(\varepsilon_n - \varepsilon_m)^2 + \omega^2} \quad , \qquad \text{(C-2)}$$

where the integration contour C_1 is shown in Fig.C-1, and $f(z) \equiv [\exp(\beta z)+1]^{-1}$ is the Fermi distribution function which has poles at $z=i\varepsilon_n=(2n+1)\pi i k_B T$ with the residue of $k_B T$. Here, the chemical potential μ has been set to zero for brevity. Next, the integration contour C_1 is transformed to the contour C_2 which is shown in Fig.C-2. Then,

$$\int_{C_1} dz\ f(z)\ G(\mathbf{k}',z) \left\{ \frac{1}{i\varepsilon_n - z + \omega} - \frac{1}{i\varepsilon_n - z - \omega} \right\}$$

$$= \int_{C_2} dz\ f(z)\ G(\mathbf{k}',z) \left\{ \frac{1}{i\varepsilon_n - z + \omega} - \frac{1}{i\varepsilon_n - z - \omega} \right\}$$

$$+ 2\pi i [f(i\varepsilon_n+\omega)\ G(\mathbf{k}', i\varepsilon_n+\omega) - f(i\varepsilon_n-\omega)\ G(\mathbf{k}', i\varepsilon_n-\omega)] \quad , \qquad \text{(C-3)}$$

where the second term on the right-hand side is essentially originated from the poles of the phonon Green's function, $z=i\varepsilon_n \pm \omega$. Further, it is easily found that

$$f(i\varepsilon_n \pm \omega) = \frac{1}{\exp[(2n+1)\pi i]\cdot\exp(\pm\beta\omega) + 1}$$

$$= \begin{cases} -\,n(\omega) & ; \text{ for positive (+) sign} \\ n(\omega) + 1 & ; \text{ for negative (-) sign} \end{cases} , \qquad (C\text{-}4)$$

where $n(\omega)\equiv[\exp(\beta\omega)-1]^{-1}$ is the Bose distribution function. From eqs.(C-2), (C-3) and (C-4) the following equation can be obtained:

$$2\pi i k_B T \sum_{m=-\infty}^{\infty} G(\mathbf{k}', i\varepsilon_m) \frac{2\omega}{(\varepsilon_n-\varepsilon_m)^2 + \omega^2}$$

$$= \int_{-\infty}^{\infty} d\varepsilon' f(\varepsilon')\, G(\mathbf{k}', \varepsilon'+i\delta)\left\{ \frac{1}{i\varepsilon_n - \varepsilon' + \omega} - \frac{1}{i\varepsilon_n - \varepsilon' - \omega} \right\}$$

$$- \int_{-\infty}^{\infty} d\varepsilon' f(\varepsilon')\, G(\mathbf{k}', \varepsilon'-i\delta)\left\{ \frac{1}{i\varepsilon_n - \varepsilon' + \omega} - \frac{1}{i\varepsilon_n - \varepsilon' - \omega} \right\}$$

$$- 2\pi i\{n(\omega)\, G(\mathbf{k}', i\varepsilon_n+\omega) + [n(\omega) + 1]\, G(\mathbf{k}', i\varepsilon_n-\omega)\} , \qquad (C\text{-}5)$$

where the first term of the right-hand side has arised from the summation about the Matsubara frequencies for $\varepsilon_m>0$ (i.e. $m\geqq 0$) and the second term has arised from that for $\varepsilon_m<0$ ($m\leqq -1$).

It is noted that the analytic continuation of the thermal Green's function $G(\mathbf{k},i\varepsilon_n)$ just above and below the real-axis is identical with retarded $G^R(\mathbf{k},\varepsilon)$ and advanced $G^A(\mathbf{k},\varepsilon)$ Green's function, respectively. And they are complex conjugate of each other, i.e. $G^G(\mathbf{k},\varepsilon)=G^A(\mathbf{k},\varepsilon)^*$, for real ε. Hence, the following

relation can be obtain:

$$G(\mathbf{k},\varepsilon+i\delta) = G(\mathbf{k},\varepsilon-i\delta)^{*} \quad . \tag{C-6}$$

Further, the spectral representation for $G(\mathbf{k},z)$ is known to be given by:

$$G(\mathbf{k}',z) = -\frac{1}{\pi}\int_{-\infty}^{\infty} d\varepsilon' \, \frac{\mathrm{Im}\, G(\mathbf{k}',\varepsilon'+i\delta)}{z-\varepsilon'} \tag{C-7}$$

for Im $z>0$. By using the relations (C-6) and (C-7), it is found that for $\varepsilon_n>0$ (i.e. $n>0$) eq.(C-5) becomes:

$$\pi k_B T \sum_{m=-\infty}^{\infty} G(\mathbf{k}',i\varepsilon_m) \frac{2\omega}{(\varepsilon_n-\varepsilon_m)^2+\omega^2}$$

$$= \int_{-\infty}^{\infty} d\varepsilon' \mathrm{Im}[G(\mathbf{k}',\varepsilon'+i\delta)] \left\{ \frac{n(\omega)+f(\varepsilon')}{i\varepsilon_n-\varepsilon'+\omega} + \frac{n(\omega)+1-f(\varepsilon')}{i\varepsilon_n-\varepsilon'-\omega} \right\} . \tag{C-8}$$

Using this expression, eq.(C-1) is rewritten as:

$$\Sigma^{G}(\mathbf{k},i\varepsilon_n)$$

$$= \frac{1}{N(E_F)} \sum_{\mathbf{k}'} \int_0^{\infty} d\omega \, \alpha^2 F(\mathbf{k},\mathbf{k}';\omega) \cdot \frac{1}{\pi} \int_{-\infty}^{\infty} d\varepsilon' \mathrm{Im}[G(\mathbf{k}',\varepsilon'+i\delta)]$$

$$\times \left\{ \frac{n(\omega)+f(\varepsilon')}{i\varepsilon_n-\varepsilon'+\omega} + \frac{n(\omega)-f(-\varepsilon')}{i\varepsilon_n-\varepsilon'-\omega} \right\} , \tag{C-9}$$

where a relation $1-f(\varepsilon')=f(-\varepsilon')$ has been used. Finally, by

continuating analytically the self-energy $\Sigma^G(\mathbf{k},i\varepsilon_n)$ onto the real-axis $\varepsilon+i\delta$, it follows that

$$\Sigma^G(\mathbf{k},\varepsilon+i\delta)$$

$$= \frac{1}{N(E_F)} \sum_{\mathbf{k}'} \int_0^\infty d\omega\ \alpha^2F(\mathbf{k},\mathbf{k}';\omega) \cdot \frac{1}{\pi} \int_{-\infty}^{\infty} d\varepsilon' \mathrm{Im}[G(\mathbf{k}',\varepsilon'+i\delta)]$$

$$\times \left\{ \frac{n(\omega) + f(\varepsilon')}{\varepsilon - \varepsilon' + \omega + i\delta} + \frac{n(\omega) + f(-\varepsilon')}{\varepsilon - \varepsilon' - \omega + i\delta} \right\} . \qquad \text{(C-10)}$$

The similar expression for $\Sigma^F(\mathbf{k},\varepsilon+i\delta)$ is again given by replacing $G(\mathbf{k}',\varepsilon'+i\delta)$ with $F(\mathbf{k}',\varepsilon'+i\delta)$ on the right-hand side of eq.(C-10).

Essentially the same procedure with that developed in Sec.4-1-2 shall be employed hereafter to derive the final expression of the Eliashberg equation. First, in order to obtain the self-consistent equations for self-energies the explicit expression for the Green's function, eqs.(4-73) and (4-74), are substituted in eq.(C-10) and the similar equation for $\Sigma^F(\mathbf{k},\varepsilon+i\delta)$. Then, neglecting (or averaging over the Fermi surface) the wave-vector dependence of the self-energies, the equations can been reduced to the isotropic form. Further, the self-energy for normal state $\Sigma^G(\varepsilon+i\delta)$ is devided into odd $\xi(\varepsilon)$ and even $\eta(\varepsilon)$ part. Then,

$$\xi(\varepsilon) = \int_{-\infty}^{\infty} d\varepsilon' \mathrm{Re}\left\{ \frac{\varepsilon' - \xi(\varepsilon')}{\Omega(\varepsilon')} \right\} \cdot \mathrm{sign}[\mathrm{Im}\ \Omega(\varepsilon')]$$

$$\times \int_{0}^{\infty} d\omega\ \alpha^2 F(\omega) \left\{ \frac{n(\omega) + f(\varepsilon')}{\varepsilon - \varepsilon' + \omega + i\delta} + \frac{n(\omega) + f(-\varepsilon')}{\varepsilon - \varepsilon' - \omega + i\delta} \right\} , \tag{C-11}$$

where $\Omega(\varepsilon)$ has been defined by eq.(4-102) and written in terms of the renormalization function $Z(\varepsilon) \equiv 1 - \xi(\varepsilon)/\varepsilon$ and the gap function $\Delta(\varepsilon) \equiv \Sigma^F(\varepsilon)/Z(\varepsilon)$ as

$$\Omega^2(\varepsilon) = [\varepsilon - \xi(\varepsilon)]^2 - [\Sigma^F(\varepsilon)]^2$$

$$= Z(\varepsilon)^2 [\varepsilon^2 - \Delta(\varepsilon)^2] \quad . \tag{C-12}$$

By using this the final expression can be derived as

$$\xi(\varepsilon) = \int_{-\infty}^{\infty} d\varepsilon' \mathrm{Re}\left\{ \frac{\varepsilon'}{[(\varepsilon')^2 - \Delta(\varepsilon')^2]^{1/2}} \right\}$$

$$\times \int_{0}^{\infty} d\omega\ \alpha^2 F(\omega) \left\{ \frac{n(\omega) + f(\varepsilon')}{\varepsilon - \varepsilon' + \omega + i\delta} + \frac{n(\omega) + f(-\varepsilon')}{\varepsilon - \varepsilon' - \omega + i\delta} \right\} . \tag{C-13}$$

Another party of the Eliashberg equation, i.e. the equation for gap function $\Delta(\varepsilon)$ can also be derived in the same way:

$$\Delta(\varepsilon) = \frac{1}{Z(\varepsilon)} \int_{-\infty}^{\infty} d\varepsilon' \mathrm{Re}\left[\frac{\Delta(\varepsilon')}{[(\varepsilon')^2 - \Delta(\varepsilon')]^{1/2}} \right]$$

$$\times \int_0^{\infty} d\omega\ \alpha^2 F(\omega) \left[\frac{n(\omega) + f(\varepsilon')}{\varepsilon - \varepsilon' + \omega + i\delta} + \frac{n(\omega) + f(-\varepsilon')}{\varepsilon - \varepsilon' - \omega + i\delta} \right] . \tag{C-14}$$

By concerning the parity of $\xi(\varepsilon)$ and $\Delta(\varepsilon)$, i.e.

$$\xi(-\varepsilon) = -\xi(\varepsilon)$$

$$\Delta(-\varepsilon) = \Delta(\varepsilon)$$

the integration about ε' for $(-\infty,\infty)$ in eqs.(C-13) and (C-14) can be folded into the semi-infinite interval $(0,\infty)$:

$$\xi(\varepsilon) = \int_0^{\infty} d\varepsilon' \mathrm{Re}\left[\frac{\varepsilon'}{[(\varepsilon')^2 - \Delta(\varepsilon')]^{1/2}} \right] \int_0^{\infty} d\omega\ \alpha^2 F(\omega)$$

$$\times \{[n(\omega) + f(\varepsilon')] \cdot \left[\frac{1}{\varepsilon - \varepsilon' + \omega + i\delta} + \frac{1}{\varepsilon + \varepsilon' - \omega + i\delta} \right]$$

$$+ [n(\omega) + f(-\varepsilon')] \cdot \left[\frac{1}{\varepsilon - \varepsilon' - \omega + i\delta} + \frac{1}{\varepsilon + \varepsilon' + \omega + i\delta} \right]\} , \tag{C-15}$$

$$\Delta(\varepsilon) = \frac{1}{Z(\varepsilon)} \int_0^{\infty} d\varepsilon' \mathrm{Re}\left[\frac{\Delta(\varepsilon')}{[(\varepsilon')^2 - \Delta(\varepsilon')]^{1/2}} \right] \int_0^{\infty} d\omega\ \alpha^2 F(\omega)$$

$$\times \{[n(\omega) + f(\varepsilon')] \cdot \left[\frac{1}{\varepsilon - \varepsilon' + \omega + i\delta} - \frac{1}{\varepsilon + \varepsilon' - \omega + i\delta} \right]$$

$$+ [n(\omega) + f(-\varepsilon')] \cdot \left[\frac{1}{\varepsilon - \varepsilon' - \omega + i\delta} - \frac{1}{\varepsilon + \varepsilon' + \omega + i\delta} \right]\} . \tag{C-16}$$

In case of T=0 K the Bose factor $n(\omega)$ and the Fermi factor $f(\varepsilon')$ go to zero, while $f(-\varepsilon')$ goes to unity since $\varepsilon'>0$. Hence, the Eliashberg equations for T=0 K can be given by

$$\xi(\varepsilon) = \int_0^\infty d\varepsilon' \mathrm{Re}\left[\frac{\varepsilon'}{[(\varepsilon')^2 - \Delta(\varepsilon')]^{1/2}} \right] \times \int_0^\infty d\omega\, \alpha^2 F(\omega) \left\{ \frac{1}{\varepsilon - \varepsilon' - \omega + i\delta} + \frac{1}{\varepsilon + \varepsilon' + \omega + i\delta} \right\} . \tag{C-17}$$

$$\Delta(\varepsilon) = \frac{1}{Z(\varepsilon)} \int_0^\infty d\varepsilon' \mathrm{Re}\left[\frac{\Delta(\varepsilon')}{[(\varepsilon')^2 - \Delta(\varepsilon')]^{1/2}} \right] \times \int_0^\infty d\omega\, \alpha^2 F(\omega) \left\{ \frac{1}{\varepsilon - \varepsilon' - \omega + i\delta} - \frac{1}{\varepsilon + \varepsilon' + \omega + i\delta} \right\} . \tag{C-18}$$

List of Publications

1. N. Suzuki and M. Shirai:
Magnetic Excitations and Successive Transition in $RbFeBr_3$-type Modified Triangular Antiferromagnets.
Physica 136 B (1986) 346.

2. M. Shirai, N. Suzuki and K. Motizuki:
Microscopic Theory of Electron-Phonon Interaction and Superconductivity of $BaPb_{1-x}Bi_xO_3$.
Solid State Commun. 60 (1986) 489.

3. M. Shirai, N. Suzuki and K. Motizuki:
Electron-Lattice Interaction, Lattice Dynamics and Superconductivity in $BaPb_{1-x}Bi_xO_3$.
Jpn. J. Appl. Phys. Series 1
Superconducting Materials (1988) 225.

4. M. Shirai, N. Suzuki and K. Motizuki:
Electron-Phonon Interaction and Lattice Dynamics in $BaPb_{1-x}Bi_xO_3$.
to be published in Ferroelectrics (1989).

5. M. Shirai, N. Suzuki and K. Motizuki:
Superconductivity in $BaPb_{1-x}Bi_xO_3$ and $Ba_xK_{1-x}BiO_3$.
to be published in J. Phys., Cond. Matter (1989).

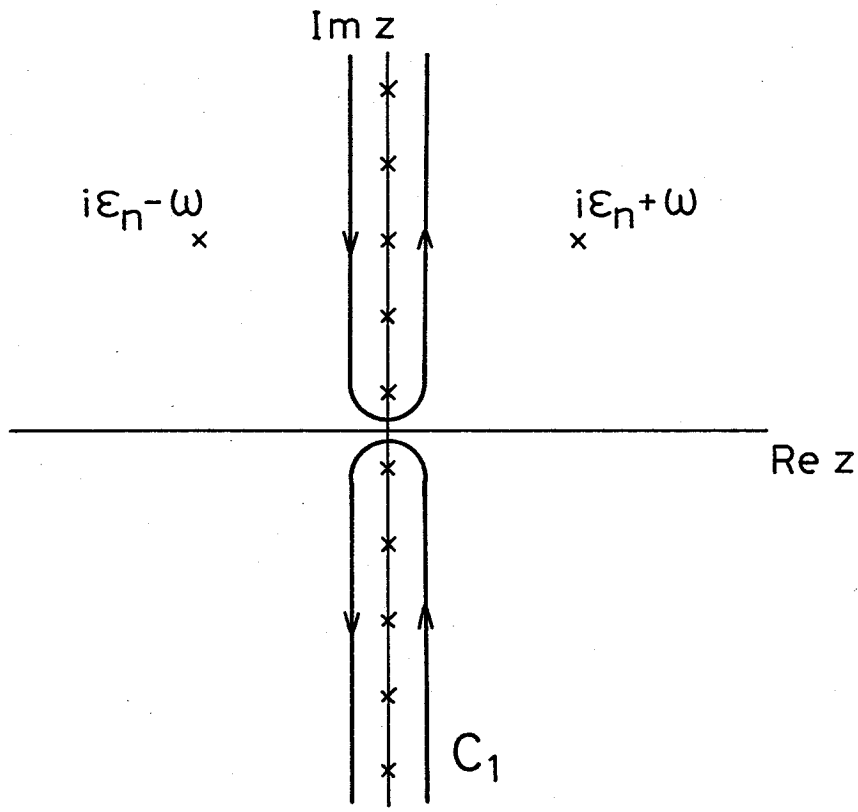

Fig.C-1. Contour of integration C_1 in the complex (z) plane.

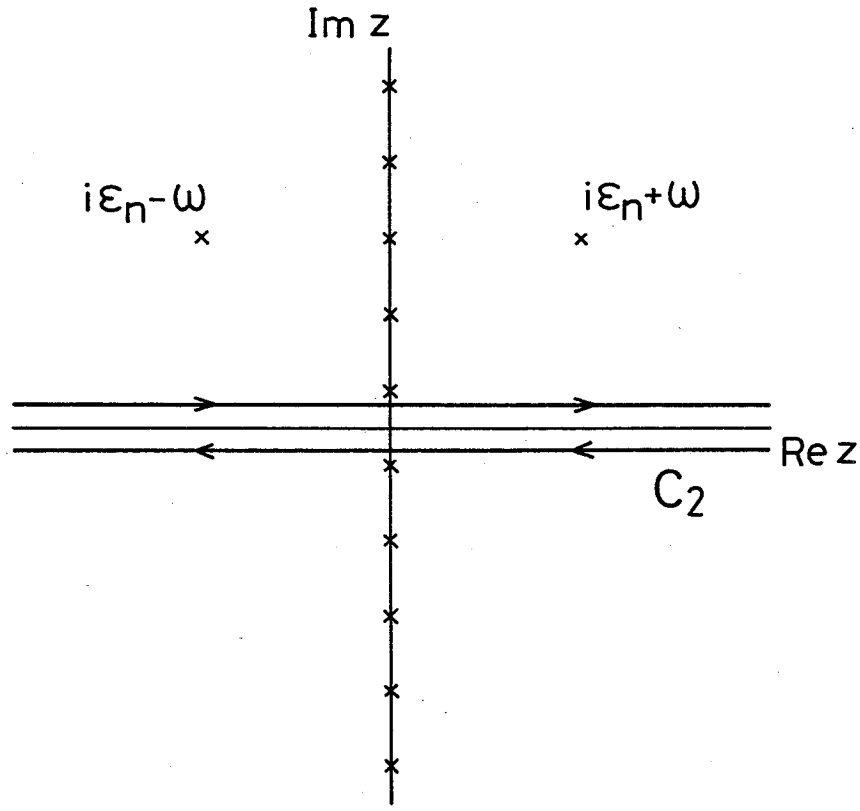

Fig.C-2. Contour of integration C_2 in the complex (z) plane.